THE DISSERTATION COMMITTEE FOR BRIAN ROONEY CERTIFIES THAT THIS IS THE APPROVED VERSION OF THE FOLLOWING DISSERTATION:

RESTORING BLADDER FUNCTION BY PROMOTING NEURONAL REGENERATION

Committee:

Claire Hulsebosch, Ph.D., Supervisor

Doug Dewitt, Ph.D.

Ping Wu, M.D., PhD.

Simon Lewis, Ph.D.

Leif Havton, Ph.D.

Dean, Graduate School

RESTORING BLADDER FUNCTION BY PROMOTING NEURONAL

REGENERATION

BY

BRIAN ANTHONY ROONEY, B.A. MOD. ZOO.

DISSERTATION

Presented to the Faculty of the Graduate School of

The University of Texas Medical Branch

in Partial Fulfillment

of the Requirements

for the Degree of

DOCTOR OF PHILOSOPHY

THE UNIVERSITY OF TEXAS MEDICAL BRANCH

AUGUST, 2010

DEDICATION

To my parents, Tony and Bríd.

ACKNOWLEDGEMENTS

Firstly I would like to give most thanks to my mentor Dr Claire Hulsebosch, without whose guidance, encouragment and patience I would not have made it through this. I greatly appreciate the opportunities for learning that she has provided for me over the years and I will miss the enthusiasm and kindness she demonstrates everyday. Thanks also to Debbie Pavlu and everyone I worked alongside in the Hulsebosch Lab. I learned something from each and every one of you and I will miss our Christmas lunches at the Pelican Club. I am very grateful to Tony Rossomondo who, while at Biogen Idec, provided us with the Artemin that made this project exciting to work on. Without the support of the MD Anderson Foundation, the West, Strake and Dunn Foundations, Mission Connect of TIRR, Mr. F. Liddell and NIH grants NS 11255 and 39161 I would not have been able to carry this project to completion.

I need to give special thanks to the extended Ortiz family for taking me into your homes, especially during hurricane Ike, your kindness will never be forgotten. I am particularly grateful for the support and constant encouragement of my family and friends back in Ireland and for making me feel like I had never been away whenever I came to visit. I love you all. Ely, your love, your support and your belief in me was second to none, thank you for everything.

Last but not least, I would like to thank the countless rats who tolerated me, kept me company on those late nights in the lab and who truly did all the work. Hopefully your sacrifice was not in vain.

RESTORING BLADDER FUNCTION BY PROMOTING NEURONAL REGENERATION

Publication No._____

Brian Anthony Rooney, Doctor of Philosophy (Ph.D),

The University of Texas Medical Branch, 2010

Supervisor: Claire Hulsebosch

ABSTRACT

Following dorsal root injury, dorsal root ganglion neurons can regenerate their severed axons but are unable to cross the dorsal root entry zone (DREZ) due to the presence of an inhibitory environment produced in part by chondroitin sulfate proteoglycans (CSPGs) manufactured by reactive astrocytes and oligodendrocytes. We examined the influence of the GDNF family neurotrophin artemin on the neuroarchitecture and extracellular matrix composition of the dorsal spinal cord following a bilateral dorsal root crush (DRC) at L6 and S1. Our functional assessment involved recording from the bladder and external urethral sphincter (EUS). Systemic artemin treatment resulted in significant increases in the laminar fine fiber population and reinnervation of the sacral parasympathetic nucleus. In a tracer study, where AAV-GFP was injected into the dorsal root ganglia of crushed roots, artemin treatment resulted in an the reappearance of GFP-filled afferents in the medial dorsal horn and of GFP-filled rostrocaudally oriented afferent cross-sections in the dorsal column, which we interpret as regeneration. To find out if sensorimotor functional improvements resulted from reafferentation of the dorsal spinal cord, we carried out urodynamic analysis of the bladder and EUS. Artemin treatment resulted in significant reductions in dysfunctional EUS electromyographic (EMG) activity, and normalization of bladder threshold volumes and residual volumes. To examine how artemin facilitates regeneration of primary afferents across the DREZ, we studied post-injury expression of CSPGs in the DREZ following artemin administration. Artemin had

no effect on the post-injury increase in the CSPGs neurocan or NG2 in the DREZ. However, there was a delay in the post injury increase in phosphacan in the DREZ in the artemin treatment group. There was a rightward shift in the expression profile of phosphacan in the DREZ as a result of artemin treatment. This data accompanied by recent work reporting the influence of artemin on neuronal RhoA activity suggests that artemin encourages regeneration across the DREZ by ramping up the intrinsic regenerative capacity of injured afferents to overcome the inhibitory barrier rather than breaking the barrier down.

TABLE OF CONTENTS

LIST OF TABLES

LIST OF ABBREVIATIONS

AAV-GFP:	Adeno-Associated Viral Vector-Green Fluorescent Protein
ANOVA:	Analysis of Variance
ARTN:	Artemin
BBB:	Blood Brain Barrier
BMPs:	Bone Morphogenic Proteins
Cdc42:	Cell Division Control Protein 42
CFL:	Complete Freund's Adjuvant
CGRP:	Calcitonin Gene Related Peptide
CNS:	Central Nervous System
CS:	Chondroitin Sulfate
CSPG:	Chondroitin Sulfate Proteoglycan
ΔP:	Pressure Change
ΔV:	Volume Change
DC:	Dorsal Column
DCM:	Dorsal Commissure
DH:	Dorsal Horn
DRC:	Dorsal Root Crush
DREZ:	Dorsal Root Entry Zone
ECM:	Extracellular Matrix
EMG:	Electromyography
Ephs:	Ephrins
EUS:	External Urethral Sphincter
GAG:	Glycosaminoglycan
GDNF:	Glial Derived Neurotrophic Factor
GFAP:	Glial Fibrillary Acidic Protein

GFRα:	GDNF Family Receptor-α
GFLs:	GDNF Family Ligands
GPI:	Glycosyl-Phosphatidylinositol
GTPase:	Guanosine triphosphatase
IB4:	Isolectin subunit B4
ICI:	Inter-Contraction Interval
IVP:	Intravesical Pressure
L6:	Lumbar 6
LAR:	Leucocyte Antigen-Related
LCP:	Lateral Collateral Pathway
LPS:	Lipopolysaccharide
LT:	Lissauer's Tract
MAG:	Myelin Associated Glycoprotein
MCP:	Medial Collateral Pathway
mRNA:	Messenger Ribonucleic Acid
NgR:	Nogo Receptor
NT3:	Neurotrophin 3
NTN:	Neurturin
OMgp:	Oligodendrocyte Myelin Glycoprotein
PNS:	Peripheral Nervous System
PSP:	Persephin
PTP:	Protein Tyrosine Phosphatase
RARβ2:	Retinoic Acid Receptor β2
RPTPβ:	Receptor Protein Tyrosine Phosphatase β
S1:	Sacral 1
SCG:	Superior Cervical Ganglion
SCI:	Spinal Cord Injury
SEM:	Standard Error of the Mean
Sema:	Semaphorin
SPN:	Sacral Parasympathetic Nucleus
T13:	Thoracic 13
TGFβ:	Transforming Growth Factor
TRPV1:	Transient Receptor Potential Vanilloid type 1
VGLUT1:	Vesicular Glutamate Transporter 1

CHAPTER 1: INTRODUCTION

SPINAL CORD AND CAUDA EQUINA INJURY

In the United States alone there are an estimated 12,000 new cases of spinal cord injury (SCI) a year, with approximately 250,000 individuals living with an injury. The majority of SCIs result in permanent loss of muscle function and physical sensation below the area of injury, significantly reducing the quality of life and lowering the life expectancy of the individual. Currently, there is no clinical treatment to regenerate the severed or degenerated axons of an injured spinal cord, only ways to prevent further damage from occurring. Furthermore, with medical expenses and patient care costing between $200,000 and $700,000 in the first year and up to $3 million in a lifetime, SCI can be a financial hardship on both the individual and his or her family (Jackson, 2008).

Injuries to the thoracolumbar junction (T11-L2) and lumbosacral spine together account for 23% of all spinal injuries (Fife and Kraus 1986). The unique anatomy of the thoracolumbar junction and lower lumbar vertebrae make this region the second most injured part of the spine (Meyer *et al.* 1991). The upper thoracic spine, held rigid by the ribs, transitions to a lumbar region where intervertebral discs are thicker and the lumbar body articulating facets orient in such a way as to allow increased flexion, extension and lateral bending of the spine. The susceptibility of the weakly supported T11-L2 and lumbar spine to injury is due to isolation between the rigidly supported thoracic and fused sacral vertebrae. The end of the spinal cord, the conus medullaris, is located at the L1 level from where nerve roots extend caudally as the cauda equina. Lesions of the cauda

1

equina are mainly due to compression. Common etiologies of cauda equina compression are herniations of intervertebral discs (Nielsen *et al.* 1980, Hellstrom *et al.* 1986, Kennedy *et al.* 1999), fractures of the spine (Pavlakis *et al.* 1983) and iatrogenic lesions during intervertebral disc surgery (Hellstrom *et al.* 1986). Injury to the cauda equina results in damage to the roots innervating the lower urinary tract and in loss of below level segmental reflexes and muscular atrophy including external sphincters, causing impaired urethral closure and inability to initiate micturition (Pavlakis *et al.* 1983; Fowler *et al.* 1984; Beric and Light, 1992; Hoang and Havton 2006).

It should be remembered that the spinal roots are part of the peripheral nervous system as opposed to the spinal cord and thus exhibit regeneration following injury. The neuronal somata from which sensory axons emanate are situated in the dorsal root ganglia (DRG), which are located just outside the spinal column. One branch of a DRG neuron travels centrally into the spinal cord and the other travels peripherally. Thus, a root injury within the spinal canal damages the central branch of primary afferent neurons whereas peripheral injury damages the peripheral branch. It is well known that axotomized motor efferent nerves, including somatic and preganglionic autonomic nerves, can re-establish connection by allowing the surviving neurons to regrow along their original tracts, frequently resulting in restoration of function (Carlstedt 2000). By contrast, the sensory axon must grow back into the spinal cord in order to restore function. This however does not happen in the adult mammal due to the presence of axonal growth inhibitors at the PNS-CNS (Peripheral nervous system-Central nervous

system) barrier in the DREZ (Dorsal root entry zone), a fact that was established and first described in the early twentieth century (Ramon y Cajal 1928). Thus, since motor neurons have an intrinsic capacity to regenerate and reform lost connections and sensory neurons do not, we will concentrate on isolating the sensory aspect using a model of cauda equina injury affecting the central branches of DRG neurons that innervate the bladder. However, to place the model in context it is important to understand bladder function, dysfunction, innervation and response after injury. These issues are discussed in the following sections.

LOSS OF BLADDER FUNCTION AFTER SPINAL CORD INJURY

Research in the field of spinal cord injury (SCI) is largely focused on attempts to improve the functional recovery of locomotion and skilled motor tasks. Few studies focus on areas of research that would be of greatest immediate benefit to the SCI population. When the SCI population was surveyed, the recovery of bladder, bowel and sexual function was listed as a far greater concern that ranked above locomotion as having greater potential impact on quality of life (Anderson 2004). In another study, neuropathic pain is listed as the most common non-locomotor topic, followed closely by bladder function (Rosenzweig and McDonald 2004).

Renal failure as a result of neurogenic bladder dysfunction is one of the leading causes of death amongst SCI people (National Spinal Cord Injury Statistical Center). SCI results in functional impairment of the urinary tract, including bladder areflexia that leads to initial urinary retention followed by bladder hyperreflexia and detrusor-sphincter

3

dyssynergia (Blaivas *et al.* 1981, Kaplan *et al.* 1991). Nerve root trauma resulting from lumbar disc herniation (LDH), lumbar spinal stenosis (LSS) and any injury that results in narrowing of the spinal canal or intervertebral foraminae is known to result in urologic dysfunction (Cheek *et al.* 1973, Jones and Moore 1973, Mosdal *et al.* 1979, Susset *et al.* 1982, Kostuik *et al.* 1986, Bodner *et al.* 1990, Deen *et al.* 1994). A dysfunctional lower urinary tract is accompanied by high intravesical pressures resulting in life threatening complications such as hydronephrosis, renal calculi, bladder calculi and vesiculourethral reflux (Yoshiyama *et al.* 1999, Benevento & Sipski 2002), as well as producing detrusor muscle hypertrophy, incontinence and recurrent urinary tract infections (Kruse *et al.* 1993, de Groat 1995). Thus research that leads to understanding mechanisms that contribute to improved bladder function after SCI is critically important.

ANATOMY OF THE LOWER URINARY TRACT

The lower urinary tract consists of the urinary bladder, urethra and associated sphincters (Fig 1.1). Upper urinary tract refers to the kidneys and ureters. The bladder can be anatomically divided into two main components: the bladder body, located above the ureteral orifice, and the bladder base, consisting of the anterior bladder wall and trigone, the specialized area with both uretro-vesical junctions and the urethral opening forming its triangulation points.

The bladder wall has three distinct layers: the urothelium lines the intravesical space, surrounding this is the lamina propria layer and then the outermost smooth muscle layer called the muscularis. The urothelium, historically viewed as merely a passive

4

barrier, is known to have specialized sensory and signaling properties that allow it to respond to chemical and mechanical stimuli and to engage in reciprocal chemical communication with neuronal ending lying beneath (Apodaca 2004). These properties
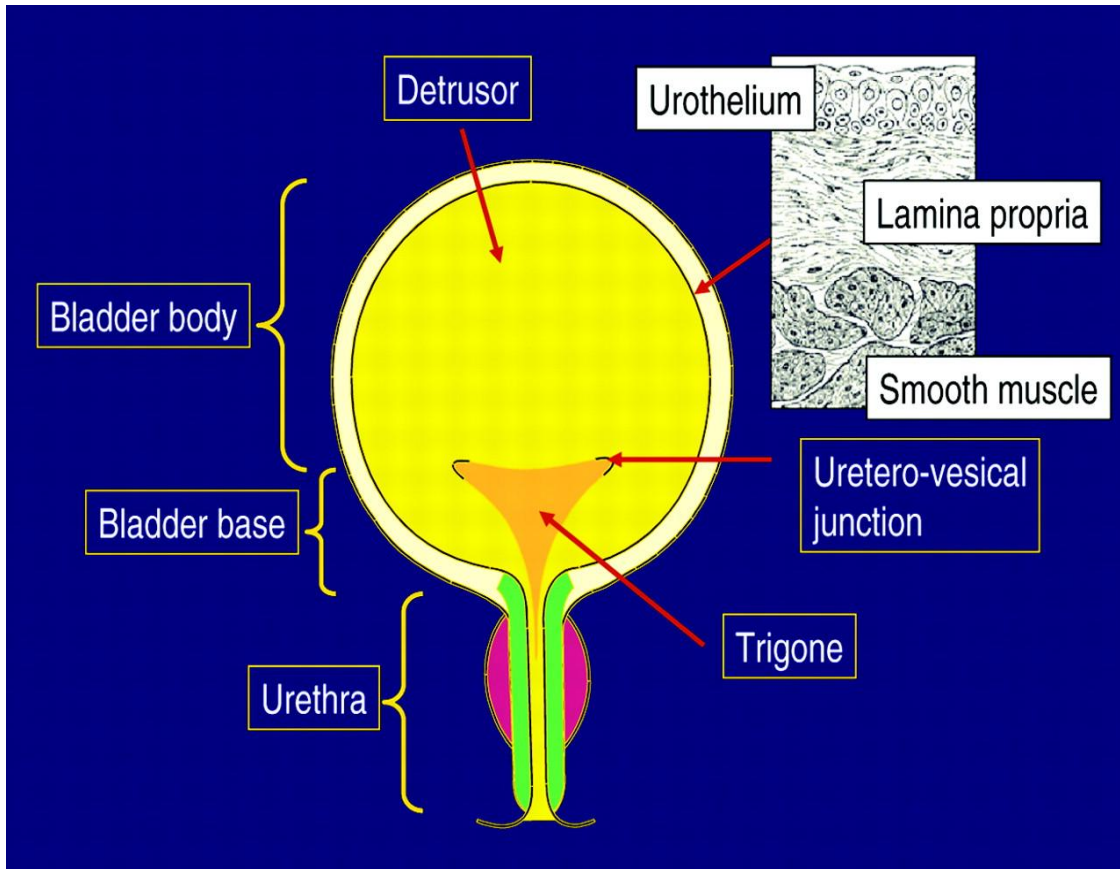
Figure 1.1 Anatomy of the lower urinary tract and bladder wall.
 (Modified from Andersson & Arner 2004)

include the expression of nicotinic, muscarinic, tachykinin, adrenergic, bradykinin and vanilloid receptors (Birder *et al.* 2002a,b, Beckel *et al.* 2006, Hanna-Mitchell *et al.* 2007); responsiveness to transmitters (neuropeptides) released by afferent nerves (Birder *et al* 2002a.); close physical association with afferent nerve endings; and the ability to

5

release chemical mediators such as ATP, acetylcholine and nitric oxide, which can regulate the activity of adjacent nerves that trigger local vascular changes or reflex bladder contractions (Ferguson *et al.* 1997, Andersson 2002). The lamina propria contains a dense layer of interwoven collagen fibers that provide structural strength and prevent bladder over distension (Murakumo *et al.* 1995). The muscular layer is formed of highly innervated smooth muscle cells, which comprise the detrusor muscle. Three layers of smooth muscle have been described (Gabella and Uvelius 1990). The inner and outer layers are oriented longitudinally and the middle layer is circular.

INNERVATION OF THE LOWER URINARY TRACT

The storage and periodic elimination of urine requires a complex neural control system that coordinates the activities of a variety of effector organs including the smooth muscle of the urinary bladder and the smooth and striated muscle of the urethral sphincters (Kuru 1965, Kluck 1980, de Groat 1993).

PERIPHERAL INNERVATION OF THE LOWER URINARY TRACT

Three neural pathways regulate the lower urinary tract (Fig 1.2): 1) the parasympathetic neurons of the pelvic nerve provide excitatory input to the bladder; 2) the sympathetics of the hypogastric nerve provide an inhibitory input to the bladder and an excitatory input to the bladder neck and urethra; and 3) the somatic neurons of the pudendal nerve innervate the striated muscle of the sphincter (De Groat and Steers 1990, Middleton and Keast 2004).
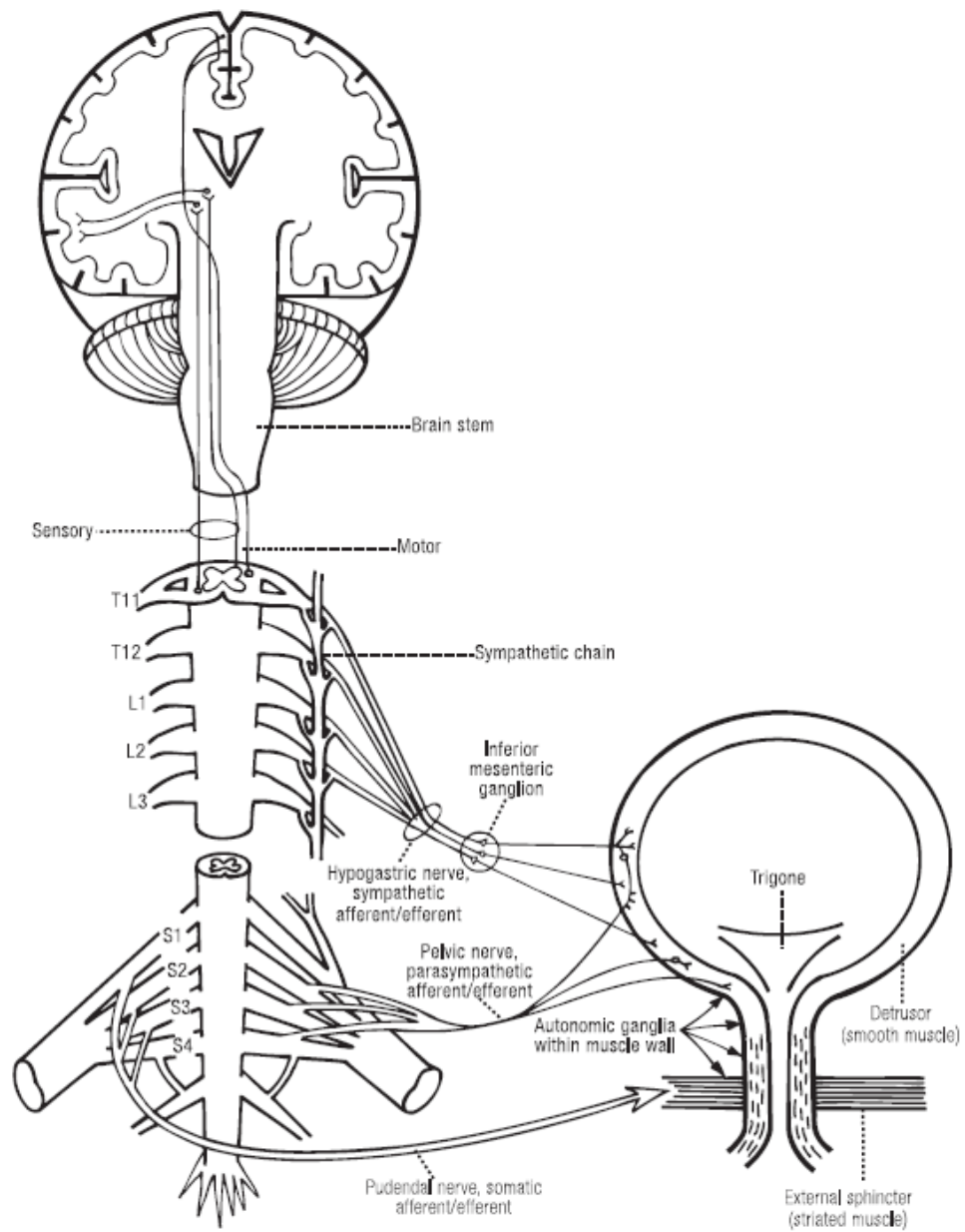
Figure 1.2 Sympathetic, parasympathetic and somatic innervation of the human lower urinary tract. (Modified from Fernandez 2002).

EFFERENT INNERVATION: HYPOGASTRIC NERVE (SYMPATHETIC)

The hypogastric nerves arise from the ventral roots of the 2nd to 4th or 5th lumbar segments in humans and T11-L2 in the rat (Hulsebosch and Coggeshall 1982, Baron and Janig 1991). These preganglionic fibers end partly in the inferior mesenteric plexus. Others continue without synapsing through the hypogastric nerves to reach the vesical plexus in the bladder wall (Moseley 1936). Post ganglionic fibers, originating in the inferior mesenteric plexus, also join the pelvic nerves and reach the bladder musculature, in addition to the very short postganglionic fibers of the vesical plexus (Gruber 1933). Roughly 83% of all sympathetic innervation to the bladder arises from the sympathetic chain ganglia with approximately half of these fibers carried by the pelvic nerve in the rat (Hulsebosch and Coggeshall 1982, Vera and Nadelhaft 1992). Sympathetic postganglionic nerves release norepinephrine, which activates β-adrenergic inhibitory receptors in the detrusor muscle and vesical plexus to relax the bladder, and α-adrenergic excitatory receptors in the urethra and bladder neck to contract the bladder outlet (De Groat and Booth 1993, Andersson and Arner 2004). Much early provided evidence that activity of the hypogastric nerve is inhibitory and responsible for urine storage and maintaining continence. The response to stimulation of the hypogastric nerves varies from species to species (Ingersoll and Jones 1958). In the cat, stimulation causes relaxation of the bladder (Elliott 1907) and also induces closure of the bladder neck and sphincter (Flood *et al.* 1990). Hypogastric nerve section caused relaxation of the ureteric orifices, trigone and internal sphincter of the bladder and dilation of blood vessels (Bucy *et al.* 1937, Voris and Landes 1940).

The parasympathetic outflow originates in the sacral parasympathetic nucleus (SPN) in the intermediolateral cell column of the spinal segments S2 to S4 in humans and L6 to S1 in rats (de Groat 1993). Preganglionic neurons send their fibres through the ventral spinal nerves to form part of the pelvic nerves that synapse with postganglionic neurons in the pelvic plexus or on ganglia on the bladder surface (vesical ganglia) or ganglia within the bladder and urethral walls (de Groat 1976). Parasympathetic postganglionics release acetylcholine as the major excitatory transmitter in the bladder (Andersson and Arner 2004). Acetylcholine release results in detrusor contraction mediated principally by the M_3 muscarinic receptor, although bladder smooth muscle also expresses M_2 receptors (Matsui *et al.* 2002). Muscarinic receptors are also present on parasympathetic nerve terminals at the neuromuscular junction and in the parasympathetic ganglia (Somogyi *et al.* 1998). Activation of these receptors on the nerve terminals can enhance (via M_1 receptors) or suppress (via M_4 receptors) transmitter release, depending on the intensity of neuronal firing. Various investigative paradigms have been used over the decades to investigate the functional input the pelvic nerve has on the bladder. In dogs and cats, section of the pelvic nerve resulted in retention of urine with overflow. The animals continued to pass small quantities of urine reflexively, and the bladder contained a large amount of residual urine (Barrington 1941, Fowler 1999) and its muscle was hypertrophied (Langworthy and Kolb 1933, Carpenter 1951). Pelvic nerve stimulation induces bladder contraction (Sato *et al.* 1989).

EFFERENT INNERVATION: PUDENDAL NERVE (SOMATIC)

Pudendal motor neurons that originate in Onuf's nucleus and innervate the EUS exit the spinal cord through the S2-S4 ventral roots in humans and the L6 and S1 ventral roots in the rat (Nadelhaft and Vera 1996). The somatic innervation of the pudendal nerve provides conscious control of the lower urinary tract and pelvic floor muscles.

AFFERENT INNERVATION

Sensations of bladder fullness are conveyed to the spinal cord by the pelvic and hypogastric nerves, whereas sensory input from the bladder neck and urethra is carried by the pudendal and hypogastric nerves. The response to passive distention and active contractions of the bladder was monitored by recording from the hypogastric, pelvic and pudendal nerves (Talaat 1937). In this study, several groups of sensory ending were found. One group made up of endings in the bladder wall adapted quickly to the stimulus and responded to rapid changes in bladder content or contraction of the detrusor muscle. Other endings in this group responded to a rise in intravesical pressure and adapted slowly to the stimulus. Action potentials from single fibers of the pelvic plexus were also recorded (Iggo 1955). No discharge occurred with an empty bladder. During bladder filling an increased frequency of impulses was observed. Because passive distension and active contraction were effective in exciting receptors in the bladder only when occurring simultaneously but not separately, it was concluded that these receptors were tension receptors arranged in series with muscle fibers (Iggo 1955). There are, however, at least two types of tension receptors which are concerned with micturition (Talaat 1937); one which accommodated rapidly and responds to changes in bladder content and contraction,

the other accommodates slowly and is briefly excited by a rise in bladder pressure. The urothelium of the bladder greatly changes its configuration with different vesicle volumes and it is likely, therefore, that the receptors concerned with these responses are situated in the urothelium and in the suburothelium.

A dense network of sensory nerves has been identified in the suburothelium layer of the urinary bladder (Gosling and Dixon 1974, Gabella 1995), with some terminals projecting into the urothelium (Birder *et al.* 2001, Wiseman *et al.* 2002). This suburothelial plexus is most prominent in the bladder base and neck and is critical for sensory function in the urothelium (Gabella and Davis 1998). Afferent fibers are seen to terminate as Pacinian corpuscles or contact with other encapsulated ending in the submucosa and the smooth muscle layer of the urethra. The majority of encapsulated ending appear to have some connection with the responses observed with passive distention and active contraction of the bladder (Bors and Blinn 1957).

Two main types of mechanisms have been demonstrated to operate during mechanotransduction in afferent systems: 1) an indirect, chemical transduction mechanism, which relies on activation of afferents by mediators being released from non-neuronal cells bymechanical stimulation, and 2) a direct, physical transduction, which is due to mechano-gated ion channels in the afferent endings, without involvement of extracellular mediators (Burnstock 2001). Upon bladder wall distension, ATP is release by urothelial cells (Ferguson *et al.* 1997, Andersson 2002) and P2 purinergic receptor-expressing mechanosensitive afferents fire (Cockayne *et al.* 2000, Rong *et al.* 2002). It is

11

also believed that mechano-gated channels of the TRP family are responsible for transduction of mechanical stimuli (Hamill and McBride 1996).

The primary afferents involved in sensory function consist of myelinated Aδ- and unmyelinated C-fibers. The Aδ-fibers respond to passive distension and active contraction (Janig and Morrison 1986) and thus convey information about bladder filling. The C-fibers are insensitive to bladder filling under physiological conditions (termed 'silent' C-fibers) and respond primarily to noxious chemical irritation (Habler *et al.* 1990) or cold (Fall *et al.* 1990). Most of the pelvic nerve afferents are mechanoreceptive and the vast majority of hypogastric nerve afferents are nociceptive (Sengupta and Gebhart 1994, Wen and Morrison 1995).

Afferents from the bladder project to specific regions of the spinal cord dorsal horn (Fig 1.3) in a cytoarchitecturally unique pattern (Morgan *et al.* 1981, Steers *et al.* 1991). Pelvic nerve afferents enter the spinal cord through Lissauer's tract and travel rostrocaudally giving off collaterals that terminate in the superficial laminae of the dorsal horn (laminae I and II) (Nadelhaft and Booth 1984). Bladder afferents follow two pathways to reach deeper laminae of the dorsal horn. The most prominent pathway is the lateral collateral pathway (LCP) which extends from Lissauer's tract running laterally until it reaches the SPN in the lateral edge of lamina V (de Groat 2006). The second and less prominent pathway runs medially (medial collateral pathway; MCP) from Lissauer's tract to the dorsal commissure (DCM) in lamina X (Steers *et al*. 1991). Pudendal

12

afferents from the urethra and sphincter exhibit a similar pattern of termination (Thor *et al.* 1989). The overlap between bladder and urethral afferents in the lateral dorsal horn and dorsal commissure indicates that these regions are probably important sites of viscerosomatic integration that might be involved in coordinating bladder and sphincter reflex activity.
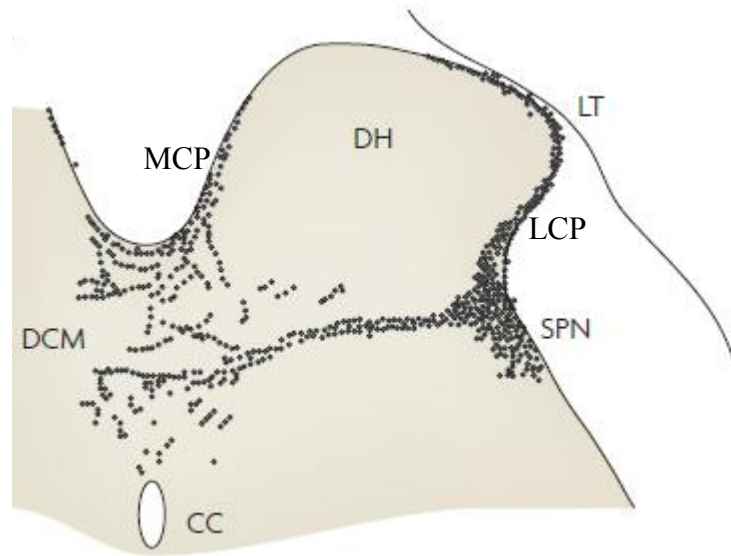
Figure 1.3 Central projection territory of bladder primary afferents.
LT: Lissauer's Tract; DH: Dorsal Horn; MCP: medial Collateral Pathway; LCP: Lateral Collateral Pathway; DCM: Dorsal Commisure; SPN: Sacral Parasympathetic nucleus; CC: Cental Canal. (Modified from Fowler *et al.* 2008).

REFLEX MICTURITION

The storage and voiding of urine is a far more complex process than it may first appear, involving the integration of a number of reflexive components. Studies of reflex micturition by Barrington revealed numerous reflexive components, discussed below. The following reflexes are responsible for continence being maintained and voiding proceeding to completion once initiated.

The Storage Reflex: Tension receptors in the bladder wall send information about the increase in bladder volume to the medulla through the pelvic nerves, the sacro-bulbar tract and the pelvic sensory vagus. These impulses excite the vesical relaxer center in the dorsomedial reticular formation in the medulla leading to inhibition of detrusor contractions so that the relaxation of the detrusor muscle continues in spite of bladder filling. The efferent connections for this reflex are in the ventral reticulospinal tract and pelvic nerves (Kuru *et al.* 1960).

The Continence Reflex: This reflex is also initiated by tension receptors in the bladder wall and prevents urine passing the sphincter. This reflex activity is detected as an increase in discharge frequency of the EUS in response to bladder filling (Garry *et al.* 1959). The afferent fibers are in the pelvic nerves and efferents in the pudendal nerves. The reflex center is hypothesized to be in the ventral horns of the 3rd and 4th sacral cord segments.

The Guarding Reflex: Increases in the contraction of the EUS occur after urine enters the proximal urethra and stimulates urethral stretch receptors. This reflex has afferent and efferent fibers in the pudendal nerves and central connections in the anterior horns of the 3rd and 5th sacral cord segments.

The Multiplication Reflex: The continuation of micturition once initiated depends on centers situated rostral to the medulla oblongata. Electrical stimulation of the pontine detrusor nucleus causes marked contraction of the bladder (Wang and Ranson 1939). This nucleus has bilateral connections with the bulbar vesical constrictor center and the

14

lateral horn of the lumbosacral cord which is the spinal vesicomotor center. Excitation of this nucleus can, therefore, result in the summation of the vesical constrictor effects, hence the use of the term 'multiplication reflex' (Kuru 1965).

The Bulbar Vesical and Relaxer Inhibiting Reflexes: These two closely related inhibitory reflexes result in reduced EUS activity and inhibition of bladder relaxation as a result of sustained detrusor contraction. An area which is concerned with the tone of the EUS is found in the lower pons close to the pontine detrusor nucleus and stimulation of this nucleus inhibits the activity of the EUS (Kuru *et al.* 1963). During the activity of the bulbar vesical detrusor reflex, the external sphincter is simultaneously relaxed. The continuation of vesical contraction during reflex micturition is dependent on the relaxer inhibiting reflex.

The Urethro-vesical and Urethro-sphincteric Reflexes: Feedback from the urethra helps to sustain detrusor contraction and EUS relaxation. Both irrigation of the urethra and distention of the proximal urethra are important in maintaining continuous micturition. Irrigation of the urethra is the more effective stimulus and afferents pass through the pudendal nerves whereas distention of the urethra, though less effective, has afferents in the hypogastric, pelvic and pudendal nerves. The transmission of afferent impulses from the urethra, bladder mucosa, sphincter and perineal muscles was thought to be entirely in the dorsal columns (Nathan 1956). Some reflexes which might be involved in the continuation of micturition have their centers in the spinal cord.

THE DORSAL ROOT ENTRY ZONE (DREZ): INTERFACE BETWEEN CNS AND PNS

THE DREZ AS A USEFUL MODEL OF CNS REGENERATION FAILURE

The DREZ can provide considerable insight into the success or failure of axon regeneration in relation to astrocytes made reactive by neurotrauma or lesion. In this context, the DREZ, as well as being of interest as a biological interface with distinctive and variable geometry, has proven to hold considerable potential for analyzing the problem of the failure of axonal regeneration into the CNS environment, which is of major significance for clinical neuroscience. Specifically, the response of the DREZ to dorsal root injury forms a useful model of these events.

At the DREZ the myelinating glia of the CNS (oligodendrocytes) and PNS (Schwann cells) come into contact. The principle supporting tissues are astrocytes centrally and endoneurium peripherally (Fraher and Kaar 1984). The superficial plasma membranes of the many astrocyte processes which form the surface of the CNS glia limitans are covered by a basal lamina that is continuous with the inner covering of the endoneurial tubes surrounding the nerve fibers of the PNS (Rossiter and Fraher 1990). Astrocyte processes within the CNS form a cone of tissue that extends distally into the root. Myelinated axons cross the DREZ singly, from the PNS into the CNS, swapping Schwann cell myelination peripherally for oligodendrocyte myelination centrally. Most unmyelinated axons cross the DREZ in unsegregated bundles at a less defined transition point due to the absence of a glial barrier (Fraher 1982, Doucette 1991).

During the degeneration sequence, the DREZ glial barrier does not break down. Nor do the Bands of Bungner formerly occupied by degenerated axons permit axon

16

regeneration in a central direction through them. On the contrary, the DREZ astrocyte processes proliferate, the cone of astrocytic outgrowth extends further into the peripheral territory of the dorsal root for a considerable distance (Liu *et al.* 2000) and contributes to a glial scar. If untreated, this gliotic interface inhibits regeneration and prevents the regenerating axons from growing into the CNS, by both physical and molecular means (Carlstedt *et al.* 1989, Bovolenta *et al.* 1992, Bovolenta *et al.* 1993). For example, astrocytes exhibiting reactive gliosis in response to neural injury, extend numerous filopodia that form intercellular gap junctions between adjacent astrocytes and juxtaposed filopodia from the same astrocyte. The filopodia result in a dense network that forms a physical impediment to growing neurites. In addition, the astrocytes secrete a variety of growth inhibitory molecules such as chondroitin sulfate proteoglycans that result in both a molecular and/or chemical barrier to neurite extension (Stichel and Muller 1998).

In using the DREZ as a model in which to study axon regeneration, the objective is to induce axons to grow from the PNS into the CNS through DREZ astrocytic tissue which is undergoing gliosis following dorsal root fiber interruption central to the ganglion. The DREZ model provides a broader understanding of axonal regeneration in the CNS in general since its response to root injury is almost identical to direct CNS lesion.

REGENERATION FAILURE IN THE CENTRAL NERVOUS SYSTEM
Axons fail to exhibit regeneration for long distances in the central nervous system (CNS) following injury (Ramon y Cajal 1928, Horner and Gage 2000); historically, this

was considered to be a property inherent to neurons of the CNS (Clark 1943). As in the PNS, central axons attempt to regrow following interruption, but the regenerative sprouts are largely unsuccessful (Carlstedt 1985b, Carlstedt 1985a, Carlstedt *et al.* 1988, Carlstedt 1997) with growth reported for 1mm but no further (Ramon y Cajal 1928). Furthermore, while limited neurite sprouting has been observed in the injured CNS (Liu and Chambers 1958), the growth cones quickly become dystrophic and are incapable of entering the lesion site (Misgeld and Kerschensteiner 2006, Misgeld *et al.* 2007). Given a favorable environment, an injured axon has the ability to regenerate and grow for significant distances (Richardson *et al.* 1980, David & Aguayo 1981). Success is readily achieved in immature animals (Carlstedt *et al.* 1987, Carlstedt 1988,), or by using embryonic material transplanted into the mature nervous system (Kozlova *et al.* 1995, Kozlova *et al.* 1997). Hence, it is now believed that regenerative failure is due to the extrinsic molecular environment at the site of injury (or in the case of a dorsal root injury, at the DREZ), rather than the intrinsic nature of the cells. In particular, there are several classes of molecules locally released at the dorsal root entry zone following dorsal root injury that are potentially inhibitory to neuronal regeneration.

There are two main sources of regenerative inhibition in the CNS: 1) central myelin and 2) activated glial cells. Berry (Berry 1982) suggested that central myelin proteins may act as major axon growth-inhibitory ligands . Several other factors contribute to this failure, however. This includes oligodendrocytes and myelin breakdown products (Caroni and Schwab 1988b, Caroni and Schwab 1988a, Schnell and Schwab

18

1990, Pindzola *et al.* 1993, Schwab 1996a, Schwab 1996b, Schwab and Brosamle 1997, Spillmann *et al.* 1997, Tatagiba *et al.* 1997, Guest *et al.* 1997,). Another important factor is the gliotic reaction. Astrocyte processes at the injury site or DREZ play a major role in this by contributing to scar formation.

MYELIN RELATED INHIBITORS

Neurite inhibition has been largely attributed to the release of several molecules from disrupted CNS myelin, commonly referred to as the myelin related inhibitors. These molecules include myelin-associated glycoprotein (MAG) (McKerracher *et al.* 1994, Mukhopadhyay *et al.* 1994, Filbin 1995), Nogo (Chen *et al.* 2000, GrandPre *et al.* 2000, Prinjha *et al.* 2000), and oligodendrocyte myelin glycoprotein (OMgp) (Kottis *et al.* 2002, Wang *et al.* 2002). All three bind to the same receptor, the Nogo-66 receptor (NgR). NgR is a glycosyl phosphatidylinositol-linked molecule, which signals via a partner, identified as the p75 low-affinity neurotrophin receptor. Subsequently, the Rho GTPase pathway is activated (Fournier *et al.* 2001, Domeniconi *et al.* 2002, Wang *et al*. 2002) which induces growth cone collapse (Mizuno *et al.* 2004).Thus, myelin associated inhibitors are promising therapeutic targets for promoting CNS regeneration. For example, *in vivo* neutralization of Nogo, using anti-Nogo antibodies (Bregman *et al.* 1995, Fouad *et al.* 2004) or NgR receptor antagonists (GrandPre *et al.* 2002), results in significantly improved axon sprouting in the corticospinal tract. However, little or no regeneration occurs in Nogo (Simonen *et al.* 2003), MAG (Bartsch *et al.* 1995), or NgR (Kim *et al.* 2004) knockout models (an OMgp KO does not exist), particularly in the

19

cortical spinal tract. For this reason, it is a generally accepted that although the myelin related inhibitors impede neurite outgrowth, they are not the key inhibitory components.

GLIAL SCAR AND RELATED INHIBITORS

Despite the effects of myelin related inhibitors on neurite outgrowth, the primary cause of regenerative failure is believed to be the formation of the highly inhibitory glial scar, which presents both biochemical and physical barriers. The glial scar reaction is the result of a multicellular response to injury involving astrocytes, microglia, macrophages, oligodendrocyte projenitors, fibroblasts, leptomeningial cells, and Schwann cells activated at different times and with diverse roles (Bunge *et al.* 1997, Fitch *et al.* 1999, Fawcett and Asher 1999, Dawson *et al.* 2000). Disruption of the blood brain barrier (BBB) and initial cell death following injury results in substantially increased levels of cytokines and growth factors in the area, activating astrocytes (reactive astrocytes) (Eng *et al.* 1987) and microglia (activated microglia) (Kreutzberg 1996). Consequently, production of the intermediate filament protein, glial fibrillary acidic protein (GFAP), is immediately upregulated in reactive astrocytes, causing the cells to become hypertrophic and extend filopodia, thereby generating a barrier that participates in the repair of the BBB, sequestering the injured area and protecting healthy tissue from damage (Bush *et al.* 1999, Faulkner *et al.* 2004). Unfortunately, this barrier is not permissive to axon growth, and, in turn, prevents functional recovery after injury. Hence, the glial scar acts as both a physical and chemical barrier to axonal regeneration; the dense meshwork of hypertrophic cells and the ECM proteins produced by these cells physically impede

20

growth cone migration (Windle and Chambers 1950). Among the inhibitory ECM molecules secreted by reactive astrocytes and activated microglia are the chondroitin sulfate proteoglycans (CSPGs) (Fawcett and Asher 1999), which generate a biochemical barrier to axonal regeneration (McKeon *et al.* 1991).

THE EXTRACELLULAR MATRIX AND CHONDROITIN SULFATE PROTEOGLYCANS

THE CNS EXTRACELLULAR MATRIX

Since the presence of an extracellular matrix (ECM) in the CNS was recognized (Tani and Ametani, 1971) the molecular composition has been a focus of research in mammalian systems. The ECM of the CNS has a relative scarcity of fibrous collagens and fibronectins (Rutka *et al.* 1988, Sanes 1989) and is rich in hyaluronan and chondroitin sulfate proteoglycans (CSPGs) (Margolis *et al.* 1975) resulting in a loose and relatively flexible meshwork. Proteoglycans of the hyalectan-family (named hyalectans because they are CSPGs that bind Hyaluronan) dominate this distinctive ECM along with their binding partners, hyaluronan, link proteins and tenascins (Ruoslahti 1996, Yamaguchi 2000, Bandtlow and Zimmermann 2000, Novak and Kaye 2000, Rauch 2004).

Hyaluronan, a simple glycosaminoglyacan (GAG), free of any core protein binding (Toole 2000) extends extracellularly, from the intracellular enzyme that assembles it, out into the pericellular space and becomes incorporated into the extracellular matrix (Spicer and Tien 2004). It is with this GAG that the members of the hyalectan family of proteoglycans bind and aggregate when secreted into the neural ECM

(Iozzo and Murdoch 1996, Bandtlow and Zimmermann 2000). Link proteins, known as hyaluronan and proteoglycan binding link proteins (HAPLNs), serve to reinforce bonds between hyaluronan and hyalectans (Spicer *et al.* 2003). Tenascins represent a fourth class of basic neural ECM constituents and this glycoprotein binds with all the hyalectans, phosphacan, NG2, many cell adhesion molecules and numerous other ECM and cell surface ligands (Jones and Jones 2000). When the individual components of the CNS ECM come together to aggregate, hyaluronan acts as the backbone, remaining fixed to the cell it was produced in. Large supramolecular complexes assemble into a dense cross-linking meshwork as hyalectans bind to hyaluronan and link proteins, and tenascins bind multiple CSPGs (including phosphacan and NG2) and cell surface molecules to one tenascin glycoprotein. Therefore, hyaluronan and tenascin are important as scaffold proteins to which secreted CSPGs bind during the formation of the inhibitory glial scar.

CHONDROITIN SULFATE PROTEOGLYCANS

CSPGs are ECM molecules with a varied and complex structural composition of both the transmembrane and secreted varieties. Both types have a central core protein covalently attached to chondroitin sulfate (CS) and glycosaminoglycan (GAG) side chains. The structure of CSPGs is diversified by variations in the core protein with the addition of N- and O-linked oligosaccharides; number, length, and sulfation patterns of CS GAG side chains; and proteolysis of translation products (Esko *et al.* 1999). The core proteins, known to carry mainly chondroitin sulfate GAGs, are hyalectans (brevican, neurocan, versican and aggrecan), NG2, phosphacan, appican, decorin, biglycan and

neuroglycan C (Bandtlow and Zimmermann 2000). The hyalectans along with phosphacan and apican are mainly secreted molecules, NG2 and neuroglycan C are transmembrane proteins, and decorin and biglycan are small ubiquitously expressed leucine-rich proteoglycans (Properzi and Fawcett 2004). In the present study we have concentrated on three of these CSPGs: the secreted hyalectan neurocan, phosphacan and the transmembrane NG2 (Fig 1.4). These three CSPGs were chosen because they have all demonstrated neurite growth inhibition, their expression is increased in the CNS following neurotrauma and they represent three distinctive subtypes of CSPG.
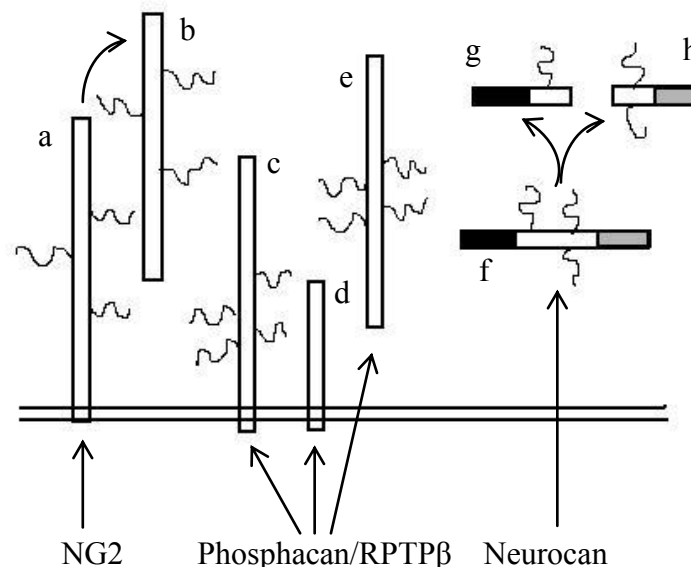
Figure 1.4 Chondroitin Sulfate Proteoglycan, soluble and membrane-bound forms.
A number of different CSPGs have been shown to be upregulated following CNS injury. NG2 (a) is synthesized as a transmembrane protein, but also exists in a soluble form (b) following proteolytic cleavage. RPTPβ (c) is another transmembrane CSPG. Its splice variant, the short receptor form (d), lacks the CS-binding domain and does not carry GAG sidechains, whilst a third splice variant produces a secreted CSPG, phosphacan (e). Neurocan (f) is a secreted hyalectan possessing a C-terminal lectin-like domain (black), an N-terminal hyaluronic acid binding region (gray) and an intervening region to which CS sidechains are attached. Neurocan can undergo proteolytic processing to produce neurocan-N_{130} (g) and neurocan-C (h).

23

NEUROCAN

Neurocan is so named because under non-pathological conditions it is primarily synthesized by neurons (Inatani *et al.* 2000). Neurocan is produced by GFAP-positive astrocytes in the CNS following injury (Haas *et al.* 1999, McKeon *et al.* 1999). It is a secreted molecule and undergoes posttranslational modification in the CNS, resulting in a 150 kD C-terminus and 130 kD N-terminus fragment (Matsui *et al.* 1994, Meyer-Puttlitz *et al.* 1995). Neurocan interacts with a cell surface glycosyltransferase (Li *et al.* 2000), a GPI-linked protein that modulates important cell adhesion molecules such as β1-integrin, N-cadherin, L1, and N-CAM (Friedlander *et al.* 1994), and may inhibit neurite outgrowth in vivo by disrupting growth cone cell-substrate cell adhesion molecule interactions (Grumet *et al.* 1993). Neurocan has axon-growth-inhibitory properties in vitro and is upregulated following CNS injury (Friedlander et al. 1994, McKeon et al. 1999). There is a very large increase in neurocan mRNA in the DREZ and a lesser but significant increase in the dorsal column following rhizotomy (Waselle *et al.* 2009).

PHOSPHACAN

The CSPG phosphacan is a secreted isoform of the receptor-type protein-tyrosine phosphatase β (RPTPβ) that lacks the intracellular and transmembrane domains (Maurel *et al.* 1994). Unlike the previously mentioned CSPGs, phosphacan does not bind to hyaluronan but instead just binds to tenascin-R and tenascin-C (Milev *et al.* 1997), and thus interacts *in vitro* with numerous cell adhesion molecules including N-CAM, Ng-CAM, TAG-1 and contactin (Peles *et al.* 1995, Milev *et al.* 1996). Phosphacan is expressed during the embryonic and postnatal period where it could, according to various

in vitro studies, play a role in the regulation of axon growth (Garwood *et al.* 1999), cell migration (Maeda & Noda 1998) and myelination (Harroch *et al.* 2000). Substantial overlap of phosphacan and O4-positive and O1-negative oligodendrocytes has been found (Faissner *et al.* 1994, Schnadelbach *et al.* 1998). Phosphacan and its splice variant RPTPβ are strongly expressed by oligodendrocyte precursors (Canoll *et al.* 1996). In the adult rat brain, phosphacan occurs in the circumference of a selected subpopulation of neurons which expressed the calcium binding protein, parvalbumin, occupying the extracellular space in close vicinity to the cell body, surrounding axon terminals and glial end feet, but not synaptic clefts i.e. perineuronal nets (Wintergerst *et al.* 1996). Phosphacan is inhibitory to axon growth in vitro (Milev *et al.* 1994) and is also found at the site of a CNS lesion (McKeon et al. 1999). Phosphacan mRNA does not increase in either the DREZ or DC following rhizotomy (Waselle et al. 2009).

NG2

NG2 has a primary structure unrelated to other CSPGs and is expressed by NG2-glia (Butt *et al.* 2002), which represent a fourth major population of glial cells distinct from astrocytes, oligodendrocytes and microglia. NG2-positive cells are also found in peripheral nerves, dorsal root ganglia (Rezajooi *et al.* 2004) and at nodes of Ranvier (Martin *et al.* 2001). Under pathological conditions, astrocytes have been reported to express NG2 (Hirsch and Bahr 1999). NG2 is produced as a cell surface molecule but becomes a soluble component of the ECM after cleavage from its transmembrane domain (Nishiyama *et al.* 1995). This CSPG is considered to be a major axon growth-inhibitory

25

molecule in the CNS (Dou and Levine 1994). Following SCI, NG2 is highly expressed by NG2-glia and macrophages (Jones *et al.* 2002). In the past, NG2-glia (or oligodendrocyte precursor cells, as they were all originally thought to be) were considered the primary source of NG2 expression in the CNS following injury (Dawson *et al*. 2000). However, recent work suggests that a considerable portion of this expression is from peripheral macrophages migrating to sites of gliosis, such as the DREZ following rhizotomy (Zhang *et al.* 2001, Bu *et al.* 2001). It has been reported that NG2 mRNA expression becomes upregulated in the DREZ and dorsal column rapidly following rhizotomy, peaking at 1 day post lesion (Waselle *et al.* 2009).

THE INTRACELLULAR MECHANISM MEDIATING NEURON-GLIA AND NEURON-ECM INTERACTIONS

Most axon growth-inhibitory ligands either repel or collapse growth cones via the Rho GTPase signaling pathway (Mueller, 1999; Tang, 2003) after binding to specific surface receptors, located on the axolemma. Axonal growth cones rely heavily on F-actin dynamics and microtubule assembly to drive growth and guidance. The Rho family of small GTPases regulates the actin cytoskeleton and most attention has been focused on the three most widely expressed family members, RhoA, Cdc42, and Rac1. In the injured CNS, inhibitory molecules change the balance of intracellular Rac1, Cdc42, and Rho signaling, so that the activity of RhoA is elevated and that of Rac1/Cdc42 decreased, leading to paralysis of growth cone mobility and induction of growth cone collapse/repulsion. Coupling of neurite-inhibitory molecule receptors to the Rho family of G-proteins is a common thread shared by Ephs, Nogo, MAG, OMgp and Sema to

induce growth cone collapse, and seems probable that this pathway is involved in CSPG signaling (Sandvig *et al.* 2004). Therefore, preventing the increase of intracellular RhoA in injured neurons will enhance their regenerative capacity by rendering them relatively unresponsive to the inhibitory extracellular environment. Among the neurotrophins which are capable to improving the intrinsic regenerative capacity of neurons is artemin.

ARTEMIN

Artemin [also known as neublastin (Rosenblad *et al.* 2000)] is one of four members of the Glial Cell Line-Derived Neurotrophic Factor (GDNF) family ligands (GFLs). GDNF, originally, isolated from the rat glial cell line B49 supernatant, was shown to promote the survival and differentiation of dopaminergic neurons in the midbrain (Lin *et al.* 1993). After the discovery of GDNF came the purification of neurturin, the cloning of persephin and most recently the purification of artemin (Kotzbauer *et al.* 1996, Milbrandt *et al.* 1998, Baloh *et al.* 1998). All four family members are distant members of the transforming growth factor-β (TGF-β) superfamily due to their seven conserved cysteine residues. Unlike other members in the TGF- β family (TGF- β s, BMPs, Activins, etc.) which signal through direct engagement of two different types of serine/threonine receptor kinases (Massague and Chen 2000), GFLs exert their activities through the nucleation of a tertiary complex containing a nonsignaling, ligand specific GFRα receptor and a signaling tyrosine kinase receptor RET (Durbec *et al.* 1996, Treanor *et al.* 1996, Trupp *et al.* 1996, Worby *et al.* 1996). All four GFLs naturally form homodimers and each binds with individual preference to one

of four glycosyl-phosphatidylinositol (GPI)-anchored co-receptors called the GDNF family receptor-α (GFRα). The protein-GFR-α complex then binds to and dimerizes the transmembrane receptor tyrosine kinase Ret that is found in lipid rafts (Saarma and Sariola, 1999, Takahashi 2001). Artemin preferentially binds to the co-receptor GFRα3, however it can also activate the GFRα1-Ret complex to which GDNF itself binds (Baloh *et al.* 1998).
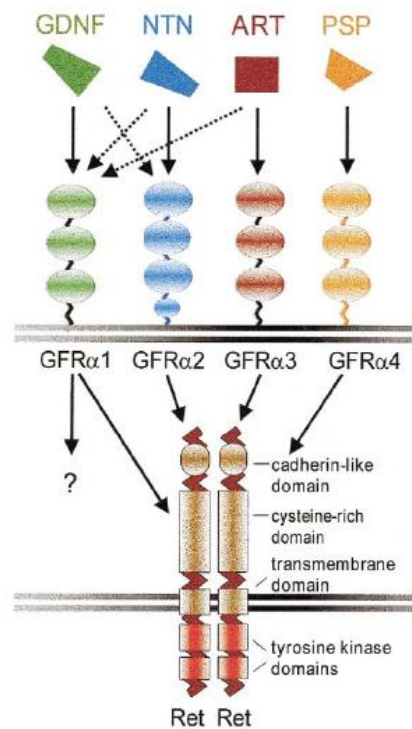
Figure 1.5 The components of RET signalling: GFLs, GFRαs and RET.
GFLs (GDNF, NRTN, ARTN and PSPN) each bind a specific coreceptor GFRα (GFRα1, GFRα2, GFRα3 and GFRα4) and activate the common signalling receptor RET (in light pink). The crosstalk between GFRα1 and other GFLs, apart from PSP, is shown (dotted arrows). GDNF: Glial derived neurotrophic factor; GFL: GDNF family of ligands; GFR: GDNF family receptors; ARTN: Artemin; NRTN: Neurturin; PSPN: Persephin. (Modified from Sariola and Saarma, 2003).

28

The GDNF family of proteins functions to guide the development, migration, outgrowth, and maintenance of a number of sensory and autonomic neurons. GFRα3 is expressed in embryonic superior cervical ganglion (SCG) neurons; therefore, artemin was thought to play a role in the development of sympathetic neurons (Luukko et al., 1998). Artemin's role as a survival factor for sensory and sympathetic neurons in culture suggested it could influence the same neurons *in vivo* (Baloh et al. 1998). Subsequent studies supported the idea that artemin, acting through GFRα3 and Ret, is involved in the rostral migration of SCG precursors. For example, the SCG of mice lacking artemin, Ret or GFRα3 are found caudal to their normal location and an artificial source of artemin induces their migration (Durbec et al. 1996, Nishino *et al.* 1999). Artemin is expressed in the smooth muscle of blood vessels and, along with its receptor complex, plays a role in the segmentation of cells into the individual ganglia of the sympathetic chain (Honma *et al.* 2002). Coupled with the fact that sympathetic axons grow preferentially toward artemin in vitro (Yan *et al.* 2003), it is suggested that artemin induces sympathetic axon outgrowth along blood vessels (Young *et al.* 2004). Artemin appears to act neurotropically (growth or migration attractant) during development but neurotrophically (promoting cell survival) in maturity (Carmeliet 2003).

In animal models of neurological diseases, neurotrophic factors usually only show therapeutic potential when delivered locally by surgical procedures. In clinical application, less invasive delivery through blood flow and cerebrospinal fluid was ineffective because of the poor bioavailability at target tissues due, in part, to poor BBB

penetration, low tissue diffusion, and short half-life (Pardridge 2002, Wu 2005, Bespalov and Saarma 2007). Moreover, administration of high-dose neurotrophic factors frequently led to adverse effects, because of their systemic, pleiotropic actions, and interference with normal brain functions. However, recent reports show artemin to be efficacious when delivered systemically (Wang *et al.* 2008, Gardell *et al.* 2003), perhaps due to its relative specificity for primary afferents neurons (Baloh et al. 1998). The fact that the artemin receptor, GFRα3, is almost exclusively expressed by primary afferent DRG neurons (Baloh *et al.* 1998) necessitates extra caution in assessing its unwanted side effects, particularly relating to hyperalgesia.

ARTEMIN'S ROLE IN INFLAMMATION AND HYPERALGESIA

Although neurotrophic factors were previously thought to be responsible only for the growth and maintenance of sensory neurons, it is now maintained that they play a significant role in inflammatory hyperalgesia (Shu and Mendell 1999). The levels of GFLs in the joint capsule and plasma of patients with osteoarthritis, Crohn's disease, and interstitial cystitis are greatly increased compared to control subjects (Okragly *et al.* 1999, von Boyen *et al.* 2004). Artificially induced inflammation by injection of complete Freund's adjuvant (CFA) or lipopolysaccharide (LPS) results in increased levels of the GFLs, GDNF, neurturin and artemin (Amaya *et al.* 2004, Hashimoto *et al.* 2005, Malin *et al.* 2006). There is a growing body of evidence that, through binding to and translocation of GFRα receptors, the above three GFLs play a role in the induction of hyperalgesia (Amaya et al. 2004, Malin et al. 2006, Vellani *et al.* 2006). Equally

important is evidence of significant overlap in expression of the GFRα1-3 receptors and the transient receptor potential vanilloid type 1 (TRPV1) receptor, a ligand-gated ion channel that is activated by noxious stimuli, including heat and acidic pH (Aoki *et al.* 2005, Malin *et al.* 2006). Schmutzler and colleagues (Schmutzler *et al.* 2009) demonstrated that all GFLs except persephin were capable of sensitizing the central terminals of sensory neurons through an interaction with TRPV1. These GFLs were able to produce an enhancement in the capsaicin-stimulated release of calcitonin gene related peptide (CGRP), not only in sensory neurons in culture but also in spinal cord slices. Recently it was suggested that the coincidental presence of artemin in dura mater vasculature, and GRFα3 in the afferents that innervate the dura, indicates a contribution to migraine pain (McIlvried *et al.* 2009). However, it was reported that systemic, intermittent administration of artemin produces dose- and time-related reversal of neuropathic pain behavior, together with a normalization of the morphological and neurochemical features of the injury state (Gardell *et al.* 2003).

SUMMARY AND EXPERIMENTAL DESIGN

The central hypothesis of this project is that recovery of normal sensory function in the bladder can be achieved by breaking down the regenerative barrier that exists at the dorsal root entry zone (DREZ) and encouraging reentry of regenerating afferent axons into the dorsal horn. Urinary retention due to bladder and external urethral sphincter (EUS) dysfunction is the most consistent finding after injury to the cauda equina and often leads to death due to infection. Whilst management of the symptoms of a

neurogenic bladder has improved over the past few decades through improved catheterization techniques, drug treatment and surgery, little has been done to address the "root" cause, namely neural damage. To remedy this, we propose a treatment to restore sensory innervation to the bladder using a newly developed model of cauda equina injury in which we have isolated and injured those dorsal roots in the rat that constitute the sensory innervation of urinary bladder.

Here we characterize a model of bladder dysfunction due to cauda equina injury, isolating the dorsal roots, using a recently developed technique that simultaneously records bladder pressure and external urethral sphincter electromyographic activity. We also describe the effects a dorsal root crush injury has on the primary afferent neuroarchitecture and chondroitin sulfate proteoglycan expression levels in the dorsal spinal cord. Finally, in this study we bring together these two experimental techniques to test the efficacy of systemically administered artemin in promoting regeneration of centrally directed primary afferents across the dorsal root entry zone and the restoration of lower urinary tract function. The results were obtained through the following experimental design.

Hypothesis 1: Cauda equina injury produces bladder dysfunction that can be measured in a rodent model.

Specific Aim 1: To record the functional outcome of a cauda equina injury on the bladder and EUS of the rat using cystometric and electromyographic recording techniques.

Experiment: Recordings of both intravesical pressure and electrical activity of the EUS will be performed on three groups: 1) animals with cauda equina injury, 2) animals that received sham surgery and 3) age matched naïve controls.

Hypothesis 2: Dorsal root crush injury results in permanent deafferentation of the spinal cord and the upregulation of chondroitin sulfate proteoglycan (CSPGs) expression in the DREZ coincides with this permanent loss.

Specific Aim 2.1: To determine the extent of loss of sensory innervation to the dorsal horn using immunocytochemical techniques to stain for calcitonin gene-related peptide (CGRP), isolectin B4 (IB4) and the vesicular glutamate transporter 1 (VGLUT1)

Experiment: Immunocytochemistry will be used to stain for CGRP, a marker for peptidergic primary afferents, IB4, a marker for unmyelinated primary afferents and VGLUT1, a marker for myelinated afferents to assess the loss of sensory innervation to the dorsal horn of animals given a dorsal root crush injury compared to control animals 3, 7, 14 and 30 days post-surgery.

Specific Aim 2.2. To determine the expression of the CSPGs neurocan, phosphacan and NG2 at the DREZ in injured, sham and naïve controls animals using immunocytochemical techniques.

Experiment: Immunocytochemistry will be used to stain for the CSPGs neurocan, phosphacan and NG2 at the L6 and S1 DREZ of injured animals and sham and naïve controls at 3, 7, 14 and 30 days post-surgery.

Hypothesis 3: Systemic administration of artemin promotes functional regeneration of sensory fibers across the dorsal root entry zone.

Specific Aim 3.1: To determine the level of functional recovery achieved by comparing injured artemin-treated animals, injured vehicle-treated animals, sham artemin-treated control animals and sham vehicle-treated control animals using cystometric and electromyographic recording. To test for the possible development of mechanical allodynia, the same groups will be testing using abdominal Von Frey stimulation.

Experiment: Cystometry and EMG recording will be carried out at 3, 7, 14 and 30 days post-surgery on four groups of animals. Group 1 will consist of injured animals treated with artemin, Group 2 will be a control group that has been injured but administered vehicle, Group 3 will have sham surgery and artemin-treated, Group 4 will have sham surgery and vehicle-treated. Mechanical sensitivity will be tested in all animals at 7 and 30 days post-surgery.

Specific Aim 3.2: To determine the extent of regeneration of primary afferent fibers across the PNS/CNS barrier in injured-artemin-treated animals, injured-vehicle-treated animals, sham artemin-treated control animals and sham vehicle-treated control animals using immunocytochemical techniques.

Experiment: Immunocytochemistry will be used to stain for CGRP, IB4 and VGLUT1 to assess the extent of regeneration of primary afferent fibers across the PNS/CNS barrier

34

in injured artemin-treated animals, injured vehicle-treated animals, sham artemin-treated control animals and sham vehicle-treated control animals at 3, 7, 14 and 30 days post-surgery.

   Specific Aim 3.3: To determine the extent of regeneration of sensory fibers from the bladder across the PNS/CNS barrier in injured-artemin-treated animals, injured-vehicle-treated animals, sham artemin-treated control animals and sham vehicle-treated control animals using antrograde tracing techniques after injection of AAV-GFP into the dorsal root ganglia.

<u>***Experiment:***</u> Antrograde tracing techniques will be used to determine the regenerative capacity of crushed primary afferents involved in bladder function after systemic administration of artemin.

   Specific Aim 3.4: To determine the expression of the CSPGs neurocan, phosphacan, brevican and NG2 at the DREZ in injured-artemin-treated animals, injured-vehicle-treated animals, sham and naïve controls using immunocytochemical techniques.

<u>***Experiment:***</u> Immunocytochemistry will be used to stain for the CSPGs neurocan, phosphacan and NG2 at the L6 and S1 DREZ of injured-artemin-treated animals, injured-vehicle-treated animals, sham artemin-treated control animals and sham vehicle-treated control animals at 3, 7, 14 and 30 days post-surgery.

CHAPTER 2: CHARACTERIZING LOWER URINARY TRACT DYSFUNCTION

INTRODUCTION

Research in the field of spinal cord injury (SCI) is largely focused on attempts to improve the functional recovery of locomotion and skilled motor tasks. Few studies focus on areas of research that would be of greatest immediate benefit to the SCI population. When the SCI population was surveyed, the recovery of bladder, bowel and sexual function was listed as a far greater concern, ranked above locomotion, as having greater potential impact on quality of life (Anderson, 2004). In another study, neuropathic pain is listed as the most common non-locomotor topic, followed closely by bladder function (Rosenzweig and McDonald, 2004). Injury to the thoracolumbar junction (T11-L2) and lumbosacral spine together account for 23% of all spinal injuries (Fife and Kraus, 1986). Since the end of the spinal cord, the conus medullaris, is located at vertebral level L1 in humans and the roots innervating the lower urinary tract make up part of the cauda equina, injuries at this level often result in bladder dysfunction. In addition, there is a loss of below level segmental reflexes and muscular atrophy including external urethral sphincter, causing impaired urethral closure and inability to initiate micturition (Pavlakis, *et al.* 1983, Fowler, *et al.* 1984, Beric and Light, 1992, Hoang and Havton, 2006). Thus, it is critical to develop models that permit study of bladder function recovery after spinal injuries.

A normal functioning lower urinary tract carries out two primary tasks: the storage of urine without leakage and the voluntary voiding of urine by the coordinated act

36

of micturition. Sensory feedback supplied by the dorsal roots, along with intact motor input via ventral roots are vital for normal function. Parasympathetic afferents that course through the pelvic nerve from the bladder musculature and urothelium to the lumbosacral cord of the rat relay information essential for passive filling of the bladder and initiation of the micturition reflex (De Groat and Lalley, 1972, de Groat and Theobald, 1976, Yoshimura, et al., 1998). Consequently, injury to spinal dorsal roots often results in irreversible sensory and parasympathetic deficits (Al-Qattan, 2003, Qiu, et al., 2005) due to regenerative failure at the dorsal root entry zone (Liuzzi and Lasek, 1987). Disrupting normal afferent function is known to contribute to the development of an overactive bladder with reduced continence and compliance (de Groat, 1997, Wein, 2005). The effects of ventral root injury alone on bladder function (Hoang, et al., 2006, Hoang, et al., 2006) and on methods of surgical repair (Carlstedt *et al.* 1986, Hallin *et al.* 1999, Gu *et al.* 2004, Hoang *et al.* 2006) have been described; whereas deafferentation and its impact on bladder function remains understudied.

A direct test of sensory decentralization that eliminates the afferent arms of the urogenital reflex arc and its influence on urine storage and micturition in anaesthetized animals is lacking. Thus, to examine the effects of injury to the dorsal roots on acute and long-term bladder function, we tested for functional changes in the lower urinary tract (LUT) using urodynamic analysis following bilateral L6 and S1 dorsal root crush (DRC) injury. The bladders of subjects were weighed and measured to assess any resulting morphological changes. We report that a bilateral dorsal root crush injury (DRC)

37

significantly interrupted normal EUS function, resulted in shorter intercontraction intervals (IVIs), lower compliance, greater threshold volumes and larger residual volumes relative to sham controls. Electromyographic (EMG) activity in the EUS was also adversely affected. DRC animals showed a reduction in the frequency of high amplitude voiding bursts and the average amplitude of filling phase EMG activity is significantly increased to voiding phase levels. DRC also had a major impact on the physical properties of the bladder itself. Bladder weight increased significantly 7 days post-surgery. However at later time points bladder weight was not significantly greater in DRC animals compared to sham but capacity was significantly larger indicating over distension.

MATERIALS AND METHODS

EXPERIMENTAL DESIGN

Two experimental groups were examined: a sham surgical group (n=20) and bilateral dorsal root crush (DRC) injury group (n=20). At 3, 7, 14 and 30 days post-surgery 5 animals from each group were tested for urodynamic function and the bladder and spinal cord tissue was harvested. To monitor their health and to assess the impact of the surgery, animals were weighed prior to surgery and at each time point (Fig. 1). Both DRC and sham surgery resulted in very significant weight loss. Sham animals reached their lowest weight two days after surgery and DRC animals continued to drop weight until 7 days after surgery, after which they slowly recovered to just above pre-surgical

weight by 28 days. Female rats were used to allow for ease of insertion of the urethral catheter and recording electrodes.

SURGERY

Female Sprague-Dawley rats, 225-250g, (Harlan Sprague-Dawley, Inc.) were housed with a light/dark cycle of 16h/8h. Rats were deeply anesthetized by intraperitoneal injection of sodium pentobarbital (0.5mg/kg) as determined by the absence of the paw withdrawal reflex to pinch and the absence of the corneal blink reflex. The dorsum was shaved, a midline incision was made, the dorsal musculature was retracted and a laminectomy performed for vertebra L1 and L2. The L1 and L2 vertebrae were identified by counting 6 and 5 vertebrae rostrally from the first sacral verterbra, respectively. The first sacral vertebra was identified due to its lack of articulation with the vertebra immediate caudal to it. This method of vertebral identification was employed for each sham and injury surgery in order to ensure consistency. For bilateral dorsal root crush injury, the dura was opened, the dorsal surface of the spinal cord was exposed and L6 and S1 dorsal roots were crushed by inserting one arm of a fine forceps underneath each root and compressing it twice for 10 seconds. The crush was given 5 mm from the dorsal root entry zone and deemed successful when the opaque root turned transparent across its entire width at the site of compression. The musculature and fascia were then closed with 3-0 silk suture, followed by closure of the skin. For a control group, sham surgery was done in the same way as the injury surgery with the exception that the dorsal

roots were not crushed. All surgeries and experiments were in compliance with the Institutional Animal Care and Use Committee.

URODYNAMIC RECORDING

Lower urinary tract function was assessed using a non-surgical urodynamic procedure that allowed rapid collection of simultaneous bladder pressure and sphincter electromyography (EMG) data over a number of consecutive voiding cycles. In preparation for bladder cystometry and sphincter EMG recordings animals were anesthetized by intraperitoneal injection of sodium pentobarbital and placed in a supine position. A catheter (PE-50, ~10cm) was inserted into the intravesical space of the bladder through the urethra. Accurate insertion depth was ensured by first making a black mark 2.5cm from the end of the catheter, the catheter was inserted to the mark and then secured to the animals' tail to prevent catheter displacement. Two, fine Teflon coated platinum-iridium wire electrodes (0.002'' stripped, 0.0045'' coated, A-M Systems Inc., Carlsborg, WA) were then placed percutaneously into the muscle of the external urethral sphincter (EUS) along the side of the catheter using a 30 gauge needle as an insertion cannula. In detail, the electrodes were threaded through a 30 gauge needle and hooked at the stripped end forming an insertion assembly. Two assemblies were inserted along either side of the urethral catheter until the muscular resistance of the EUS was encountered and the assemblies were advanced a few more millimeters into the muscle. The needle cannula for each assembly was withdrawn leaving only the hooked wire electrode embedded internally within the EUS musculature. The animals were then

40

restrained and allowed to recover 3 to 4 hrs from the anesthetic. The animals were fully awake, responding to auditory stimulus and the eye blink and foot pinch test. To ensure each recording session began with an empty bladder, each bladder was emptied by manual expression before connecting the catheter to the infusion pump, allowing urine to flow out through the catheter. Bladder intravesical pressure (IVP) was recorded by infusing warm saline (0.22 mL/min) through the catheter and into the bladder using an infusion pump (Harvard Apparatus, Holliston, MA). During the bladder detrusor contractions, fluid is released by flowing around the catheter in the urethra. The signal from the attached pressure transducer (Biopac Systems Inc., Goleta, CA) in the form of resistance to the flow of saline through the catheter, is amplified and sampled using an analogue-to-digital converter (Biopac Systems Inc., Goleta, CA) and acquired on a computer using Acq*Knowledge*® Software (Biopac Systems Inc., Goleta, CA). The EMG activity recorded from the urethral sphincter electrodes was amplified using a separate amplifier attached to the same analogue-to-digital converter as above allowing for simultaneous acquisition of EMG and intravesical pressure (Fig 2).

Before beginning a recording session and connecting the catheter to the infusion pump tubing, the rat's bladder was manually expressed. The bladder was deemed empty when urine stopped flowing from the catheter. Recordings were carried out on the awake, restrained animal over maximum period of 20 minutes at 3, 7, 14 and 30 days post-surgery. The animals did not have their bladders expressed manually at any time post

injury because they retain a limited ability to micturate and this would interfere with the development of post-injury changes to the bladder.

URODYNAMIC ANALYSIS

Data for a single micturition cycle was gathered at the beginning of each recording session by noting the volume of saline infused into the empty bladder to elicit the first voiding event (Threshold Volume). The volume of saline voided was collected, measured and subtracted from the infused volume to give the volume of saline remaining inside the bladder (Residual Volume). Voiding efficiency was calculated as the percentage of the infused volume that was successfully voided.

Recording sessions lasted 20 mins per animal. The inter-contraction interval (ICI) was calculated by averaging the length of time between the end of one bladder contraction and the beginning of the next for each 20 min period. Bladder compliance, which described the relationship between change in bladder volume and change in bladder pressure, was calculated using the equation $\Delta V/\Delta P$, where ΔV is the volume of saline infused into the bladder during each ICI and ΔP is the difference between the baseline pressure and the intravesical pressure (IVP) at the moment a contraction begins. A low $\Delta V/\Delta P$ value indicates poor compliance during which high IVPs were recorded at low volumes and in the absence of detrusor muscle activity (Fig 2b). Physiologically normal animals show compliance values closer to zero. To analyze sphincter EMG activity the waveform data was integrated by rectifying it to provide an interpretable waveform that can be easily compared between groups. The Acq*Knowledge* software

collects the absolute value of the input data prior to summing and a plot of the waveform's mean envelope over 20 samples was obtained. The average filling phase EMG amplitude is expressed as a percentage of the average voiding phase EMG amplitude. The frequency of the phasic bursts characteristic of the EUS of the rat was measured in Hz or bursts per second, during voiding phase of the micturition cycle.

PHYSICAL ANALYSIS OF THE BLADDER

At each of the afore mentioned time points 5 injured, sham and naïve subjects were overdosed with sodium pentobarbital (100 mg/kg) and transcardially perfused with 250 ml cold heparinized (1 ml/1 l) saline (0.9%). A lower abdominal incision was made and the bladder was dissected out, blotted dry and weighed.

STATISTICAL ANALYSIS

Quantitative data were expressed as mean ± SE. For bladder morphological analysis as well as urodynamics studies, a two way ANOVA test followed by the Tukey test (SPSS 14.0, SPSS Inc., Chicago, Illinios). Repeated measures ANOVAs were performed to test the weight change data over time post-surgery. In all cases the level of statistical significance was set at $p<0.05$.

RESULTS

POST-SURGERY BODY WEIGHT

Animals in the three groups, naïve, sham and DRC were weighed right before surgery (Day 0) and then 3, 7, 14 and 30 days after surgery. Pre-surgical weight for all three groups was normalized to a baseline of 0% ± 0. Any weight change was expressed as a percentage of their weight before surgery. Surgery, regardless of injury, resulted in a negative change in body weight. The sham group lost a maximum of 3.52% ± 0.7 on day 3 post-surgery and the DRC group lost a maximum of 6.26% ± 0.75 on day 7 post-surgery however, there was never any significant difference between the groups at any time point. Sham and DRC group weight changes were significantly less than the naïve on all four post-surgical days (Fig 2.1). Despite the significant drop in post-surgical weight as a result of sham surgery, there was no impact on urodynamic functions which remained statistically similar to naïve animals throughout.

URODYNAMIC ANALYSES

The intravesical pressure (IVP) of the bladder and EMG activity of the external urethral sphincter (EUS) were simultaneously recorded from all animals in the DRC group (n=5), and the sham (n=5) and naïve (n=5) control groups. Representative urodynamic recordings are shown in Figure 2 illustrate micturition cycles of a sham animal (Fig. 2.2a), and DRC animals 14 days (Fig. 2.2b) and 30 days (Fig. 2.2c) post-surgery over 4 minutes of a 20 minute recording period of continuous saline infusion. There were no statistically significant differences in urodynamic records between naïve

and sham animals. For both sham and naïve rats (Fig. 2.2a), during the filling phase of the cycle, a low baseline level of both bladder IVP (< 10 mmHg) and low level tonic EUS EMG activity (< 0.01 Volts) was maintained. As the infused volume of saline reached a threshold bladder capacity, there was a sharp increase in bladder IVP, high-amplitude phasic EMG activity was initiated and synergy between the detrusor muscle of the bladder and the EUS muscle was demonstrated during voiding. When voiding ended, IVP peaked and fell back to baseline and EMG activity was reduced. At a constant infusion rate, such cycles of filling and voiding occurred approximately once every 3 min in the uninjured animal.

For rats that received a bilateral L6 and S1 dorsal root crush injury 14 days or 30 days prior to recording (Fig. 2.2b and 2.2c), during the filling phase there was a gradual increase in bladder IVP from baseline over time with small non-voiding contractions present and the EUS showed increased EMG non-voiding activity. The filling phase was shorter in 14 day animals; however, 30 days post-surgery a long micturition cycle (extended filling phase followed by voiding) was followed by 2 short micturition cycles. When a voiding contraction began, bladder IVP was already high and rose further to voiding pressure. High-amplitude tonic EUS EMG activity was present between voiding contractions, decreased as voiding began and returned to noisy pre-voiding levels once voiding had stopped. During voiding, saline exited the external urethral orifice slowly and often in a broken stream of high pressure bursts.

Voiding contractions of the bladder detrusor muscle were recorded as an increase in resistance to the flow of saline through the transurethral catheter as a result of an increase in pressure within the intravesical space, accompanied by an outflow of saline through the urethra. Measuring the time between voiding events, or Inter-Contraction Interval (ICI), provides important information about the health of the lower urinary tract. ICIs of naïve and sham control animals were compared with animals that received a crush injury to the L6 and S1 dorsal roots in Figure 2.4a. At 3 days post-surgery the average length of time between voiding contractions of the DRC group (151.92 sec ± 20.48) dropped significantly below naïve (209.27 sec ± 20.88; $p<0.05$) and sham (221.55 sec ± 16.83; $p<0.05$) controls. The average ICI of DRC animals remained significantly shorter at 7 and 14 days post-surgery (152.28 sec ± 14.77 and 140.24 sec ± 16.36; $p<0.05$; $p<0.05$) compared to naïve and sham animals (229.85 sec ± 20.31; $p<0.05$ and 210.14 sec ± 22.28; $p<0.05$; 238.31 sec ± 25.6; $p<0.05$ and 236.24 sec ± 29.15; $p<0.05$). At 30 days post-surgery however, ICIs were statistically similar in all three groups (naïve: 201.18 sec ± 17.73; sham: 238.16 sec ± 42.77; DRC: 214.28 sec ± 26.09). The data in figure 2.3a show the average length of time between voiding contractions of the bladder, however, the lack of separation between the DRC group and controls at 30 days does not reflect the still dysfunctional state of the DRC bladder at this time point. For example, long, extended ICIs were quickly followed by 1, 2 and sometime 3 much shorter ICIs in the injured 30 day animals (see Fig. 2.2c) thus the mean ICI of all voiding contractions might imply a return to normal function when in fact ICI values alternate between prolonged

time periods and multiple shortened time periods. This conclusion was supported by the lack of any significant effect of time post surgery on the DRC group. Two way ANOVA tests showed no significant difference between naïve and sham, a significant separation between naïve and DRC (p=0.003, F= 8.92) and a significant separation between sham and DRC (p<0.001, F= 15.407).

Bladder compliance is a measure of the relationship between change in bladder volume and change in detrusor pressure under artificial filling conditions and is defined as $\Delta V/\Delta P$, or the inverse of the tangent to the cystometry curve. Compliance values depend on filling rates which vary between species and experimental design; therefore general statements about compliance are used such as "low", "normal" or "high". The rise in pressure that causes low compliance is a function of the viscoelastic nature of the detrusor under higher than physiologic filling rates, i.e. if the muscle is stretched quickly it cannot accommodate completely. The average compliance of the DRC bladder was significantly lower than either naïve or sham (p=0.002, F= 9.56 and p<0.001, F= 11.529; two way ANOVA) (Fig. 2.3b). When isolating individual time points, post hoc Tukey pairwise comparisons showed a significant difference only after 30 days between DRC compliance (0.066 mL/mmHg ± 0.011) compared to naïve (0.274 mL/mmHg ± 0.098; p<0.05) and sham (0.229 mL/mmHg ± 0.085; p<0.05) controls.

Urodynamic analysis of just a single micturition cycle at the beginning of a recording session allows the investigator to examine how the bladder performs when starting out completely empty and eliminates the influence of possible muscle fatigue

47

resulting from back to back contractions over a short time period. Most importantly, starting out with an empty bladder allows for an accurate calculation of Threshold Volume (the volume of saline infused into the bladder to elicit the first voiding contraction, sometimes referred to as Bladder Capacity) and Residual Volume (the volume of saline remaining within the bladder after a voiding contraction, sometimes referred to as the Post Void Residual). Threshold volume of sham animals was compared to DRC animals at 3, 7, 14 and 30 days post-surgery in Figure 2.4c. The average infused volume of saline required to elicit the first micturition response was statistically larger in the DRC group compared to the sham group (p=0.004, F= 9.599; two way ANOVA). There was no significant effect of time post-surgery. The threshold volume of DRC animals remained between 2.38 mL ± 0.36 mL and 2.94 mL ± 0.23 mL over all four time points. The threshold volume of sham animals was at its lowest after 7 days (1.48 mL ± 0.35 mL) and greatest after 14 days (2.18 mL ± 0.2 mL). There was a significant difference between sham and DRC at 7 days (1.48 mL ± 0.35 mL and 2.7 mL ±0.51 mL respectively; p<0.05; Tukey test) but at no individual time point before or after that. The amount of saline remaining within the bladder after the first micturition was calculated by collecting the volume voided and subtracting this from the volume infused. The effects of a bilateral dorsal root crush at L6 and S1 on the efficiency of bladder voiding are illustrated in Figure 3d. There was a clear and significant difference between the groups as indicated by two way ANOVA (p<0.001, F= 21.357). DRC animals had a significantly larger residual volume compared to shams at 3 days (1.41 mL ± 0.42 and 0.095 mL ±

0.033; p<0.05; Tukey test), 14 days (1.45 mL ± 0.35 and 0.25 mL ± 0.14; p<0.05; Tukey test) and 30 days (1.62 mL ± 0.3 and 0.36 mL ± 0.25; p<0.05; Tukey test) post-surgery. Large residual volumes were left unvoided in the bladders of the DRC group and resulted in an average voiding efficiency of 47% compared to 89% in sham animals.

External Urethral Sphincter Outcome Measures

Samples of an expansion of recording traces of both filling and voiding phases for both sham and DRC groups are shown in Figure 2.3. Examination of these 15 second periods allowed closer analysis of the contrasts in EUS EMG activity of the individual phases of micturition and the same phases in animals from different surgical groups. Sham animals (Fig. 2.3a and 2.3b) demonstrated low baseline, filling phase EMG activity of the EUS followed by robust high frequency bursting activity during voiding. The DRC group (2.3c and d) had greater EMG activity during the filling phase but no high frequency activity during the voiding phase. When the EMG data was recorded at a higher sample rate, the typical high frequency bursting period, evident in rats and dogs, during the voiding phase (2.3e) was disrupted as a result of dorsal root injury; specifically the individual bursts had a lower frequency and shorter amplitude (2.3f).

To quantitatively compare the EUS EMG activity between sham and DRC groups, the average integrated EMG amplitude recorded during the bladder filling phase was expressed as a percentage of the average amplitude recorded during bladder voiding phase [Fill EMG/Void EMG × 100] (Fig. 2.5a). There was a statistically significant difference between the Sham and DRC groups as a whole (p<0.001, F = 43.58; two way

ANOVA); however, no significant effect of time post-surgery was reported for either group. In sham animals at 3, 7, 14 and 30 days post-surgery, the average filling phase EMG amplitude was between 52.73% ± 2.68 and 56.88% ± 5.34 of the voiding phase EMG. In DRC animals the average filling phase EMG was 96.78% ± 13.18, 84.93% ± 4.02 and 93.25% ± 16.39 of voiding EMG at 3, 7 and 14 days respectively. At 30 days post-surgery the average filling phase EMG surpassed that of the voiding phase reaching 112.98% ± 9.53. At all time points there was a statistically significant difference between sham and DRC values ($p < 0.05$; Tukey test). The frequency of bursts within the voiding period were compared between both groups of animals in Figure 2.5b. The sham group was significantly different compared to the DRC group ($p < 0.001$, F= 25.19; two way ANOVA). Time post-surgery showed no significant effect on either group; however, a Tukey pairwise comparison showed a significant reduction in bursting frequency between 3 days (1.63Hz ± 0.27) and 14 days (0.76Hz ± 0.13; $p < 0.05$) post-surgery in the DRC group. There was no significant difference between the bursting frequencies of sham and DRC animals at the 3 day time point (1.95Hz ± 0.21 and 1.63Hz ± 0.27 respectively; $p > 0.05$). At 7, 14 and 30 days post-surgery there was significant separation with the number of bursts remaining between 2.09 ± 0.34 and 2.2 ± 0.4 per second in the sham group and between 1.18 ±0.19 and 0.76 ± 0.13 bursts per second in the DRC group ($p < 0.05$; Tukey test).

PHYSICAL ANALYSIS OF THE BLADDER

Bladders from animals in each surgical group (n=5) were dissected out at each time point post-surgery. Figure 6a shows the gross physical changes that occur in the bladder due to a bilateral DRC injury. The injury created a muscular, thick, opaque bladder by 7 days post-surgery however, by 30 days post-surgery the bladder was thin, transparent and balloon-like. After removal, bladders were blotted dry and weighed (Fig 6b). Bladder weight within the DRC group demonstrated a significant effect of dorsal root injury (p=0.004, F= 9.214; two way ANOVA). The average weight of a bladder from an injured animal (0.191g ± 0.016g) was significantly greater than control (0.119g ± 0.007g; p<0.05, Tukey test) at 7 days post-surgery. The average weight of sham bladders remained between 0.115g ± 0.012 and 0.125g ± 0.008.

DISCUSSION

Our study is the first to demonstrate the effects of a bilateral crush injury of the L6 and S1 dorsal roots on bladder and external urethral sphincter (EUS) function in awake rats using cystometric, sphincter EMG and morphological analysis of the bladder. We report that a bilateral dorsal root crush injury (DRC) significantly interrupted normal EUS function, resulted in shorter inter-contraction intervals (ICIs), lower compliance, greater threshold volumes and larger residual volumes relative to sham controls. Electromyographic (EMG) activity in the EUS was also adversely affected. DRC animals showed a reduction in the frequency of high amplitude voiding bursts and the average amplitude of filling phase EMG activity is significantly increased to voiding phase levels. DRC also had a major impact on the physical properties of the bladder itself. Bladder

51

weight increased significantly 7 days post-surgery. However at later time points bladder weight was not significantly greater in DRC animals compared to sham but bladder capacity was significantly larger indicating over distension.

CAUSES OF CAUDA EQUINA INJURY

Any spinal injury from low thoracic down through the lumbar segments, whether severe or incomplete, risks compromising the function of the lower urinary tract by injury to the roots innervating that region. The unique anatomy of the thoracolumbar junction and lower lumbar vertebrae make this region the second most injured part of the spine (Meyer *et al.* 1991). The upper thoracic spine, held rigid by the ribs, transitions to a lumbar region where intervertebral discs are thicker and the lumbar body articulating facets orient in such a way as to allow increased flexion, extension and lateral bending of the spine. The susceptibility of the weakly supported T11-L2 and lumbar spine to injury is due to isolation between the rigidly supported thoracic and fused sacral vertebrae. Thus, vertebral collapse or displacement and intervertebral disc herniation injures nerve roots within the spinal canal and the intervertebral forminae. Injury to the lumbosacral nerve roots in the spinal canal results in a cauda equina syndrome with variable clinical manifestations that include sensorimotor deficits in the lower limbs and areflexic bowel and bladder. While the prognosis for recovery from these injuries is similar to peripheral nerve injury and significantly better than that for cord injury (Savitsky and Votey 1997), dorsal root intraspinal regeneration remains problematic.

In this study, awake and responsive animals with an L6 and S1 dorsal root crush injury demonstrated a capacity for limited voiding activity during urodynamic tests. This voiding activity worsened in some chronically injured animals where long filling phases were followed by a combination of multiple brief voiding contractions and sphincter leakage. The presence of any kind of micturition reflex is surprising considering the neuroanatomical pathways involved and the knowledge that pelvic nerve afferent feedback is needed to maintain micturition contractions (Kruse *et al*. 1991). Considering the fact that the majority of sensory innervation mediating the initiation of micturition via the pelvic nerve is removed by injuring the L6 and S1 dorsal roots, is it possible that the intact hypogastric nerve afferents have a part to play in bladder voiding? Autonomic sensory innervation of the bladder is provided by lumbosacral pelvic parasympathetics (L6-S1 in rat; S2-S4 in human) and thoracolumbar hypogastric sympathetics (T13-L3 in rat; T11-L2 in human) (Hancock and Peveto 1979, Hulsebosch and Coggeshall 1982, Nadelhaft and Booth 1984, de Groat 1993,). Most of the pelvic nerve afferents are mechanoreceptive and the vast majority of hypogastric nerve afferents are nociceptive. (Sengupta and Gebhart 1994, Wen and Morrison 1995). Talaat, however, described weak afferent excitation of the hypogastric nerve after bladder distension in the dog, work on cats produced single-afferent fiber excitation and a small subset of activated rat nociceptors can transmit bladder filling information through the hypogastric nerve (Talaat 1937, Floyd *et al*. 1976, Bahns *et al*. 1986, Moss *et al*. 1997). It was proposed that

53

perhaps these hypogastric afferents played a unique dual role by responding to combined noxious and mechanical stimuli, i.e. noxious over distension of the bladder. In humans, the roll of the hypogastric nerve in preserving the sensation of bladder filling appears important in cases of complete spinal cord injury (Pavlakis *et al*. 1983, Wyndaele 1991, Wyndaele 1997). Ersoz and Akyuz found that a majority of people with complete lesions below T10 were aware of bladder filling and an urge to void, but that these sensations were described as "pain, tension or a burning sensation" by some in the study (Ersoz and Akyuz, 2004).

It is also possible that afferents outside the bladder in other visceral organs and in peritoneal connective tissue, that have central projections entering the spinal cord rostral or caudal to the lesioned roots, may play some part in initiating voiding (Talaat, 1937, Muellner, 1958). The anti-dogmatic existence of lumbosacral ventral root afferents has been known for decades with some innervating the bladder (Coggeshall *et al.* 1974, Clifton *et al.* 1976, Loeb 1976, Ohta *et al.* 1991). The role this small population of ventral afferents plays in initiating micturition under normal or dorsal root injury conditions is not clear. However, in combination with hypogastric afferents they may be capable of relaying just enough mechanoreceptive information centrally from the over distended bladder to induce a detrusor contraction and inefficient voiding. Pascual and collegues reported a completely areflexic bladder following injury to the L6-S2 dorsal roots (Pascual *et al*. 2002). In this case urodynamic recordings were performed in

anesthetized animals, which is known to interfere with micturition (Matsuura and Downie 2000).

SUGGESTED NEUROGENIC MECHANISM OF LOWER URINARY TRACT DYSFUNCTION

Throughout the process of urine storage and voiding there is a fine balance between inhibition, excitation and facilitation mediated by more than just one spinal reflex arc. As the storage volume of the bladder increases, gradual increments in intravesical pressure and ultimately the entry of urine into the proximal urethra will recruit the somatic innervation to the EUS to induce sphincter contraction. In human urology, these phenomena are known as the 'continence reflex' and the 'guarding reflex' respectively, with the strength of the latter increasing as micturition approaches (Garry *et al.* 1959). In the present study, the lumbosacral spinal cords of injured animals lack pelvic and pudendal dorsal root afferents as a result of deafferentation at L6 and S1. Without this input the supraspinal pontine micturition center or Barrington's nucleus (Barrington 1915) has only low level indirect information with which to conduct micturition. Under hyposensate conditions the bladder becomes over filled, distended and activates a small group of hypogastric afferents which send a weak signal about bladder fullness to the pontine micturition center. This lesser signal may be interpreted as a filling bladder but not a full bladder and thus initiates an extended guarding reflex-like response in the EUS that results in high amplitude tonic activity throughout much of the filling period, essentially functioning as a bladder outlet obstruction. A symptom and effector of this dysfunction is the presence of a large residual volume within the bladder.

Both the passage of fluid through- and distention of the proximal urethra are important stimuli in maintaining continuous and efficient voiding. The micturition reflex (detrusor contraction and sphincter opening) initiates the process of bladder emptying by forcing fluid into the urethra. Positive feedback from the important sympathetic urethrovesical and vesicosphincteric reflexes potentiates detrusor contraction and EUS phasic bursting in the rat (EUS relaxation in humans) in what Kuru termed the "multiplication reflex" (Kuru 1965, Fraser and Chancellor 2003, Shafik *et al.* 2003). Loss of pudendal afferent innervation breaks these reflex arcs which normally constitute a positive feedback mechanism to improve voiding efficiency. The adverse effects of blocking urethral afferent nerve activity on detrusor contraction frequency has been demonstrated previously (Jung *et al.* 1999). Premature cessation of detrusor contractions prevents complete voiding, accompanied by low frequency phasic activity of the EUS, as seen in the present study.

Prolonged sphincter closure, i.e. increased EUS EMG tonic activity, evident during the filling phase in DRC animals prohibits voiding until very large threshold volumes are reached. The reduction in phasic bursting frequency during voiding in the DRC animals compared to sham animals is a result of the broken urethro-vesico-sphincteric reflexes. Complete bladder voiding is not achieved and large residual volumes remain.

BLADDER WALL COMPLIANCE IS LOW AFTER DORSAL ROOT INJURY

In the clinical arena, an important tool in the diagnosis and management of the neurogenic bladder is assessment of bladder wall compliance. Compliance is a function of the passive (viscoelastic) and active (sensory inhibition) properties of the bladder wall. This is critical for maintenance of low pressures during the filling phase when the bladder stretches to accommodate the storage of urine thus preventing premature voiding of the bladder. Cauda equina injury most commonly results in a high compliance areflexic neurogenic bladder, but low compliance accompanied by a small storage volume and a large residual volume are commonly encountered (Shin *et al.* 2002) as seen in this rodent study. Changes in the passive properties of the detrusor muscle are believed to be the main effector of compliance (German *et al.* 1994).

CHANGES IN THE PHYSICAL PROPERTIES OF THE BLADDER FOLLOWING NEURAL DAMAGE

Changes in the physical anatomy of the bladder have been noted as a result of injury to the spinal cord in animal models (Mimata *et al.* 1993, Pikov *et al.* 1998, Yoshimura *et al.* 1998, Zinck *et al.* 2007). We report an increase in bladder weight in DRC animals in the present study. The bladders of animals injured 7 days prior are thick, muscular and opaque in contrast to the bladders of animals dissected 30 days post-injury. Hypertrophy of the smooth muscle in the bladder detrusor can occur in response to urinary outlet obstruction or decentralization. Regardless of the cause, the primary factor for induction of the growth seems to be stretch of the bladder wall components (Andersson and Arner, 2004). Metabolic pathways can influence the bladder structure, however it is evident that the hypertrophy associated with denervation can be prevented

57

by manually expressing the contents of the bladder (Berggren and Uvelius 1996, Malkowicz *et al.* 1985). Stress on the bladder wall by over filling is primarily responsible for initiating the significant increase in size and weight of the bladder. Hypertrophy of the bladders smooth muscle layer is not solely responsible for the increase in bladder size. There are also increases in extracellular materials, including collagen in hypertrophic bladders are also described (Gosling and Dixon 1980, Uvelius and Mattiasson 1984). Inflammation due to neurogenic causes and acute urothelial barrier disruption is likely to add to bladder weight (Apodaca *et al.* 2003, Birder 2006, Geppetti *et al.* 2008). Therefore, at 7 days post-injury over distension is countered by increasing muscle mass and extracellular support materials in order to maintain the integrity of the organ. Continued stress on the bladder wall by 30 days post-surgery, however, resulted in a flaccid structure, lacking in sufficient muscle mass to allow complete emptying.

POSSIBLE THERAPEUTIC INTERVENTIONS TO IMPROVE BLADDER FUNCTION FOLLOWING CAUDA EQUINA INJURY

Two broad approaches can be taken to improve bladder function. First, the neurogenic structures and intact circuitry can be targeted. Excessive sphincter tone can be reduced by α-2 receptor sympathetic adrenergic blockade or even sphincterotomy (Gerstenberg *et al.* 1983, Potter 2006, Pannek *et al.* 2009,). The successful use of ventral root stimulators to increase the efficacy of existing motor circuits has been well documented (Vignes *et al.* 2007).

A second approach is the restoration of afferent connections that fail to regenerate. A clear difference is reported in the regenerative capacity of motor efferents and sensory afferents following root injury. The outgrowth of regenerating axons of transected nerves is well documented in peripheral motor nerves (Fawcett and Keynes 1990) and spontaneous recovery is reported clinically in somatic nerve function in studies of lower motor neuron neurogenic lower urinary tract disorders (Esteban *et al*. 1998). Thus there is an innate ability of axotomized motor neurons to regenerate back to their peripheral targets, since the neuronal soma are undamaged within the ventral horn of the spinal cord and the regenerating axon is in the "permissive" environment of the peripheral nervous system. Following injury to dorsal roots however, afferent axons will regenerate from their peripherally located cell bodies as far as the dorsal root entry zone but will fail to penetrate this barrier and cross into the CNS due to the abundance of inhibitory factors and absence of appropriate trophic support at this location (Carlstedt 1985, Carlstedt 1985, Carlstedt 1988, Carlstedt 1997, Priestley *et al*. 2002). A conditioning peripheral nerve lesion prior to dorsal root injury is known to provide an increase in the number of regenerating axons that cross the DREZ (Neumann and Woolf 1999, Quaglia *et al*. 2008). This, however is not clinically relevant. Lentiviral-mediated expression of polysialic acid in the spinal cord created a permeable DREZ but again this required a conditioning lesion (Zhang *et al*. 2007). Over expression of the retinoic acid receptor β2 (RARβ2) in DRG neurons resulted in an increase of axonal projections from Lissauer tract into the dorsal grey matter of the spinal cord (Wong *et al*. 2006). Other

interventions that reportedly improve regeneration of sensory axons into and across the DREZ are systemic administration of Artemin (Wang *et al.* 2008), treatment with neurotrophin-3 (NT-3) (McPhail *et al.* 2007) and injection of Chondroitinase ABC (Steinmetz *et al*. 2005, Massey *et al.* 2006,) to digest the chondroitin sulfate proteoglycans that are upregulated in the DREZ after dorsal root injury (Beggah *et al*. 2005) [reviewed by Silver and Miller (Silver and Miller, 2004)]. Without considerable regrowth assistance provided by olfactory ensheathing cells (Pascual *et al.* 2002) and methlyprednisolone (Nash *et al.* 2002) or neurotrophins and proteoglycan degraders (Massey *et al*. 2006, Ramer *et al*. 2000, Steinmetz *et al.* 2005) sensory afferent regeneration across the dorsal root entry zone simply will not occur. Consequently, it is the irreversible nature of injury to dorsal roots that requires the majority of attention in the field of cauda equina injury.

We demonstrated the effects of a bilateral crush injury of the L6 and S1 dorsal roots on bladder and external urethral sphincter (EUS) function in awake rats using cystometric, sphincter EMG and morphological analysis of the bladder. We report that a bilateral dorsal root crush injury (DRC) significantly interrupted normal EUS function, resulted in shorter inter-contraction intervals (ICIs), lower compliance, greater threshold volumes and larger residual volumes relative to sham controls. Electromyographic (EMG) activity in the EUS was also adversely affected. DRC animals showed a reduction in the frequency of high amplitude voiding bursts and the average amplitude of filling phase EMG activity is significantly increased to voiding phase levels. DRC also had a

major impact on the physical properties of the bladder itself. Bladder weight increased significantly 7 days post-surgery. We suggest that the inability of afferents to regenerate across the dorsal root entry zone (DREZ) and the neurogenic dysfunction associated with cauda equina injury represent critical problems and important future therapeutic targets for investigation. Further work in this area will not only reveal the nature of the DREZ barrier and the growth inhibitory environment of the entire central nervous system, but will also help to improve the quality of life of those suffering from neurogenic bladder bowel and sexual function.
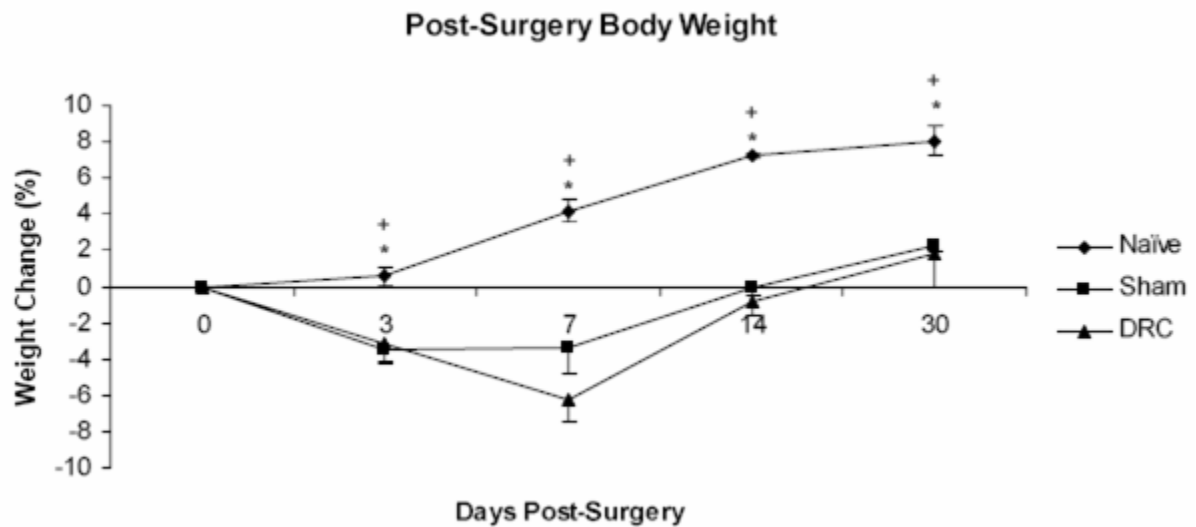
Figure 2.1 Body weight changes over time expressed as a percentage of pre-surgery weight.
Body weight changes over time expressed as a percentage of pre-surgery weight (day 0) at each of four time points (3, 7, 14 and 30 days) post-surgery demonstrate the significant effect that surgery had on the weight of subjects in each group. When compared to the naïve group, surgery resulted in a significant drop in the weight of both sham and bilateral L6 and S1 dorsal root crush (DRC) animals. Data are displayed as means (X) ± standard error (S.E.) and * $p < 0.05$ between naïve and sham groups; + $p < 0.05$ between naïve and DRC groups.

61
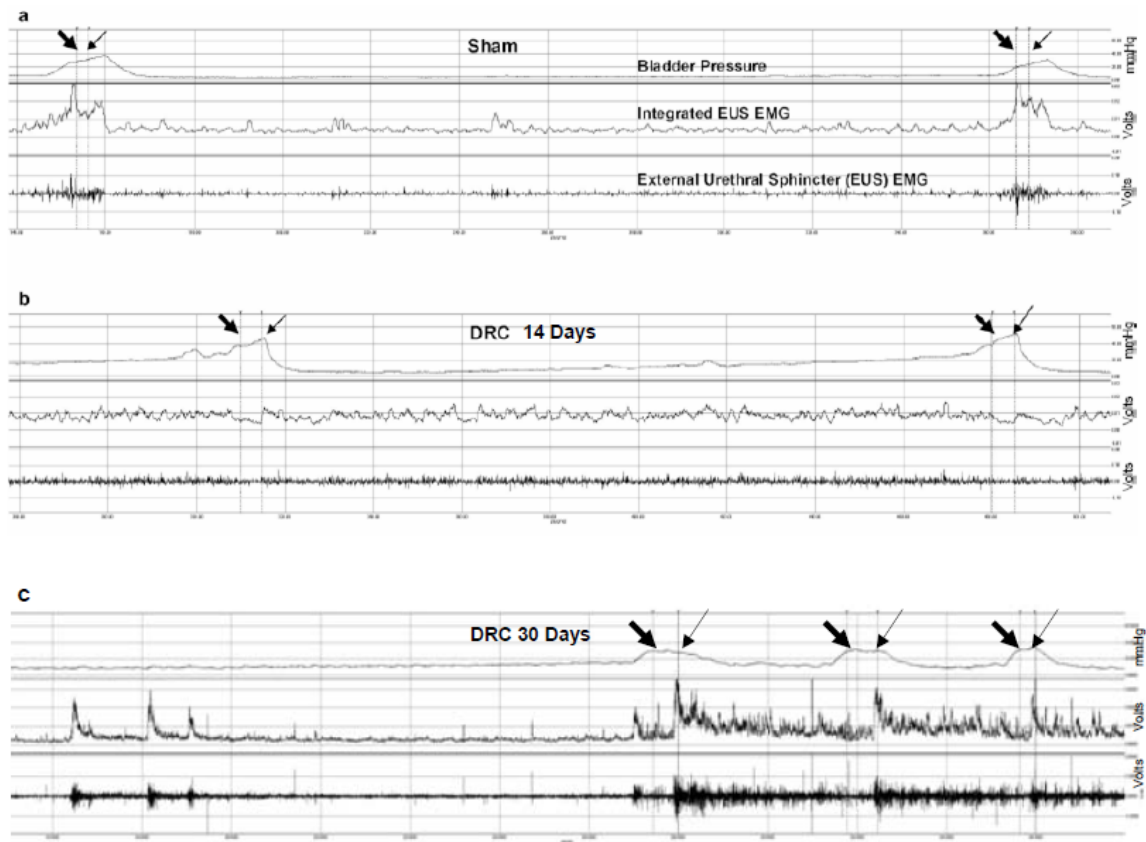
Figure 2.2 Sample urodynamic recordings.
Sample urodynamic recordings from an uninjured animal (a), and an animal 14 days after a bilateral dorsal root crush (DRC) injury at spinal level L6 and S1 (b) and from an animal 30 days after DRC (c). Each panel displays 3 traces: the top is intravesical pressure (IVP) measured in millimeters of mercury, on the bottom is external urethral sphincter (EUS) electromyography (EMG) in volts and in the center is the integrated EUS EMG during 4 minutes of a 20 minute recording period. The thick arrow indicates the beginning of saline voiding and the thin arrow indicates the end of voiding. In 2a note that during the filling phase of the micturition cycle IVP remained low and flat in uninjured animals until voiding occurred. By contrast in 2b and 2c, at both post-injury time points, a gradual increase in IVP was evident as the infused volume increased. EUS EMG tonic activity increased in amplitude during the filling phase post injury. Shortened micturition cycles at 14 days post-injury were replaced by a long cycle followed by multiple brief cycles. These recordings demonstrate a gradual change in dysfunction over time post injury.

62
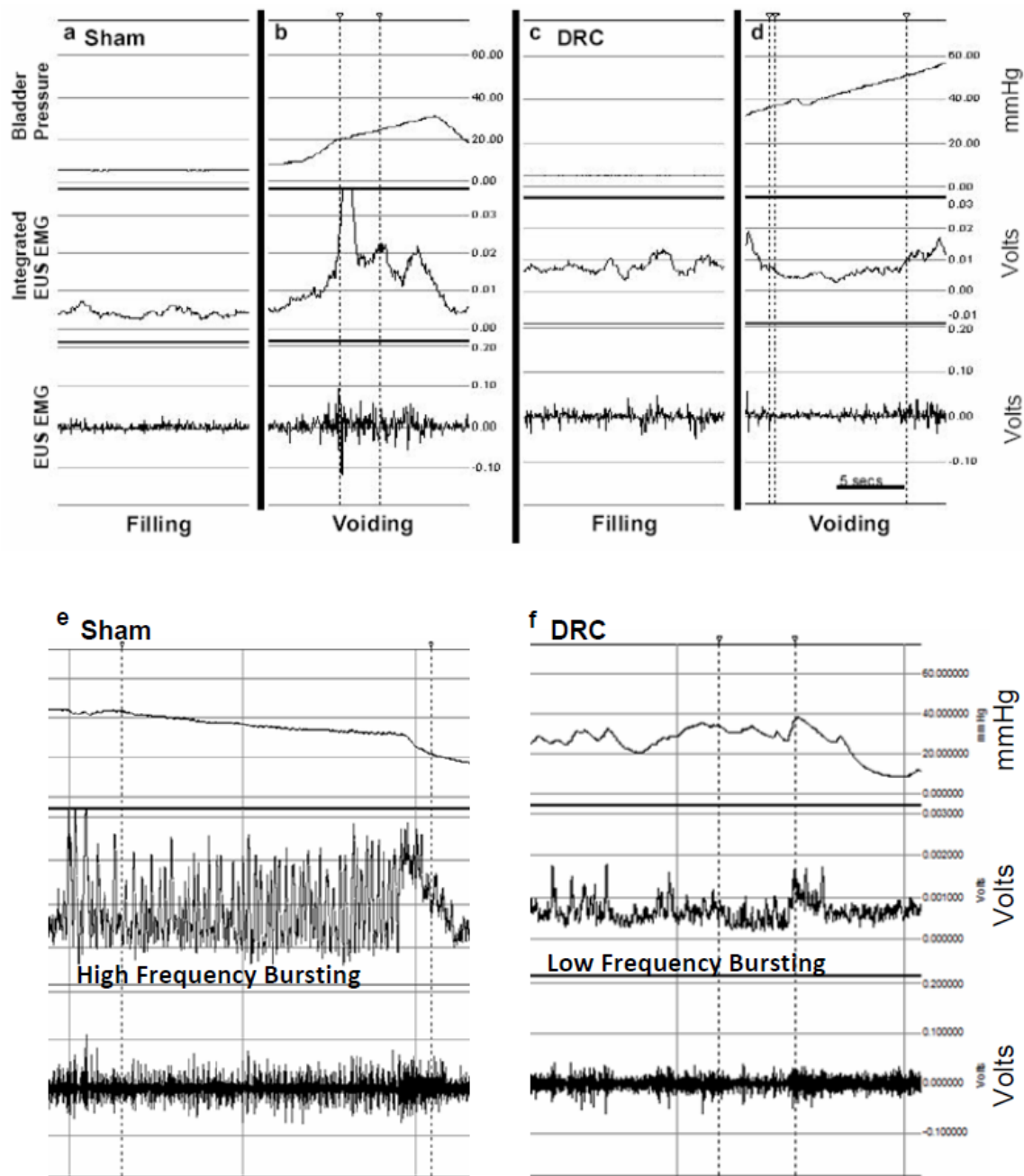
Figure 2.3 Sample urodynamic recordings demonstrate the effect of dorsal root crush (DRC) on external urethral sphincter (EUS) electromyography (EMG).

Each panel is a representative urodynamic recording showing bladder pressure on the top, integrated EUS EMG in the center and raw EUS EMG on the bottom. Panel a shows low amplitude tonic EMG activity during the filling phase in a sham animal; panel b shows high-amplitude phasic EMG activity before, during and after the voiding period (between dashed lines) in the same animal. Panel c shows higher-amplitude tonic EMG activity during the filling phase in a DRC animal; panel d shows low amplitude phasic EMG activity during voiding in the same animal. When the sample rate during recording was

63

increased and the time scale was expanded panel e shows the phasic bursts of high amplitude EMG activity during voiding in a sham animal, followed by a brief period of tonic activity as voiding is terminated. In panel f, dorsal root crush (DRC) injury reduced the frequency and amplitude of phasic bursts during voiding and increased EMG activity before and after voiding.
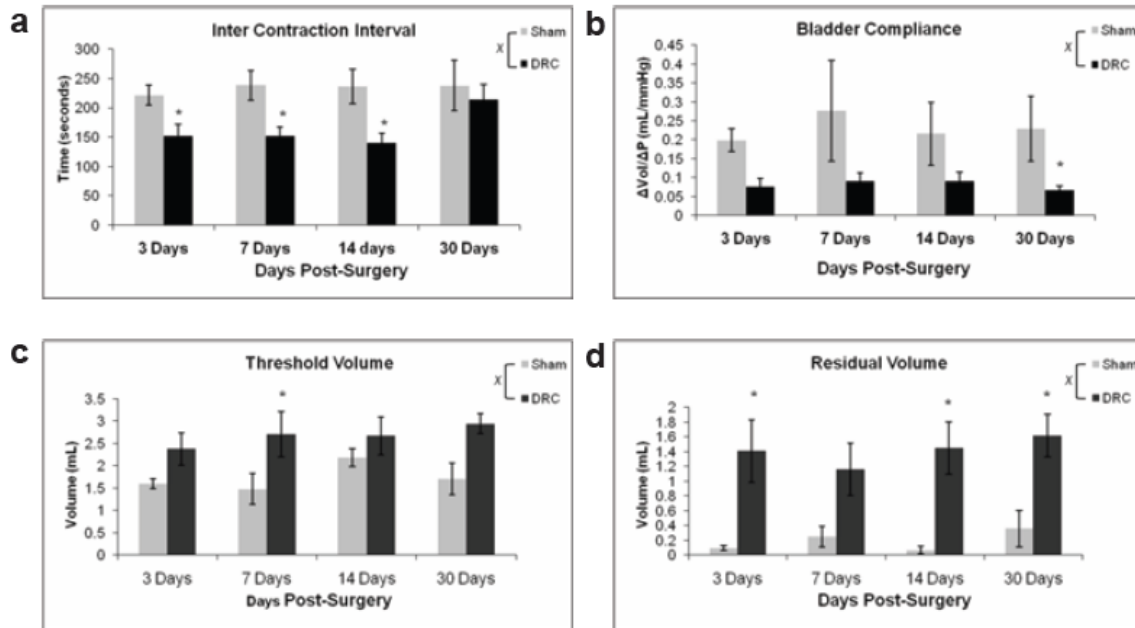
Figure 2.4 Four outcome measures of bladder function.
Four outcome measures of bladder function are shown in these figures at each of the four time points (3, 7, 14 and 30 days) post-surgery. 3a) average inter contraction intervals (ICIs) measured in seconds, in sham and dorsal root crush (DRC) animals at the four post injury time points in this study. DRC animals have significantly lower ICIs compared to sham over the full post-surgical period (x Two way ANOVA, p=0.003 and p<0.001). However, there was no statistical difference between sham and DRC ICIs when recorded at 30 days post-surgery. * indicates a statistical difference from sham at individual post-surgical days, Tukey post hoc test (p<0.05). There was no significant difference between naïve and sham (data not shown). 3b) shows bladder compliance ($\Delta V/\Delta P$) measured in milliliters per millimeter of mercury (mL/mmHg). Injury resulted in significantly lower compliance over the full post-surgical period (x Two way ANOVA, p=0.002 and p<0.001). * indicates statistical difference from sham at individual post-surgical days, Tukey post hoc test (p<0.05). There was no significant difference between naïve and sham (data not shown). 3c) shows the threshold volume of infused saline needed to induce micturition in the empty bladder in sham and DRC animals. Threshold volume was significantly greater as a result of injury over the full post-surgical period (x Two way ANOVA, p=0.004). 3d) shows the residual volume of saline remaining in the bladder (mL) of sham and DRC animals after voiding. Injury resulted in a significantly larger residual volume in the DRC group over the full post-surgical period (x Two way ANOVA, p<0.001). * indicates a statistical separation from sham by Tukey post hoc test (p<0.05).

64
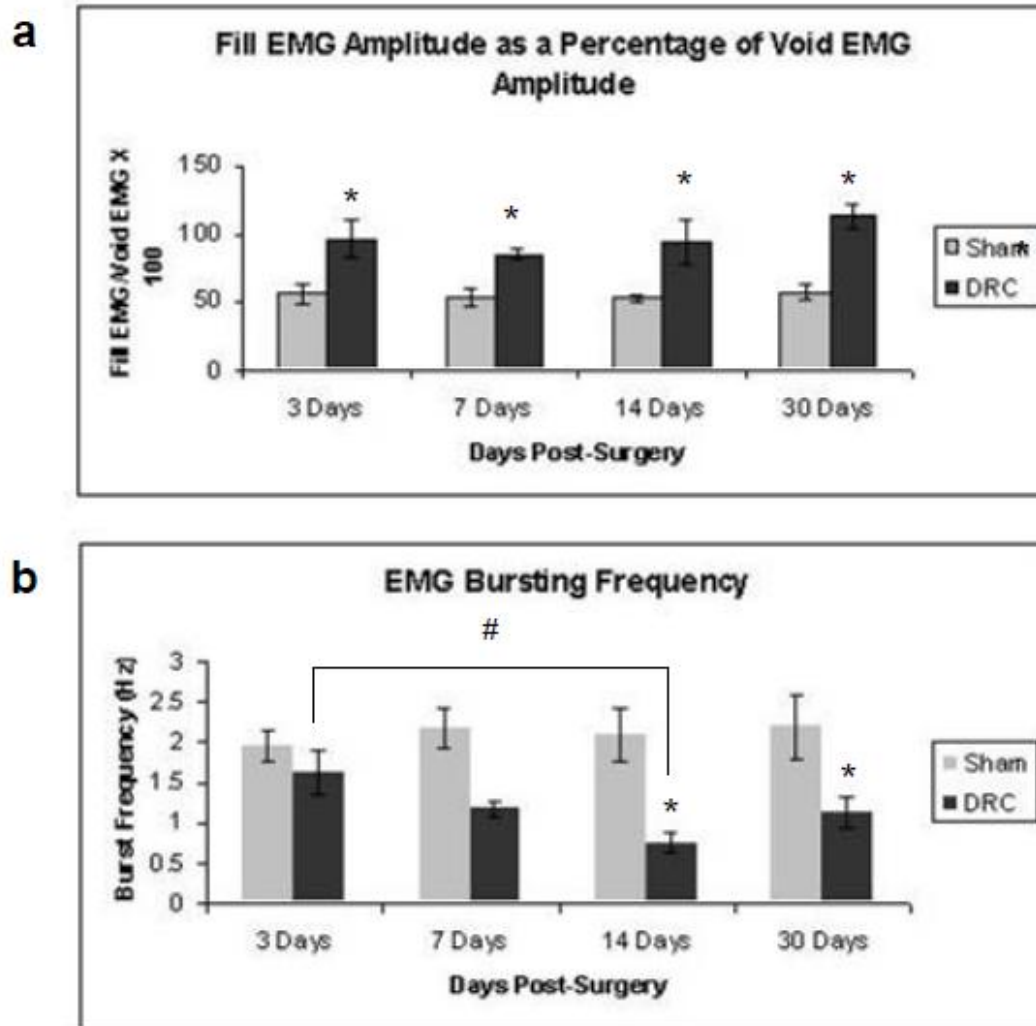
Figure 6 Quantitative analysis of external urethral sphincter electromyography (EMG).
a) The average filling phase EMG amplitude is expressed as a percentage of the average voiding phase EMG amplitude in sham and dorsal root crush (DRC) animals for the four post-surgical time points in this study. 100% indicates a 1:1 ratio. The average filling phase EMG is a significantly larger percentage of voiding phase EMG in DRC animals compared to sham over the full post surgical period (Two way ANOVA, p<0.001), rising to over 100% after 30 days. b) The average frequency of phasic bursts, measured in Hz or bursts per second, during voiding in sham animals is compared to DRC animals. There was a significant reduction in burst frequency in DRC animals (two way ANOVA, p<0.001). There is no significant effect of time post-injury on burst frequency in DRC animals as determined by two way ANOVA (p>0.05); however, there were significantly less bursts per second after 14 days compared to 3 days (# p<0.05, Tukey post hoc test). * indicates a significant difference to sham p<0.05, Tukey post hoc test).
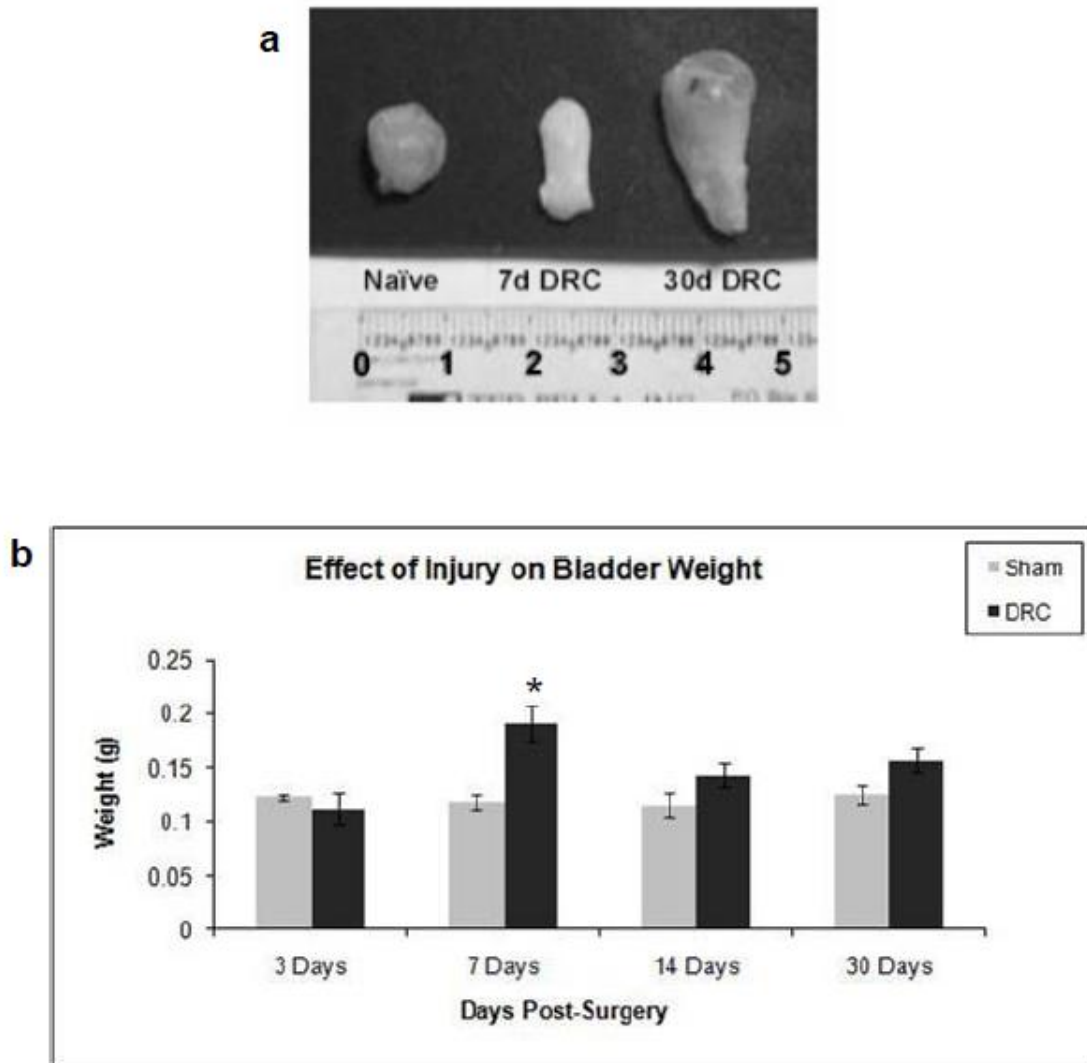
Figure 7 Effects of dorsal root crush on bladder anatomy.
Shown in a are dissected bladders from a representative naïve (N), and two bilateral dorsal root crush (DRC) animals, one at 7 days post surgery (7d DRC) and one at 30 days post surgery (30 d DRC). Ruler is shown with cm divisions. Note that the bladder size increases after bilateral DRC injury. An increase in weight (g) is demonstrated graphically in b for the four post surgical time points in this study. The bladder was removed, blotted dry and weighed following sham and DRC animals perfusion. The bladder weight was significantly greater in the DRC animal following injury compared to shams over the full post-surgical period (two way ANOVA, p=0.004) The average DRC bladder weight was significantly greater than sham 7 days post surgery (* p<0.05, Tukey post hoc test)

66

INTRODUCTION

Axons fail to exhibit regeneration for long distances in the central nervous system (CNS) following injury (Horner and Gage 2000, Ramon y Cajal 1928). Neurons within the CNS have an intrinsic regenerative capacity; however, the lack of regeneration appears to be due to the nonpermissive properties of the CNS environment. Given a favorable environment, an injured axon has the ability to regenerate and grow for significant distances (David and Aguayo 1981, Richardson *et al.* 1980). There are two major glial cell populations that prove to be sources of inhibitory molecules: 1) oligodendrocytes/myelin and 2) astrocytes. Oligodendrocytes express molecules such as Nogo and myelin associated glycoprotein (MAG), that inhibit axonal growth by causing growth cone collapse (Filbin 1995, Shibata *et al*. 1998, Chen *et al*. 2000, Fournier and Strittmatter 2001). Reactive astrocytes, associated with glial scarring, represent both a physical and molecular obstacle for regrowing axons (McKeon *et al*. 1991). The glial scar produced by astrocytes contains keratin and tenascin R, which have been shown to inhibit axonal outgrowth in vitro (Becker *et al.* 2000, Fournier and Strittmatter 2001). Chondroitin sulfate proteoglycans (CSPGs) are expressed by oligodendrocytes and astrocytes and are found in both the glial scar and in myelin, respectively. Numerous studies demonstrate that CSPGs can inhibit neurite outgrowth of various neuronal cell types in a variety of injury models (Snow *et al*. 1990, McKeon *et al. al.* 1999, Asher *et al*. 2000). More recently a third population of glial cells were described that express NG2

also undergoes reactive gliosis and upregulates the growth cone-repellent CSPG NG2 on their surface after injury (Levine *et al*. 2002). These cells, known as NG2-glia, are distinct from mature oligodendrocytes, astrocytes or resting ramified microglia and have been recently described as a fourth major glial cell population (Dawson *et al*. 2000, Butt *et al*. 2002, Nishiyama *et al*. 2002, Dawson *et al.* 2003, Peters 2004). Much of the NG2-positive cell population in the CNS gives rise to both oligodendrocytes and astrocytes (Zhu *et al.* 2008). However, approximately 50% of NG2-positive cells are non-proliferating and do not differentiate any further (Wigley and Butt 2009). Reactive NG2-glia intermingle with those of reactive astrocytes in the CNS scar and at the dorsal root entry zone (DREZ) (Zhang *et al*. 2001, Jones *et al.* 2002).

Following lumbosacral intervertebral disc herniation, foraminal stenosis or vertebral dislocation; the roots of the cauda equina are damaged most often by a compression injury that severs the axons within. Unlike motor neurons which can regenerate out to the periphery within ventral roots, sensory afferents that regenerate within the crushed dorsal root are unable to grow across the DREZ and back to their original projection territory to form appropriate central connections within the dorsal spinal cord (Carlstedt 1983) and severe often irreversible loss of function results. The DREZ responds to dorsal root injuries (injuries restricted to the PNS) similar to the way the CNS responds to direct insult, producing a glial scar which, if untreated, inhibits regeneration and prevents the regenerating axons from growing into the CNS, by both physical and molecular means (Carlstedt *et al.* 1989, Bovolenta *et al*. 1992, Bovolenta *et*

al. 1993). The DREZ is a useful model for the study of central axonal regeneration (Fraher 2002) and there is increasing use of the dorsal root crush (DRC) as an injury/rhizotomy paradigm to study this growth-inhibitory barrier (Ramer *et al.* 2004, Tang *et al.* 2007, Cafferty *et al.* 2008, Duffy *et al.* 2009, Hanna-Mitchell, *et al.* 2008, Wang *et al.* 2008, Harvey *et al.* 2009, Starkey *et al.* 2009, Andrews *et al*. 2009, Wu *et al*. 2009, Peng *et al*. 2010). Dorsal root injury results in Wallerian degeneration of severed afferents, and upregulation of extracellular matrix molecules associated with reactive gliosis and myelin disintegration within the DREZ as well as the dorsal column (DC) (Waselle *et al.* 2009), which make the dorsal root crush injury a valuable model for studying the inhibitory nature of the CNS following lesion which we characterize in the current study.

In this study we utilized immunocytochemistry to examine the neuroarchitectural and molecular changes that occur within the dorsal spinal cord following a bilateral dorsal root crush (DRC) injury at L6 and S1 in the rat. The L6 and S1 dorsal roots were chosen because they represent an understudied site of radicular neuropathology commonly caused by disk herniations and spinal arthropathy. The L6-S1 myotome in the rat includes the bladder and external urethral sphincter; thus the dorsal roots provide sensory innervation critical for lower urinary tract function. We found significant decreases in calcitonin gene related peptide (CGRP), IB4 (isolectin B4) and VGLUT1 (vesicular glutamate transporter 1) immunoreaction product and significant increases in staining for three CSPGs: neurocan, NG2 and phosphacan, in the DREZ and DC

69

following DRC. Detailed examination of the deafferentation and changes in the CSPG environment of the lumbosacral dorsal spinal cord that result from dorsal root crush injury will allow selectively targeted strategies to assist regeneration across the DREZ and restoration of lower urinary tract function.

MATERIALS AND METHODS

ANIMAL PREPARATION

A total of 30 female Sprague–Dawley (225–250g, Harlan Sprague–Dawley, Inc.) rats were used in this study. The rats were housed with a light/dark cycle of 12/12 h, and fed *ad libitum*. Experimental procedures were approved by the UTMB Animal Care and Use Committee and were carried out in accordance with the NIH Guide for the Care and Use of Laboratory Animal.

SURGERY

Two experimental groups were examined: sham surgery (n=30) and bilateral dorsal root crush (DRC) (n=30). Rats were deeply anesthetized by intraperitoneal injection of sodium pentobarbital (0.5mg/kg) as determined by the absence of the paw withdrawal reflex to pinch and the absence of the corneal blink reflex. The dorsum was shaved, a midline incision was made, the dorsal musculature was retracted and a laminectomy performed for vertebra L1 and L2. For bilateral dorsal root crush injury, the dura was opened, the dorsal surface of the spinal cord was exposed and L6 and S1 dorsal roots were crushed by inserting one arm of a fine forceps underneath each root and compressing it twice for 10 seconds. The crush was given 5 mm from the dorsal root

entry zone and deemed successful when the opaque root turned transparent across its entire width at the site of compression. The musculature and fascia were then closed with 3-0 silk suture, followed by closure of the skin. For a control group, sham surgery was done in the same way as the injury surgery with the exception that the dorsal roots were not crushed. All surgeries and experiments were in compliance with the Institutional Animal Care and Use Committee.

IMMUNOCYTOCHEMISTRY

Immunocytochemistry was used to quantitatively estimate the density of CGRP-positive and IB4-bound sensory afferents in the dorsal spinal cord, 3, 7, 14 and 30 days post-surgery, VGLUT1-positive afferents, 30 days post-surgery and to examine the expression levels of chondroitin sulfate proteoglycans (CSPG) in the dorsal column and dorsal root entry zone (DREZ) of sham and dorsal root crush rats 7 and 30 days post-surgery. CGRP and IB4 immunocytochemistry was performed at 3, 7, 14 and 30 days post-surgery to assess the acute-to-chronic post-injury population of small diameter afferent fibers before and after the influence of any regeneration or collateral sprouting. We performed VGLUT1 immunocytochemistry only at 30 days because anti-VGLUT1 is not specific for afferents plus the afferent inflow at this level of the spinal cord is almost exclusively comprised of unmyelinated C-fibers and thinly myelinated Aδ-fibers (Yoshimura and de Groat, 1997). CSPG immunoreactivity was assessed 7 and 30 days post-surgery, similar to the work of Beggah and colleagues (Beggah, et al., 2005).

Rats (5 from each group for each time point) were deeply anesthetized with sodium pentobarbital (80 mg/kg, i.p.) and perfused intracardially with heparinized physiological saline followed by 4% cold buffered paraformaldehyde solution. After perfusion, the lumbosacral spinal cord (L6/S1) was removed immediately and post-fixed overnight in 4% paraformaldehyde, followed by cryoprotection in 30% sucrose (in PBS) over the course of several days. Prior to sectioning, spinal cords were embedded in OCT compound, and then sectioned at 30 μm. Free floating sections were washed with 0.1M PBS 3x, 10 min, shaking at room temperature. Sections were then blocked with 0.1M PBS + 0.15% Triton X-100 + 5% NGS + 0.3% BSA for 45 min, shaking at room temperature. Separate sections from each animal were used for single staining each of three sensory afferent markers and three CSPGs: CGRP (1:1000, Oncogene, rabbit polyclonal, stains peptidergic thinly myelinated Aδ- and unmyelinated C-fibers), IB4 (1:1000, Invitrogen, Alexa Flour 488 conjugated, binds non-peptidergic unmyelinated C- and thinly myelinated Aδ-fibers), VGLUT1 (1:700, Synaptic systems, conjugated to Oyster 550, stains larger diameter myelinated fibers containing the vesicular glutamate transporter subunit 1), NG2 (1:700, Chemicon, rabbit polyclonal), Neurocan (1:700, 1F6, Developmental Studies Hybridoma Bank, mouse monoclonal) and Phosphacan (1:500, 3F8, Developmental Studies Hybridoma Bank, mouse monoclonal). Sections in primary antibodies were incubated with 1% NGS overnight at 4 °C. After PBS wash, sections requiring secondary antibody labeling were incubated for 2 hours with goat anti-rabbit (1:200, Molecular Probes, CGRP and NG2) or goat anti-mouse (1:500, Molecular Probes,

Neurocan and Phosphacan). Sections from sham and DRC were processed for each time point in the same solutions in partitioned plastic cubes with screened bottoms in order to eliminate intergroup variability in concentrations and timing of reactions. Sections were collected by free-floating methods and mounted on gel-coated slides with mounting media (Vectashield). Images were captured with a Fluroview confocal microscope (Olympus-Leed) and evaluated by a computer-assisted image analysis program (MetaMorph 6.1).

To measure the density of immunopositive staining, we used the Threshold Image function in Measure of MetaMorph 6.1 to set the low and high thresholds for the immunofluorescent intensity which was determined to be a signal. After setting thresholds, the Region Measurements function was selected, the Excel spread sheet was opened, and the areas of interest were traced. The predominant areas of CGRP and IB4 staining in naïve spinal cord corresponds to laminae I and IIo, and laminae IIi and IIo of the dorsal gray matter respectively; the perimeter of these same areas was traced in naïve, sham and DRC animals. VGLUT1 staining was widespread throughout all areas of the spinal cord except the substantia gelatinosa. Collaterals of larger diameter myelinated afferents are known to terminate in medial portions of laminae III, IV and V near the midline (Brown, et al., 1981); the perimeter of this area was traced in naïve, sham and DRC animals. The perimeter of the DREZ and dorsal column regions were traced in sections stained for NG2, Neurocan or Phosphacan. The same thresholds were used to measure cell areas in all experimental groups. The density of immunopositive labeling in

73

the areas of interest transferred to Excel automatically, after which analysis could be done, including statistics. Because there was no statistically significant difference in any immunoreactions product between shams and naives, only data from shams are presented.

STATISTICAL ANALYSIS

Statistical analysis of densitometric data was performed using Two-Way (comparisons between group of rats) analysis of variance (ANOVA) with repeated measures on time factor followed by the Tukey test for multiple comparisons, using the Sigmastat program (Ver. 3.1). An alpha level of significance was set at 0.05 for all statistical tests. Data are expressed as means ± standard error (means ± SEM).

RESULTS

EFFECT OF BILATERAL DORSAL ROOT CRUSH ON DORSAL HORN CGRP-POSITIVE AFFERENTS

CGRP immunocytochemistry was used to identify and locate small diameter peptidergic sensory afferent terminals within the dorsal spinal cord and to assess the effects of a bilateral crush of the L6 and S1 dorsal roots on the lumbosacral CGRP-positive neuroarchitecture. The dorsal roots and spinal cord at this level are dominated by neurons responsible for the control of the urinary bladder and external urethral sphincter. In sections taken from sham animals, peptidergic primary afferents terminate in a wide band covering the top of the dorsal horn that is made up of lamina I and parts of lamina II (Fig. 3.1a). Some fibers pass even deeper to terminate on the dendrites of interneurons in

74

laminae III, IV and V. Bilateral dorsal root crush (DRC) at the L6 and S1 spinal level resulted in a marked reduction in CGRP-positive staining in the superficial laminae. By measuring the average density of CGRP immunofluorescence in the arcing superficial laminae of sham spinal cord sections and the equivalent area of DRC spinal cord sections we were able to quantify the deafferentation resulting from DRC (Fig. 3.1b). DRC injury caused a significant reduction in the level of CGRP staining (two way ANOVA, $p<0.001$, $F=421.31$). CGRP immunofluorescence was significantly lower in DRC spinal cord sections at every time point post-surgery (Tukey post hoc test, $p<0.001$ in all cases). Post-DRC immunofluorescence was at its lowest 7 days post-surgery (63.53 ± 9.115), down from a sham level of 196.61 ± 15.403. At day three, the clearance of CGRP-positive post-axotomy debris is not complete and a laminar band is still evident. However, at a mean level of 81.55 ± 16.557, the densitometry data is not statistically different from any of the three later time points since the staining is relatively diffuse. There is no significant difference in average density between any of the time points in DRC spinal cord, indicating no significant effect of collateral sprouting or time post-injury. The presence of regenerated CGRP-positive afferents can be seen in the rootlet attached to the section taken 30 days after a DRC (Fig. 3.1a). We also quantified the apparent disappearance of the meshwork of CGRP-positive fibers from deeper laminae, i.e. laminae III, IV and V (Fig. 3.1b). There was a significant difference between sham and DRC (two way ANOVA, $p<0.001$, $F=109.89$) and this reduction was statistically significant at each time point (Tukey post hoc test, $p<0.001$ in all cases).

75

CGRP-positive collaterals also extend down the lateral and medial border of the dorsal horn gray matter forming the later collateral pathway (LCP) and the medial collateral pathway (MCP). Fibers taking the LCP terminate at the sacral parasympathetic nucleus (SPN), where the cells bodies of parasympathetic preganglionic motor neurons innervating the urinary tract are located. Fibers that make up the MCP terminate in the most medial portions of deeper laminae on both sides of the midline. Although less numerous than CGRP-positive fibers, some IB4-bound afferents travel down the LCP to terminate on the SPN and down the MCP towards the midline. There was no apparent presence of IB4-bound fibers in the laminae below lamina II.

EFFECT OF BILATERAL DORSAL ROOT CRUSH ON DORSAL HORN IB4-BOUND AFFERENTS

IB4 cytochemistry was used to identify and locate the population of unmyelinated sensory afferent terminals within the dorsal spinal cord and to assess the effects of a bilateral crush of the L6 and S1 dorsal roots on the lumbosacral IB4-bound neuroarchitecture. In sections taken from sham animals, IB4-bound primary afferents can be seen in Lissauer's tract and almost all terminate in lamina II of the dorsal horn (Fig. 3.2a). Bilateral dorsal root crush (DRC) at the L6 and S1 spinal level resulted in a marked reduction in IB4 staining in lamina II. By measuring the average density of immunolabelled IB4 fluorescence in lamina II of sham spinal cord sections and the equivalent area of DRC spinal cord sections we were able to quantify the deafferentation resulting from DRC (Fig 3.2b). DRC injury caused a significant reduction in the level of IB4 staining (two way ANOVA, $p<0.001$, $F=367.2$). The level of IB4 staining was

significantly lower in DRC spinal cord sections at every time point post-surgery (Tukey post hoc test, p<0.001 in all cases). The density of IB4 staining was at its lowest 7 days following DRC (58.279 ± 9.474), down from an equivalent sham value of 194.408 ± 6.204.

IB4 coincidentally binds to microglia and to macrophages and monocytes of peripheral origin. Microglial-bound IB4 was identified diffusely throughout the gray matter 3 days post-surgery in the DRC spinal cord. In the susequent three post-surgical time points (7, 14 and 30 days) the dorsal column (DC) region of the spinal cord became increasingly bound by IB4. This increase in immune cell-bound IB4 staining was quantified using densitometry (Fig. 3.2c). There was a statistically significant increase in IB4 staining in the DC of DRC spinal cord as a result of injury (two way ANOVA, p<0.001, F=236.37), there was a significant effect of time post-surgery (two way ANOVA, p<0.001, F=55.77) and there was a strong statistical correlation between the two (two way ANOVA, p<0.001, F=49.467). There was no statistical difference between sham and DRC 3 days post-surgery where the average density of IB4 staining in the DC was 7.883 ± 0.998 and 5.781 ± 0.642 respectively. There is a significant difference between sham and DRC at 7, 14 and 30 days post-surgery (Tukey post hoc test, p<0.001 in all cases). The density of IB4 staining was at its highest 30 days post-surgery (173.95 ± 17.684), however, there is no significant difference between densities in DRC DC at 14 and 30 days post-surgery.

77

VGLUT1 immunocytochemistry was used to identify and locate larger diameter myelinated sensory afferent terminals within the dorsal spinal cord and to assess the effects of a bilateral crush of the L6 and S1 dorsal roots on the lumbosacral CGRP-positive neuroarchitecture. In sections taken from sham animals, VGLUT1-positive primary afferents can be seen diffusely in the spinal gray matter, with the exception of the substantia gelatinosa, Lissauer's tract and medial portions of the marginal plexus (Fig. 3.3a). The descending axons of the dorsal corticospinal tract are positive for VGLUT1. Bilateral dorsal root crush (DRC) at the L6 and S1 spinal level resulted in a reduction in VGLUT1 staining, most noticeably in medial laminae III, IV and V (MLIII-V). By measuring the average density of VGLUT1 immunofluorescence in MLIII-V of sham spinal cord sections and the equivalent area of DRC spinal cord sections we were able to quantify the deafferentation resulting from DRC (Fig 3.3b). DRC injury caused a significant reduction in the level of VGLUT1 staining (one way ANOVA, $p=0.001$, $F=19.66$). There is no evidence for the termination of VGLUT1-positive afferents on the SPN.

EFFECT OF BILATERAL DORSAL ROOT CRUSH ON CSPG EXPRESSION IN THE SPINAL CORD

Immunocytochemistry was used to locate, quantify and assess any temporal changes in the expression levels of three chondroitin sulfate proteoglycans; neurocan, NG2 and phosphacan. In spinal cord sections taken from sham animals the majority of neurocan-positive staining is within the deeper laminae of the dorsal horn and absent

from white matter (Fig 3.4a). Bilateral dorsal root crush (DRC) at the L6 and S1 spinal level resulted in an increase in neurocan staining in both the dorsal root entry zone (DREZ) and dorsal column (DC). By measuring the average density of neurocan immunofluorescence in the DREZ and DC of sham spinal cord sections and the equivalent area of DRC spinal cord sections we were able to quantify the changes in neurocan expression at an acute and chronic time point following DRC (Fig 3.4b and 3.4d). There was a statistically significant, approximately 4-fold increase in staining for neurocan in both the DREZ and DC (two way ANOVA, $p<0.001$, $F=277.389$ and $p<0.001$, $F=334.32$ respectively). There was a significant difference in DC but not DREZ neurocan levels between DRC animals at 7 and 30 days post surgery; falling from 91.454 ± 4.368 to 70.409 ± 5.25 respectively (two way ANOVA, $p=0.002$, $F=10.42$).

In sham spinal cord, NG2-positive glia were present throughout the spinal cord gray matter in the form of stellate-shaped cells bearing radial processes. NG2-positive glia were present to a lesser extent in white matter where they and their processes orient along axonal tracts (Fig. 3.5a). Following DRC there is a significant increase in the amount of NG2-positive staining above the sham baseline in both the DREZ and DC (two way ANOVA, $p<0.001$, $F=184.46$ and $p<0.001$, $F=203.59$). There is no significant effect of time post-injury in either location (Fig. 3.5b).

In sham spinal cord, phosphacan is found most abundantly in the gray matter (Fig 3.6a). Following DRC there is a relatively modest but significant increase in phosphacan staining in both the DREZ and DRC (two way ANOVA, $p<0.001$, $F=50.28$ and $p<0.001$,

79

F=37.1 respectively) (Fig 3.6b and 3.6c). There is a significant effect of time post-surgery on the density of DC phosphacan immunofluorescence between 7 and 30 days in DRC spinal cord sections (two way ANOVA, p=0.047, F=4.19). For all three CSPGs there was a less robust post-injury increase in DC compared to the DREZ.

DISCUSSION

In the present study, we examined the effects of dorsal root crush (DRC) on the dorsal spinal cord, with respect to primary afferent central projections and CSPG expression. We report the following: 1) significant reductions in the laminar populations of CGRP-positive and IB4-bound primary afferents in the superficial dorsal horn and a significant depletion in projections to the collateral pathways and to the sacral parasympathetic nucleus (SPN) following DRC at all four post-surgical time points; 2) a significant reduction in VGLUT1-positive staining in deeper laminae 30 days post-surgery; 3) increased IB4, which also labels microglia, macrophages and monocytes in the dorsal root entry zone (DREZ) and dorsal column (DC) region; and 4) significant increases in staining for the three CSPGs selected (neurocan, NG2 and phosphacan) in the DREZ and DC following DRC.

CENTRAL PROJECTIONS OF PRIMARY AFFERENT SENSORY NEURONS FOLLOWING DRC

Following axotomy the distal segment of the severed axon degenerates, is phagocytized, thus, vacating the original projection territory. DRC injury successfully produces a significant reduction in immunoreactivity for three primary afferent populations within the dorsal spinal cord: CGRP, IB4 and VGLUT1. Antibodies for

CGRP label a population of unmyelinated and thinly myelinated peptidergic sensory fibers that terminate predominantly in laminae I and II, with some fibers coursing further into the deeper dorsal horn (Gibson *et al.* 1984). This group of sensory afferents is thought to consist mainly of Aδ-fibers (Light and Perl 1979). Aδ-fibers are responsible for the conduction of sharp pain, cold and pressure (McGlone and Reilly 2009, Willis and Coggeshall 1991) the sham spinal cord CGRP-positive collaterals exit Lissauer's tract, form a broad band of dense terminations in laminae I and II and also pass laterally and medially around the dorsal horn gray matter to terminate on preganglionic parasympathetic nucleus neurons and the dorsal commissure region respectively; these tracts are termed the lateral collateral pathway (LCP) and medial collateral pathway (MCP) respectively. CGRP-positive afferents were also seen extending diffusely into deeper laminae of the dorsal horn, i.e., laminae III, IV and V. Following DRC, CGRP immunoreactivity was significantly reduced in laminae I and II, and in the deeper laminae of the dorsal horn. Importantly, there was complete deafferentation of the MCP and LCP and no evidence of CGRP staining around Onuf's nucleus (sacral parasympathetic nucleus), which is a functionally significant structure at this level of the lumbosacral spinal cord, responsible for the micturition reflex.

DRC does not completely remove all immunoreactivity for CGRP in the superficial laminae. CGRP-positive staining does appear to increase with time but this apparent change is not statistically significant. Any minor increase in CGRP staining in laminae I and II is likely due to sprouting from the intact collaterals of afferents that enter

81

the spinal cord rostral and caudal to the injury and that pass within Lissauer's tract. Collateral sprouting is a commonly reported phenomenon in the dorsal spinal cord following rhizotomy (Liu and Chambers 1958, Goldberger and Murray 1974, McNeill and Hulsebosch 1987, McNeill *et al*. 1990, McMahon and Kett-White 1991, McNeill *et al*. 1991, LaMotte and Kapadia 1993). The pattern of residual CGRP immunoreactivity that was found in this study following DRC injury, compares closely to that produced by complete multiple dorsal root transections (Averill *et al*. 1995, Belyantseva and Lewin 1999, Hannila and Kawaja 2005, Brumovsky *et al*. 2006, Brumovsky *et al*. 2007, Hampton *et al*. 2007, Runyan *et al*. 2007). Thirty days following DRC, CGRP-positive axonal profiles can be seen in the attached dorsal rootlet. The profiles, which were not present at earlier time points, are interpreted to be new axons of dorsal root ganglion central processes that regenerated through the crushed dorsal root and were halted at the DREZ. These processes displayed the enlarged distal terminals characteristic of abortive regeneration at the DREZ glial scar (Carlstedt 1985, Liuzzi and Lasek 1987, Hannila and Kawaja 2005).

Isolectin B4 is a 114 kDa protein isolated from seeds of the African legume, Griffonia simplicifolia that binds, non-immunologically, to a population of unmyelinated sensory afferents that terminate in lamina II (Silverman and Kruger 1990, Kitchener *et al*. 1993). This group of IB4-binding fine fibers is composed mainly of C-fibers (Rethelyi 1977, Gobel *et al.* 1981). C-fibers are responsible for the conduction of dull burning pain, warmth, itch and pleasurable touch (Willis and Coggeshall 1991, McGlone and Reilly

82

2009). In the sham spinal cord IB4 binds to a broad band of dorsal horn gray matter corresponding to the substantia gelatinosa. The significant absence in staining between lamina II IB4 staining and the staining present in Lissauer's tract, corresponds to lamina I. It should be noted that there is extensive overlap of CGRP and IB4 staining in the L6-S1 dorsal spinal cord and that CGRP has a thicker dorsoventral distribution at this level compared to the thoracic spinal cord (Christensen and Hulsebosch 1997). Colocalization of IB4 and CGRP occurs at L6-S1, the spinal region to which the majority of bladder and external urethral sphincter sensory afferents preject (Hwang *et al*. 2005, Rethelyi *et al.* 2008), suggesting that, in a region of spinal cord where visceral afferent input outweighs cutaneous afferent input, the conventional separation of peptidergic and non-peptidergic fine fibers does not apply (Petruska *et al*. 2000, Petruska *et al.* 2002). IB4-bound fibers form the LCP and MCP and terminate densely on Onuf's nucleus. Following DRC, there is a significant reduction in IB4 staining in lamina II and a complete absence of IB4 staining on Onuf's nucleus. Similar to observations 30 days following DRC in the CGRP immunostained sections, there is also evidence of IB4-binding to the enlarged distal terminals characteristic of abortive regeneration at the DREZ glial scar.

Anti-VGLUT1 binds to the vesicular glutamate transporter-1 which is present in many large-sized, CGRP-negative, dorsal root ganglion neurons (Varoqui *et al*. 2002, Li *et al*. 2003, Oliveira *et al*. 2003, Todd *et al*. 2003). These coarse, myelinated fibers travel medially within the dorsal column and send collaterals to innervate the medial portions of the deeper dorsal horn laminae III, IV and V (Alvarez *et al*. 2004, Brumovsky *et al.* 2007,

83

Neumann *et al.* 2008). This population of afferents is composed mainly of Aαβ myelinated fibers (Brown 1982, Brown and Noble 1982). Aαβ myelinated fibers are responsible for the conduction of low-threshold mechanoreceptive and proprioceptive information (Willis and Coggeshall 1991, McGlone and Reilly 2009). In the sham spinal cord, the gray matter had considerable VGLUT1 immunoreactivity, with the notable exception of the substantia gelatinosa, or lamina II. The highest density of staining was seen in lamina III and medial portions of laminae IV and V. Following DRC, there was a significant reduction in VGLUT1-positive staining in medial laminae III, IV and IV. The patterns of VGLUT1 immunoreactivity in uninjured and DRC rat spinal cord, closely match that described in complete transection models in both the rat (Alvarez *et al.* 2004) and mouse (Brumovsky *et al.* 2007). It is important to note that at this level of the spinal cord (L6-S1), there is no evidence of VGLUT1 immunoreactivity on Onuf's nucleus, suggesting that larger-diameter myelinated afferents are not involved in the micturition reflex, confirming previous work that indicates that thinly myelinated Aδ-fibers are involved in normal micturition and C-fibers are involved in transmitting noxious stimuli from the bladder (Janig *et al.* 1991, Sengupta and Gebhart 1994) and stimulation of either can trigger micturition (Moss *et al.* 1990, Moss *et al.* 1997, Zagorodnyuk *et al.* 2006).

DRC RESULTS IN AN INCREASE IN NON-NEURONAL IB4-BINDING IN THE DORSAL SPINAL CORD.

In spinal cord sections from DRC animals, IB4 binds to more than just a subpopulation of primary afferents. IB4 binds to cells that express a particular galactose moiety (Goldstein and Winter, 1999), i.e.; all microglia, and macrophages and monocytes

of peripheral origin (Streit and Kreutzberg 1987, Ivacko *et al*. 1996, Yrjanheikki *et al*. 1998, Wang *et al*. 2002). Following DRC injury, microglial labeling is diffuse in the gray matter, as previously reported following complete transection of multiple dorsal roots (Belyantseva and Lewin 1999). Microglial and other phagocytic cell types contribute to the time-dependent increase in IB4-labeling in the DREZ and dorsal column (DC), where the degenerating remains of the central processes and collaterals of dorsal root ganglion cells are located. Macrophages from the bloodstream and microglia from the surrounding tissue migrate here to clean up the debris as would be the response to any CNS damage (Fawcett and Asher 1999). The same non-neuronal IB4 staining was reported in the dorsal columns and DREZs of chronically rhizotomized mice, colocalized with glial fibrillary acid protein (GFAP), suggesting that IB4 also binds to the fibrous processes of activated astrocytes which form the gliotic scar at the DREZ (Runyan *et al.* 2007).

INCREASED DENSITY OF CSPGS IMMUNOREACTIVITY FOLLOWING DRC

We demonstrated significant increases in the density of neurocan, NG2 and phosphacan immunoreactivity in the DREZ and DC, both acutely and chronically following DRC injury. Additionally, there was a statistically significant effect of time post-injury in reducing the density of neurocan-positive and phosphacan-positive staining in the DC of DRC spinal cord. Neurocan is produced by reactive astrocytes in the DREZ following a complete transection rhizotomy (Beggah *et al.* 2005), while neurocan mRNA levels increase transiently in both the DREZ and DC (Waselle *et al*. 2009). We confirm

85

that immunoreactivity for neurocan protein remains elevated at both acute and chronic time points.

NG2 is a CSPG found on the surface of a population of glial cells that until recently had been assumed to be just oligodendrocyte precursor cells (OPCs); however, up to 50% of cells positive for NG2 do not appear to be normally involved in generating oligodendrocytes, astrocytes or neurons (Rivers *et al.* 2008). The functions of non-proliferating NG2-glia in the adult CNS are unknown and are believed to represent a new class of glia; simply NG2-glia, or as Butt and colleagues have named them, synantocytes (Butt *et al.* 2002, Butt *et al.* 2005). NG2 immunoreactivity remains elevated in the DREZ and DC following complete transection of dorsal root (Zhang *et al.* 2001), a pattern we confirm and extend in the present study with a DRC injury model.

Phosphacan is expressed in the CNS as a secreted splice variant of the gene encoding the extracellular domain of the transmembrane receptor-type tyrosine phosphatase (RPTPβ) (Maurel *et al.* 1994). We demonstrate a significant increase in phosphacan immunoreactivity in both the DREZ and DC following DRC. However, previous work has shown that following complete transection there is no apparent change in the expression of mRNA for phosphacan in either the DREZ or DC (Waselle *et al.* 2009). Phosphacan is notably decreased in expression acutely post-injury in other models of CNS injury (McKeon *et al.* 1999, Tang *et al.* 2003). RPTPβ has three isoforms: the long and short membrane bound isoforms and a third consisting of the extracellular domain of the long form of RPTPβ minus the transmembrane domain; this third secreted

isoform is also called phosphacan (Garwood *et al*. 2001). The antibody used in the present study recognizes both phosphacan, the secreted extracellular domain, and RPTPβζ, the long transmembrane isoform of this glycoprotein. It is possible that the source of phosphacan in the DREZ and DC in the present study is from migrating cells infiltrating this degenerating environment. A good candidate cell type would be oligodendrocytes or OPCs which have been shown to express phosphacan in culture (Sakurai *et al.* 1996, Schnadelbach *et al.* 1998).

The increased expression of all three CSPGs in the DREZ and DC contributes to the post-injury growth-inhibitory environment present at the PNS/CNS border (Carlstedt 1985). The precise mechanism mediating axonal growth inhibition by CSPGs is beginning to emerge. The inhibitory nature of CSPGs is reflected in growth cone collapse and repulsion, and the formation of dystrophic axonal retraction bulbs (Tom *et al*. 2004). It is known that inhibition of CSPGs is due to the actions of the chondroitin sulfate (CS) side chains attached to the protein core, since chondroitinase ABC digestion of the CS side chains promotes sprouting, regeneration and restored function in many cases (Bradbury *et al.* 2002, Houle *et al.* 2006, Pizzorusso *et al.* 2006, Tester and Howland 2008, Cafferty *et al.* 2008). The sulfation pattern of the individual CS side chains modulates neuronal outgrowth in vitro (Properzi and Fawcett 2004). However, removal of the CS side chains does not always remove inhibition implying that the protein core contributes to inhibition (Dou and Levine 1994, Schmalfeldt *et al.* 2000). Because of the lack of a neuronal CSPG receptor, various non-receptor mediated mechanisms were

proposed such as by negatively charged sulfates (Gilbert *et al.* 2005) or the occlusion of substrate adhesion molecules (McKeon *et al.* 1995). Recent work has suggested that neuronal transmembrane protein tyrosine phosphatase-σ (PTPσ), a member of the leucocyte antigen-related (LAR) subfamily, can act as a receptor for CSPGs (Shen *et al.* 2009). PTPs are highly expressed by the growth cones of neurons (Baker and Macagno 2000), PTPσ is presynaptically involved in excitatory synaptic formation (Kwon *et al.* 2010) and has long been suggested to regulate cell-cell and cell-extracellular matrix interactions. Tyrosine phosphorylation of intracellular signaling molecules occurs in a diverse range of cellular processes but the exact transduction mechanism that follows PTPσ-CSPG binding is not known.

In conclusion, dorsal root crush injury as a model of dorsal rhizotomy/deafferentation results in the decreased presence of three different labels of primary afferents in the dorsal horn, similar to observations after multiple complete dorsal root transections. We also demonstrate that the CSPGs, neurocan, NG2 and phosphacan showed both short-term and long-term increases in immunoreactivity in the DREZ and DC following injury that reflects the development and maintainance of an inhibitory environment. Thus, we have been able to show that in the lumbosacral spinal cord it is possible to produce an effective rhizotomy and stimulate astroglial responses by crushing the L6 and S1 dorsal roots on a par with that seen following complete transection. Not only does the crush model act as a more clinically relevant model of cauda equina injury, it preserves the connection between the DRG and spinal cord,

thereby providing a potential pathway for successful regeneration of dorsal root axons given appropriate therapeutic interventions.
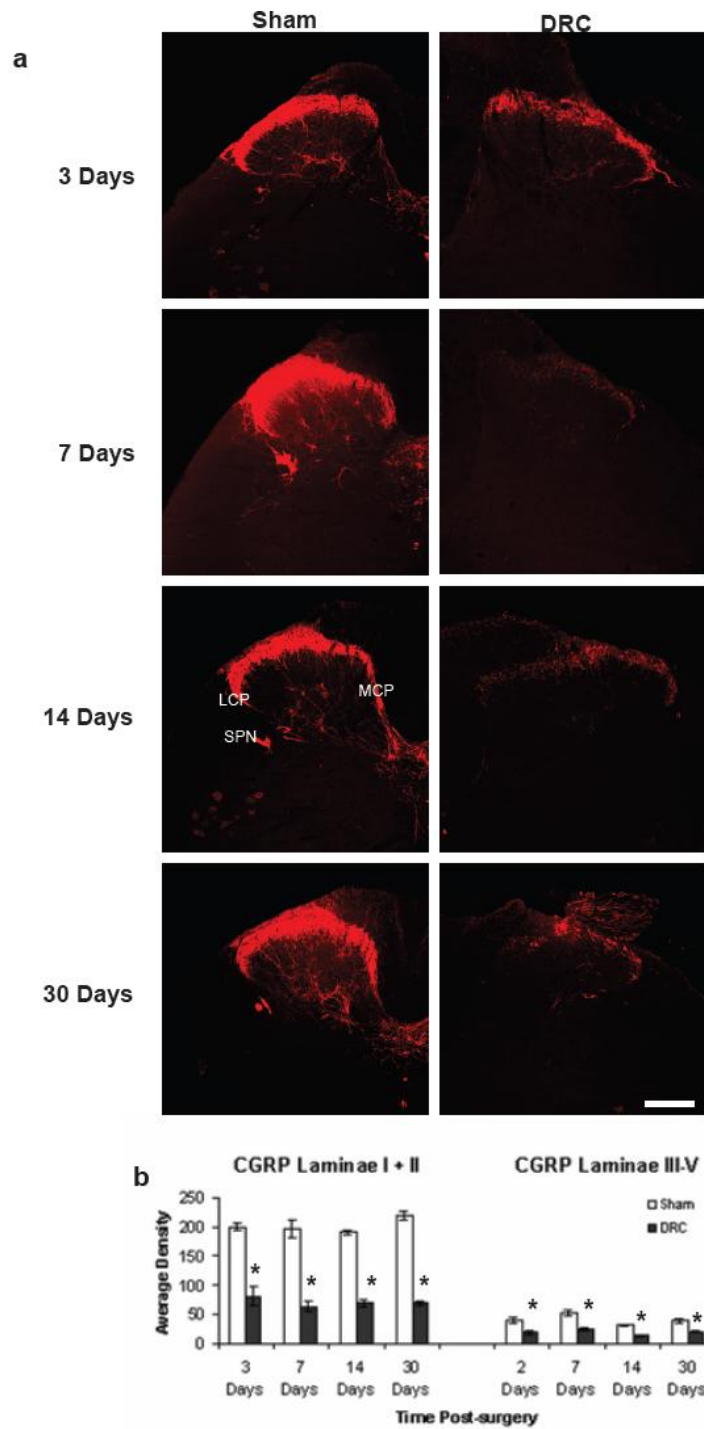
Figure 8 The effects of DRC on CGRP density in the dorsal horn.
Shown in a are confocal immunofluoresent micrographs displaying the dorsal horn of sections from the L6-S1 spinal cord stained for CGRP. Sections were taken from rats 3, 7, 14 and 30 days following sham surgery (left column) or a bilateral dorsal root crush (DRC; right column). Sections on the same post-

90

surgical day were taken from different animals. The dashed white line indicates the approximate outline of the dorsal horn gray matter. In the unlesioned lumbosacral spinal cord CGRP-positive afferent nerve endings terminate in laminae I and II, extend along the lateral collateral pathway (LCP) to the sacral parasympathetic nucleus (SPN) and along the medial collateral pathway to the dorsal gray commissure. CGRP-positive afferents also extend deeper into the dorsal horn to terminate on interneurons in laminae III-V. Dorsal root crush results in a marked reduction in CGRP in the superficial laminae, deeper laminae and complete deafferentation of the SPN. The section from 30 days post-DRC has a rootlet still attached that is full of regenerated CGRP positive afferents unable to cross the dorsal root entry zone. The reduction in the density of CGRP-positive staining in laminae I and II, and III-V is demonstrated graphically in b for all four post-surgical time points in this study. DRC significantly reduced CGRP-positive staining, compared to sham in both the superficial dorsal horn (two way ANOVA, $p < 0.001$, F=421.31) and the deeper dorsal horn (two way ANOVA, $p < 0.001$, F=109.89). * indicates a significant difference between sham and DRC at individual time points (Tukey post hoc test, $p < 0.001$ in all cases). Error bars = Standard Error of the mean. Scale bar = 200 μm.
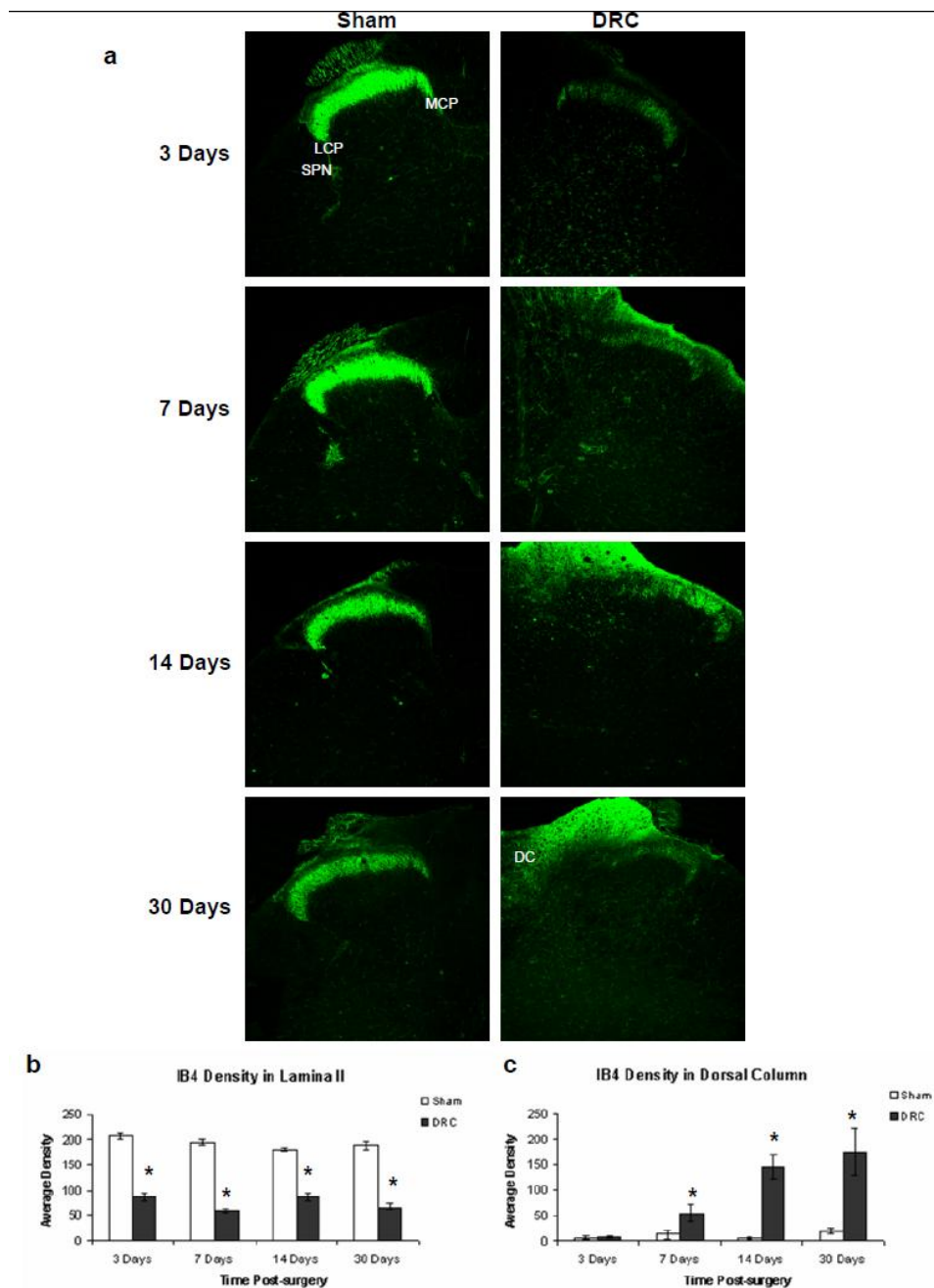
Figure 9 The effects of DRC on IB4 density in the dorsal horn.

Shown in a are confocal immunofluoresent micrographs displaying the dorsal horn of sections from the L6-S1 spinal cord labeled with IB4. Sections were taken from rats 3, 7, 14 and 30 days following sham surgery (left column) or a bilateral dorsal root crush (DRC; right column). Sections on the same post-surgical day were taken from different animals. The dashed white line indicates the approximate outline of the dorsal horn gray matter. In the unlesioned lumbosacral spinal cord IB4-labeled afferent nerve endings terminate in lamina II, extend along the lateral collateral pathway (LCP) to the sacral parasympathetic nucleus (SPN) and along the medial collateral pathway to the dorsal gray commissure, but to a lesser extent than CGRP-

92

positive fibers. Dorsal root crush results in a marked reduction in IB4 in lamina II and complete deafferentation of the SPN. The reduction in the density of IB4-bound unmyelinated afferents in lamina II is demonstrated graphically in b for all four post-surgical time points in this study. DRC significantly reduced IB4 staining, compared to sham in lamina II (two way ANOVA, $p<0.001$, F=367.2) * indicates a significant difference between sham and DRC at individual time points (Tukey post hoc test, $p<0.001$ in all cases). IB4 also binds microglia, and peripheral macrophages and monocytes. IB4 labeled microglia most notably in the gray matter of the DRC spinal cord 3 days post-surgery. There is also an increase in IB4 binding in the dorsal column region of the spinal cord over time post-surgery. This time-dependent increase in IB4 staining is graphically demonstrated in c for all four post-surgical time points in this study. There is a significant difference between sham and DRC dorsal column staining as a result of both the injury and time post-surgery (two way ANOVA, $p<0.001$, F=236.37 and $p<0.001$, F=55.77 respectively). * indicates a significant difference between sham and DRC at individual time points (Tukey post hoc test, $p<0.001$ in all cases). Error bars = Standard Error of the mean. Scale bar = 200 μm.
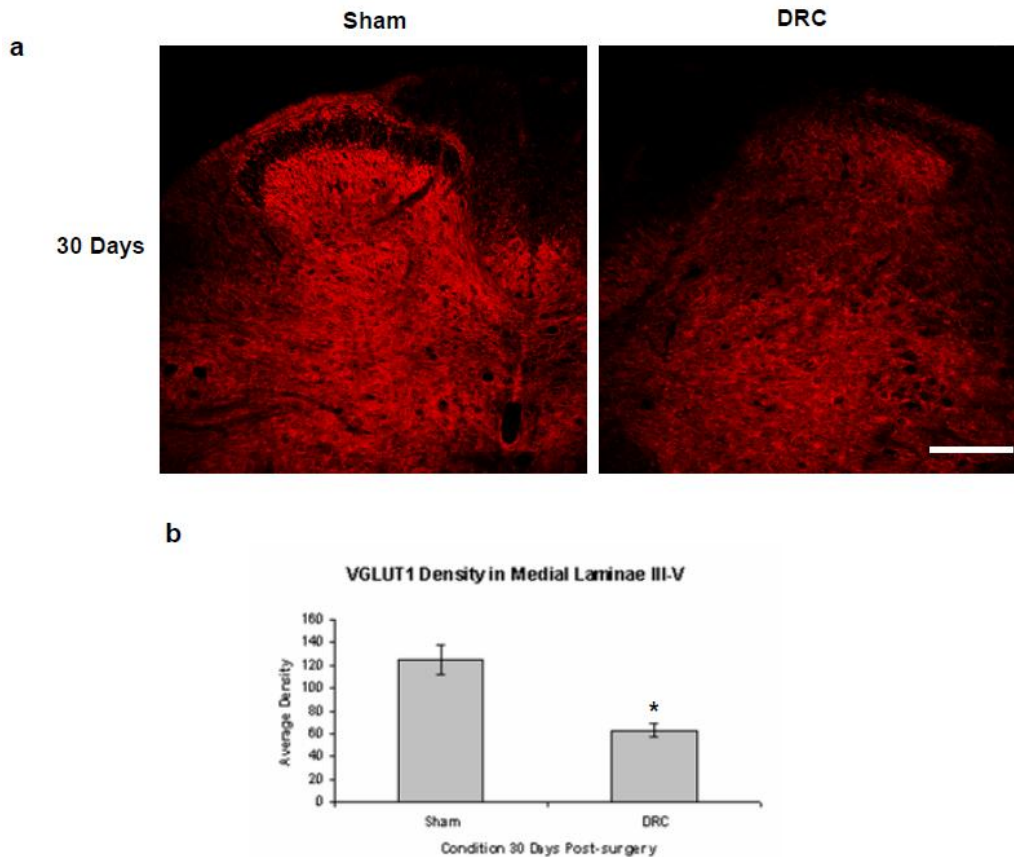

Figure 10 The effects of DRC on VGLUT1 density in the dorsal horn.
Shown in a are confocal immunofluoresent micrographs displaying the dorsal horn of sections from the L6-S1 spinal cord stained for VGLUT1. Sections were taken from rats 30 days following sham surgery (left) or a bilateral dorsal root crush (DRC; right). Both sections were taken from different animals. The dashed white line indicates the approximate outline of the dorsal horn gray matter. In the unlesioned lumbosacral spinal cord VGLUT1-positive staining is present throughout most of the dorsal and ventral gray matter with the notable exception of the superficial laminae. 30 days following DRC there was a reduction in VGLUT1-positive staining in the medial portions of laminae III-V (MLIII-V) in the dorsal horn. The reduction in the density of VGLUT1-positive myelinated afferents in this area 30 days post-surgery is

demonstrated graphically in b. DRC significantly reduced VGLUT1 staining, compared to sham in medial laminae III-V (* one way ANOVA, p=0.001, F=19.66). Error bars = Standard Error of the mean. Scale bar = 200 μm.
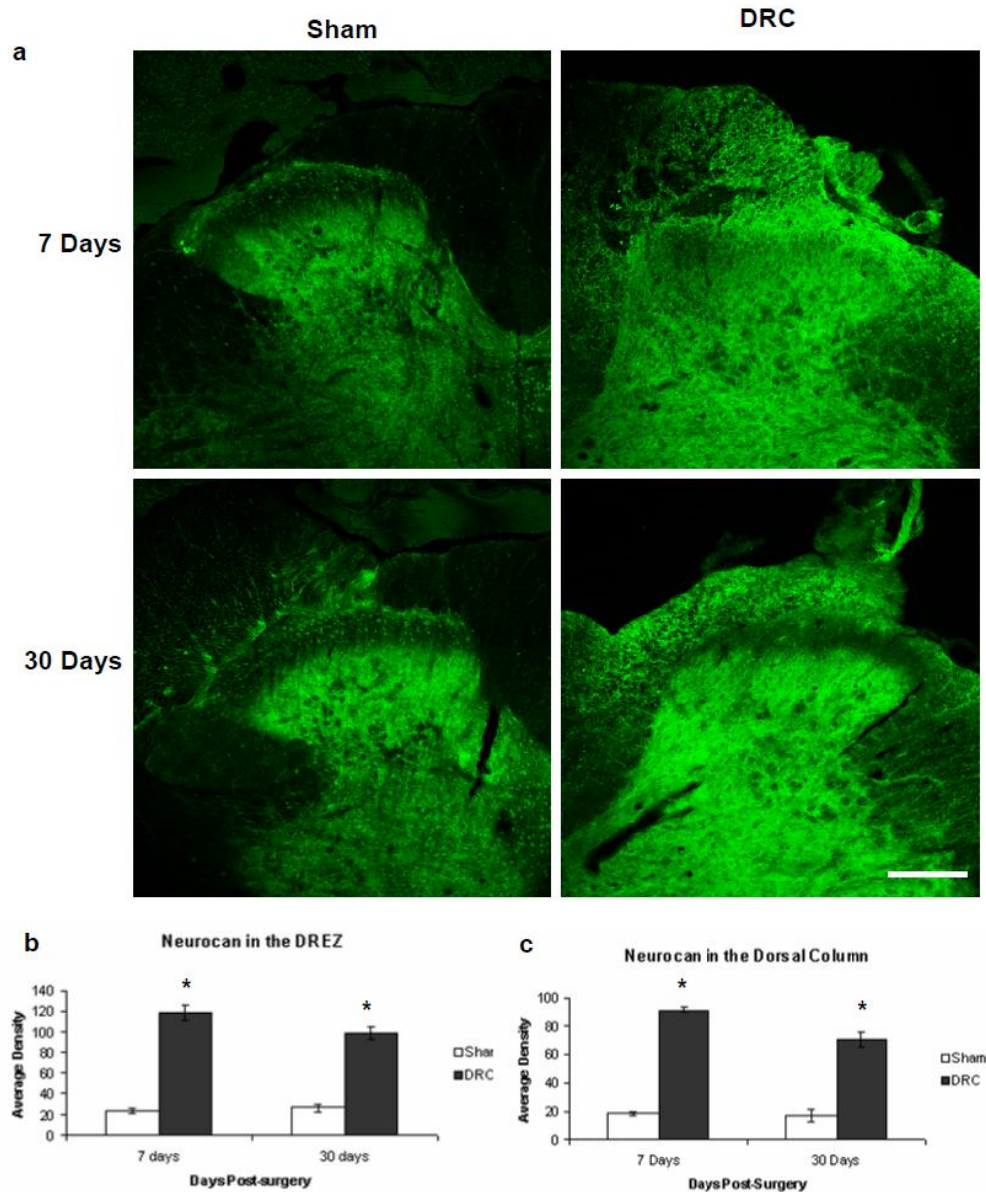
Figure 11 The effects of DRC on NEUROCAN density in the dorsal horn.
Shown in a are confocal immunofluoresent micrographs displaying the dorsal horn of sections from the L6-S1 spinal cord labeled for neurocan. Sections were taken from rats 7 and 30 days following sham surgery (left) or a bilateral dorsal root crush (DRC; right). Sections on the same post-surgical day were taken from different animals. The dashed white line indicates the approximate outline of the dorsal horn gray matter. In the unlesioned lumbosacral spinal cord, neurocan-positive staining is present in the deeper laminae of the dorsal horn and also the ventral horn gray matter but absent from white matter tracts. Dorsal root crush

results in a marked increase in neurocan in the dorsal root entry zone (DREZ) and dorsal column (DC). The increase in the density of DREZ neurocan-positive staining is demonstrated graphically in b for both post-surgical time points in this study. There is a significant difference between sham and DRC DREZ staining as a result of injury (two way ANOVA, $p < 0.001$, $F = 277.389$). * indicates a significant difference between sham and DRC at individual time points (Tukey post hoc test, $p < 0.001$ in all cases). The increase in the density of DC neurocan-positive staining is demonstrated graphically in c for both post-surgical time points in this study. There is a significant difference between sham and DRC dorsal column staining as a result of injury (two way ANOVA, $p < 0.001$, $F = 334.32$). There is a statistically significant drop in the level of DC neurocan-positive staining in DRC animals from 7 to 30 days post-surgery (# two way ANOVA, $p = 0.002$, $F = 10.4$). * indicates a significant difference between sham and DRC at individual time points (Tukey post hoc test, $p < 0.001$ in all cases). Error bars = Standard Error of the mean. Scale bar = 200 μm.
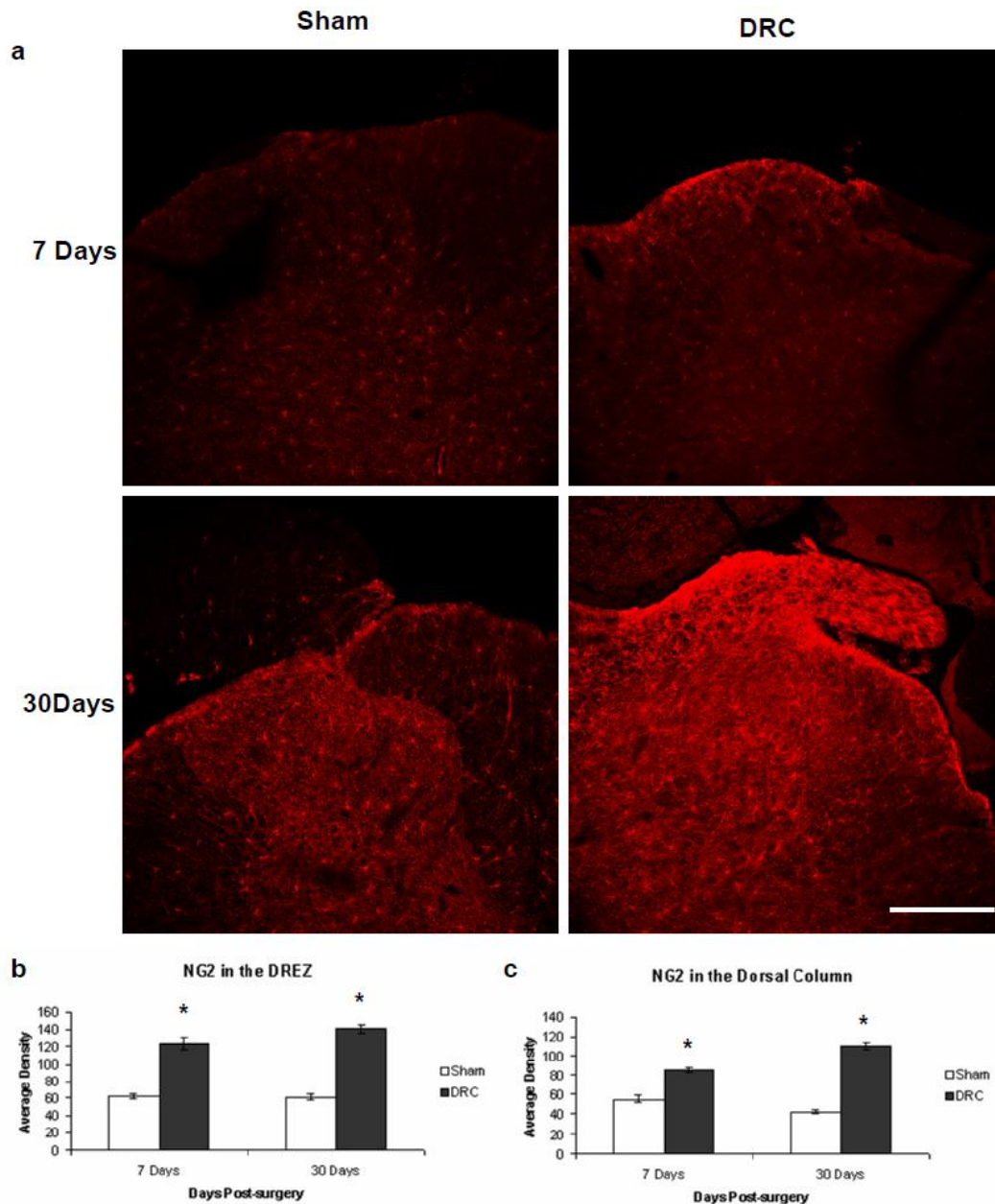
Figure 12 The effects of DRC on NG2 density in the dorsal horn.
Shown in a are confocal immunofluoresent micrographs displaying the dorsal horn of sections from the L6-S1 spinal cord labeled with NG2. Sections were taken from rats 7 and 30 days following sham surgery (left) or a bilateral dorsal root crush (DRC; right). Sections on the same post-surgical day were taken from different animals. The dashed white line indicates the approximate outline of the dorsal horn gray matter. In the unlesioned lumbosacral spinal cord, NG2-positive glia were present throughout the spinal cord gray matter in the form of stellate-shaped cells bearing radial processes. NG2-positive glia were present to a lesser extent in white matter where they and their processes orient along axonal tracts. Dorsal root crush results in a marked increase in NG2 in the dorsal root entry zone (DREZ) and dorsal column (DC). The increase in the density of DREZ NG2-positive staining is demonstrated graphically in b for both post-

96

surgical time points in this study. There is a significant difference between sham and DRC DREZ staining as a result of injury (two way ANOVA, $p<0.001$, $F=184.46$). * indicates a significant difference between sham and DRC at individual time points (Tukey post hoc test, $p<0.001$ in all cases). The increase in the density of DC NG2-positive staining is demonstrated graphically in c for both post-surgical time points in this study. There is a significant difference between sham and DRC dorsal column staining as a result of injury (two way ANOVA, $p<0.001$, $F=203.59$). * indicates a significant difference between sham and DRC at individual time points (Tukey post hoc test, $p<0.001$ in all cases). Error bars = Standard Error of the mean. Scale bar = 200 μm.
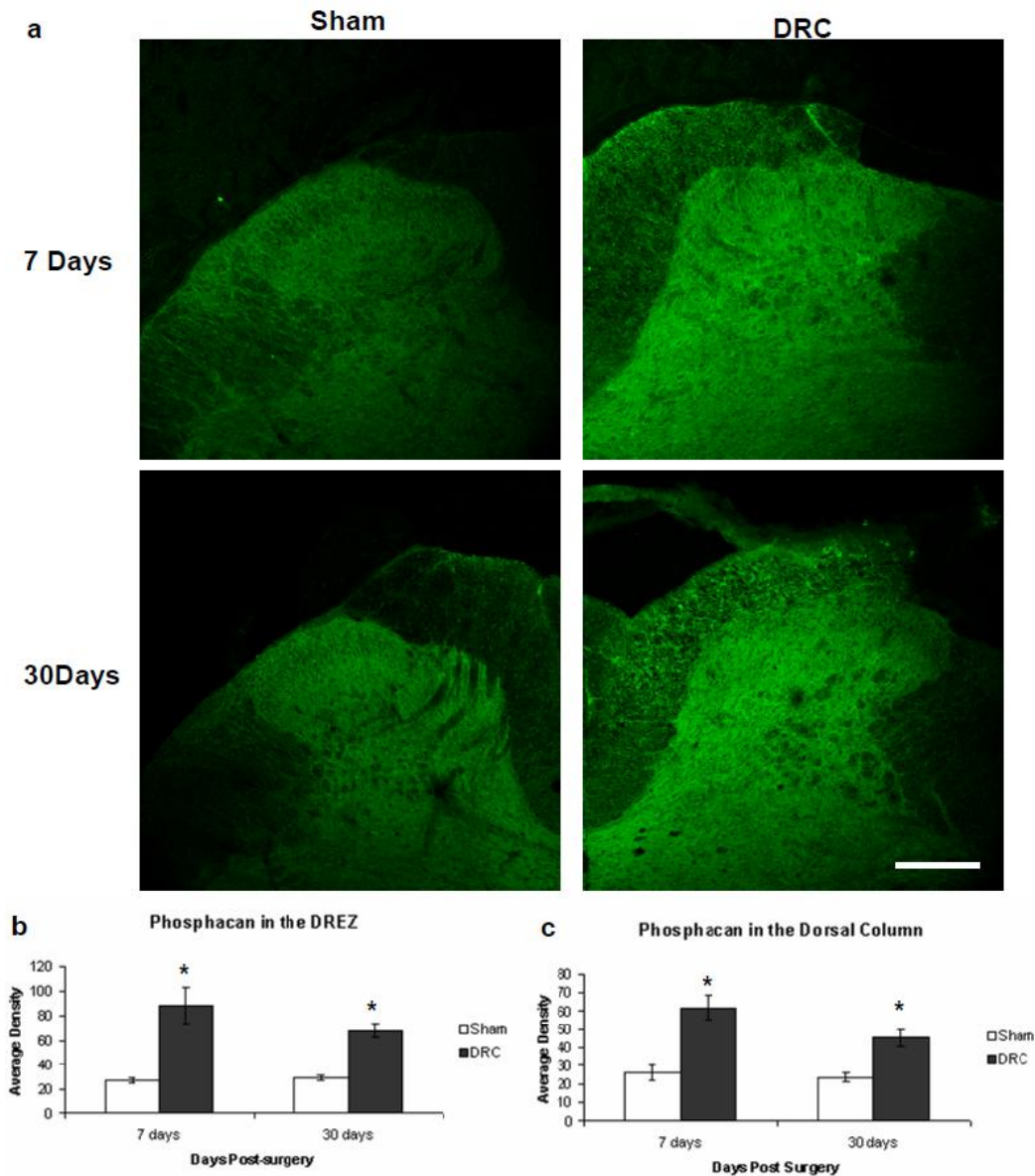

Figure 13 The effects of DRC on CGRP density in the dorsal horn.
Shown in a are confocal immunofluoresent micrographs displaying the dorsal horn of sections from the L6-S1 spinal cord labeled with phosphacan. Sections were taken from rats 7 and 30 days following sham surgery (left) or a bilateral dorsal root crush (DRC; right). Sections on the same post-surgical day were

97

taken from different animals. The dashed white line indicates the approximate outline of the dorsal horn gray matter. In the unlesioned lumbosacral spinal cord, phosphacan-positive staining is present throughout most of the gray matter but mostly absent from white matter tracts. Dorsal root crush results in a marked increase in phosphacan in the dorsal root entry zone (DREZ) and dorsal column (DC). The increase in the density of DREZ phosphacan-positive staining is demonstrated graphically in b for both post-surgical time points in this study. There is a significant difference between sham and DRC DREZ staining as a result of injury (two way ANOVA, $p<0.001$, $F=50.28$). * indicates a significant difference between sham and DRC at individual time points (Tukey post hoc test, $p<0.001$ in both cases). The increase in the density of DC phosphacan-positive staining is demonstrated graphically in c for both post-surgical time points in this study. There is a significant difference between sham and DRC dorsal column staining as a result of injury (two way ANOVA, $p<0.001$, $F=37.1$). There is a statistically significant drop in the level of DC phosphacan-positive staining in DRC animals from 7 to 30 days post-surgery (# two way ANOVA, $p=0.047$, $F=4.19$). * indicates a significant difference between sham and DRC at individual time points (Tukey post hoc test, $p<0.001$ in all cases). Error bars = Standard Error of the mean. Scale bar = 200 μm.

CHAPTER 4: *THE EFFECTS OF ARTEMIN ON AXONAL REGENERATION, BLADDER FUNCTION AND CSPG EXPRESSION*

INTRODUCTION

Nerve root trauma resulting from lumbar disc herniation, lumbar spinal stenosis and any injury that results in narrowing of the spinal canal or intervertebral foraminae is likely to result in urologic dysfunction (Cheek *et al.* 1973, Jones & Moore 1973, Kostuik *et al.* 1986, Mosdal *et al.* 1979, Susset *et al.* 1982, Deen *et al.* 1994, Bodner *et al.* 1990). The effects of ventral root injury, source of efferent innervation for bladder function have been described (Hoang *et al.* 2006b, Hoang *et al.* 2006a) as well as methods of surgical repair (Carlstedt *et al.* 1986, Hallin *et al.* 1999, Gu *et al.* 2004, Hoang et al. 2006b) which are largely satisfactory in recovery of function. However, deafferentation presents a clinical challenge. The significant dysfunction associated with bladder deafferentation due to dorsal root injury is described by our group and others (Pascual *et al.* 2002, Rooney & Hulsebosch 2010). Disruption of normal afferent function is known to reduce bladder continence and compliance (de Groat 1997, Wein 2005) and contributes to lower urinary tract dysfunction. A dysfunctional lower urinary tract results in life threatening complications such as hydronephrosis, mineral deposits in the kidneys and bladder and vesiculourethral reflux (Yoshiyama *et al.* 1999, Benevento & Sipski 2002), as well as producing detrusor muscle hypertrophy, incontinence and recurrent urinary tract infections (de Groat 1995, Kruse *et al.* 1993). Thus research that leads to understanding the mechanisms that contribute to improved bladder function after cauda equina is critically important.

99

Following injury to dorsal roots, centrally directed afferent axons will regenerate from their peripherally located cell bodies as far as the dorsal root entry zone (DREZ) but will fail to penetrate this barrier and cross into the CNS due to the abundance of inhibitory factors and absence of appropriate trophic support at this location (Carlstedt 1985b, Carlstedt 1985a, Carlstedt 1988, Carlstedt 1997, Priestley *et al.* 2002). The post-injury growth-inhibitory environment present at the DREZ is created by oligodendrocytes, reactive astrocytes, microglia and macrophages which produce inhibitory protein like Nogo, myelin associated glycoproteins (MAGs) and chondroitin sulfate proteoglycans (CSPGs), contributing to regeneration failure and growth cone collapse (Filbin 1995, Fournier & Strittmatter 2001, McKeon *et al.* 1999, Horn *et al.* 2008). Interventions that reportedly improve regeneration of sensory axons into and across the DREZ include treatment with neurotrophin-3 (NT-3) (McPhail *et al.* 2007) and injection of Chondroitinase ABC (Steinmetz *et al.* 2005, Massey *et al.* 2006) to digest the chondroitin sulfate proteoglycans that are upregulated in the DREZ after dorsal root injury (Beggah *et al.* 2005) [reviewed by Silver and Miller (Silver & Miller 2004)]. However, restoration of sensorimotor function has been limited.

A promising new therapy is the systemic administration of artemin which promoted regeneration across the DREZ and led to restoration of forelimb function in a model of deafferentation produced by dorsal root crushes in the cervical region (Wang *et al.* 2008). However, the mode of action of artemin in regeneration across the DREZ is not well understood. We hypothesized that systemic artemin administration following

lumbosacral dorsal root injury would promote functional regeneration of pelvic and pudendal afferents across the DREZ and contribute to improved bladder and external urethral sphincter function. In this study, we also tested if systemic administration of artemin had any effect on the expression of the CSPGs neurocan, NG2 and phosphacan in the DREZ.

MATERIALS AND METHODS

ANIMAL SURGERY, ARTEMIN ADMINISTRATION AND TRACING STUDIES

A total of 30 female Sprague–Dawley (225–250g, Harlan Sprague–Dawley, Inc.) rats were used in this study. The rats were housed with a light/dark cycle of 12/12 h, and fed *ad libitum*. Experimental procedures were approved by the UTMB Animal Care and Use Committee and were carried out in accordance with the NIH Guide for the Care and Use of Laboratory Animals.

Experimental Design: Four experimental groups were examined: Group 1 had sham surgery and was injected with saline vehicle (n=20). Group 2 had sham surgery and was injected with artemin at a dosage of 1mg/kg of body weight (n=20). Group 3 had a bilateral dorsal root crush of the L6 and S1 roots and was injected with saline vehicle (n=20). Group 4 had a bilateral dorsal root crush of the L6 and S1 roots and was injected with artemin at a dosage of 1mg/kg of body weight (n=20). The time points that were used are as follows: 3 days, 7 days, 14 days and 30 days post-surgery. Animals receiving artemin treatment were injected on the same day as surgery and then 2, 5, 7, 9 and 11

101

days post-surgery. Dosage and administration were based on the work of Wang and colleagues (Wang *et al.* 2008).

Surgery: Rats were deeply anesthetized by intraperitoneal injection of sodium pentobarbital (0.5mg/kg) as determined by the absence of the paw withdrawal reflex to pinch and the absence of the corneal blink reflex. The dorsum was shaved, a midline incision was made, the dorsal musculature was retracted and a laminectomy performed for vertebra L1 and L2. For bilateral dorsal root crush injury, the dura was opened, the dorsal surface of the spinal cord was exposed and L6 and S1 dorsal roots were crushed by inserting one arm of a fine forceps underneath each root and compressing it twice for 10 seconds. The crush was given 5 mm from the dorsal root entry zone and deemed successful when the opaque root turned transparent across its entire width at the site of compression. The musculature and fascia were then closed with 3-0 silk suture, followed by closure of the skin. For a control group, sham surgery was done in the same way as the injury surgery with the exception that the dorsal roots were not crushed. Artemin (1mg/kg of body weight; Biogen Idec, Cambridge, MA) or vehicle was given in six subcutaneous systemic injections over the first 11 days following bilateral DRC of the L6 and S1 dorsal roots or sham surgery. The artemin/vehicle was administered blindedly and always began on the same day as surgery. All surgeries and experiments were in compliance with the Institutional Animal Care and Use Committee.

Tracing Experiment: For the tracing experiment, a different experimental design was adopted. Three groups were examined: 1) Sham surgery plus bilateral injection of

102

viral solution (2μl) containing adeno-associated viral vector encoding green fluorescent protein (AAV-GFP) (10E11 vg titer; University of North Carolina, Vector Core) into the dorsal root ganglia (DRG) of L6 and S1 (n=5), 2) Unilateral DRC of L6 and S1, bilateral AAV-GFP injection into the DRGs and vehicle treatment (n=5) and 3) unilateral DRC, bilateral AAV-GFP injection and artemin treatment (n=5). Artemin/vehicle administration was carried out as described above. The AAV-GFP was given 30 days incubation time to allow for anterograde filling of intact and/or regenerated central processes of the DRG neurons. Rats were deeply anesthetized with sodium pentobarbital (80 mg/kg, i.p.) and perfused intracardially with heparinized physiological saline followed by 4% cold buffered paraformaldehyde solution. After perfusion, the lumbosacral spinal cord (L6/S1) was removed immediately and post-fixed overnight in 4% paraformaldehyde, followed by cryoprotection in 30% sucrose (in phosphate buffered saline; PBS) for 3 days. Prior to sectioning, spinal cords were embedded in OCT compound, and then sectioned at 30 μm. Free floating sections were washed with 0.1M PBS 3x, 10 min on an orbital shaker (Daigger) at 4rpm, at room temperature. Sections were collected by free-floating methods and mounted on gel-coated slides with mounting media (Vectashield). Images were captured with a Fluroview Radiance 2100 Confocal Microscope (Biorad) and evaluated by a computer-assisted image analysis program (MetaMorph 6.1). The number of GFP-filled axonal cross-sections in the dorsal horn were counted both ipsilateral and contralateral to the DRC injury in all three groups.

E. coli host BL21(DE3) plysS (Biogen Idec), expressing wild-type rat artemin containing an N-terminal 10 histidine tag with an enterokinase cleavage site, were lysed in phosphate-buffered saline (PBS, 5 mM NaPO4, 150 mM NaCl, pH 6.5) using a Gaulin press. After centrifugation (30 min at 4,700g) to isolate inclusion bodies, the pellets were washed twice with 20 volumes buffer (0.02 M Tris-HCl at pH 8.5 and 0.5 mM EDTA) and then washed twice with the same buffer containing Triton X-100 (2%, vol/vol) followed by two additional buffer washes without detergent. The final pellets were suspended in 50 ml of 6 M guanidine hydrochloride, 0.1 M Tris-HCl at pH 8.5, 0.1 M dithiothreitol, and 1 mM EDTA, and homogenized using a polytron homogenizer followed by overnight stirring at room temperature (18–21 ˚C). The solubilized proteins were clarified by centrifugation before denaturing chromatography through 5.5 liters of Superdex 200 preparative resin (GE Life Sciences), equilibrated with 0.05 M glycine/H3PO4 at pH 8.0 and eluted with 2 M guanidine hydrochloride at 20 ml min−1. Fractions containing artemin were pooled and concentrated approximately fivefold to 250 ml using an Amicon 2.5-liter stirred cell concentrator.

After filtration to remove any precipitate, the concentrated protein was subjected to renaturing sizing chromatography through Superdex 200 equilibrated with 0.1 M Tris-HCl at pH 7.8, 0.5 M guanidine hydrochloride, 8.8 mM reduced glutathione and 0.22 mM oxidized glutathione. The column was run using 0.5 M guanidine hydrochloride at 20 ml min−1. Fractions containing renatured artemin were identified by SDS-PAGE to determine the presence of the dimeric product under nonreducing conditions, pooled, and

104

stored at 4 1C for further processing. The N-terminal histidine tag was removed enzymatically with lysyl-endopeptidase to produce 113 amino-acid artemin. The protein sample was made with 0.1 M NaCl, 25 mM HEPES at pH 8.0, and 0.15 M guanidine hydrochloride and lysyl-endopeptidase (WAKO) added at a 1:600 (wt/wt) ratio of protease to artemin. The samples were stirred at room temperature for 2 h, and the digest was subjected to Ni-NTA chromatography (Qiagen). The flow through from this chromatography step was subjected to further purification using SP-Sepharose (GE Life Sciences) eluted with 5 mM phosphate containing 150 mM NaCl. Eluted artemin was aliquoted and stored at -70 ˚C.

The bioassay for the activity of artemin is based on the work of Harvey *et al.* (2010) demonstrating regeneration of sensory afferents across a distal root crush.

IMMUNOCYTOCHEMISTRY

Immunocytochemical techniques were used to quantitatively measure the density of calcitonin gene related peptide (CGRP) immunoreaction product (CGRP-IR), isolectin B4 (IB4) histochemistry and vesicular glutamate transporter-1 (VGLUT1) immunoreaction product (VGLUT1-IR) in sensory afferents in the dorsal spinal cord as well as the expression levels of chondroitin sulfate proteoglycans (CSPGs) in the dorsal root entry zone (DREZ). CGRP and VGLUT1 immunocytochemistry and IB4 histochemistry were performed at 3, 7, 14 and 30 days post-surgery to assess the acute-to-chronic post-injury population of afferent fibers before and after the influence of any regeneration or collateral sprouting.

Rats (n=5 from each of the four injury/treatment groups at 3, 7 14 and 30 days post-surgery) were deeply anesthetized with sodium pentobarbital (80 mg/kg, i.p.) and perfused intracardially with heparinized physiological saline followed by 250mL of 4% cold buffered paraformaldehyde solution. After perfusion, the lumbosacral spinal cord (L6/S1) was removed immediately and post-fixed overnight in 4% paraformaldehyde, followed by cryoprotection in 30% sucrose (in PBS) for 3 days. Prior to sectioning, spinal cords were embedded in OCT compound, and then sectioned at 30 μm. Free floating sections were washed with 0.1M PBS 3x for 10 min, on an orbital shaker (Daigger) at 4rpm, at room temperature. Sections were then blocked with 0.1M PBS + 0.15% Triton X-100 + 5% NGS + 0.3% BSA for 45 min, on anorbital shaker (Daigger) at 4rpm, at room temperature. Separate sections from each animal were used for single staining each of three sensory afferent markers and three CSPGs: CGRP (1:1000, Oncogene, rabbit polyclonal, labels peptidergic thinly myelinated Aδ- and unmyelinated C-fibers), IB4 (1:1000, Invitrogen, Alexa Flour 488 conjugated, binds non-peptidergic unmyelinated C- and thinly myelinated Aδ-fibers), VGLUT1 (1:700, Synaptic systems, conjugated to Oyster 550, labels larger diameter myelinated fibers containing the vesicular glutamate transporter subunit 1), NG2 (1:700, Chemicon, rabbit polyclonal), Neurocan (1:700, 1F6, Developmental Studies Hybridoma Bank, mouse monoclonal) and Phosphacan (1:500, 3F8, Developmental Studies Hybridoma Bank, mouse monoclonal). Sections in primary antibodies were incubated with 1% NGS overnight at 4 °C. After PBS wash, sections requiring secondary antibody labeling were incubated for 2 hours with goat anti-rabbit

106

(1:200, Molecular Probes, CGRP and NG2) or goat anti-mouse (1:500, Molecular Probes, Neurocan and Phosphacan). Sections from all four experimental groups were processed for each time point in the same solutions in partitioned plastic cubes with screened bottoms in order to eliminate intergroup variability in concentrations and timing of reactions. Sections were collected by free-floating methods and mounted on gel-coated slides with mounting media (Vectashield). Images were captured with a Fluroview confocal microscope (Olympus-Leed) and evaluated by a computer-assisted image analysis program (MetaMorph 6.1).

To measure the density of immunoreaction product, we used the Threshold Image function in Measure of MetaMorph 6.1 to set the low and high thresholds for the immunofluorescent intensity which was determined to be a signal. After setting thresholds, the Region Measurements function was selected, the Excel spread sheet was opened, and the areas of interest were traced. The predominant areas of CGRP-IR and IB4-histochemistry in sham spinal cord corresponds to laminae I and IIo, and laminae IIi and IIo of the dorsal gray matter respectively; the perimeter of these same areas was traced in sham and DRC animals. The sacral parasympathetic nucleus (or intermediolateral nucleus) receives innervation from both CGRP-IR and IB4-histochemically labeled afferent fibers; the perimeter of this area was traced in sham and DRC animals. VGLUT1-IR was widespread throughout all areas of the spinal cord except the substantia gelatinosa. Collaterals of larger diameter myelinated afferents are known to terminate in medial portions of laminae III, IV and V near the midline (Brown,

107

et al., 1981); the perimeter of this area was traced in sham and DRC animals. The perimeter of the DREZ and dorsal column regions were traced in sections stained for NG2, neurocan or phosphacan. The same thresholds were used to measure cell areas in all experimental groups. The density of immunoreaction product in the areas of interest transferred to Excel automatically, after which analysis could be done, including statistics. The density of immunoreaction product and histochemistry were quantified and expressed in immunodensity units.

URODYNAMICS

Recording: Lower urinary tract function was assessed using a non-surgical urodynamic procedure that allowed rapid collection of simultaneous bladder pressure and sphincter electromyography (EMG) data over a number of consecutive voiding cycles. In preparation for bladder cystometry and sphincter EMG recordings, animals were anesthetized by intraperitoneal injection of sodium pentobarbital and placed in a supine position. A catheter (PE-50, ~10cm) was inserted into the intravesical space of the bladder through the urethra. Accurate insertion depth was ensured by first making a black mark 2.5cm from the end of the catheter, the catheter was inserted to the mark and then secured to the base of the animals' tail with sticky tape to prevent catheter displacement. Two, fine Teflon coated platinum-iridium wire electrodes (0.002'' stripped, 0.0045'' coated, A-M Systems Inc., Carlsborg, WA) were then placed percutaneously into the muscle of the external urethral sphincter (EUS) along the side of the catheter using a 30 gauge needle as an insertion cannula. In detail, the electrodes were threaded through a 30

108

gauge needle and hooked at the stripped end forming an insertion assembly. Two assemblies were inserted along either side of the urethral catheter until the muscular resistance of the EUS was encountered and the assemblies were advanced a few more millimeters into the muscle. The needle cannula for each assembly was withdrawn leaving only the hooked wire electrode embedded internally within the EUS musculature. The animals were then restrained and allowed to recover 3 to 4 hrs from the anesthetic. The animals were fully awake, responding to auditory stimulus and the eye blink and foot pinch test. To ensure each recording session began with an empty bladder, each bladder was emptied by manual expression before connecting the catheter to the infusion pump, allowing urine to flow out through the catheter. Bladder intravesical pressure (IVP) was recorded by infusing warm saline (0.22 mL/min) through the catheter and into the bladder using an infusion pump (Harvard Apparatus, Holliston, MA). During the bladder detrusor contractions, fluid is released by flowing around the catheter in the urethra. The signal from the attached pressure transducer (Biopac Systems Inc., Goleta, CA) in the form of resistance to the flow of saline through the catheter, is amplified and sampled using an analogue-to-digital converter (Biopac Systems Inc., Goleta, CA) and acquired on a computer using Acq*Knowledge*® Software (Biopac Systems Inc., Goleta, CA). The EMG activity recorded from the urethral sphincter electrodes was amplified using a separate amplifier attached to the same analogue-to-digital converter as above allowing for simultaneous acquisition of EMG and intravesical pressure.

Before beginning a recording session and connecting the catheter to the infusion pump tubing, the rat's bladder was manually expressed. The bladder was deemed empty when urine stopped flowing from the catheter. Recordings were carried out on the awake, restrained animal over maximum period of 20 minutes at 3, 7, 14 and 30 days post-surgery. The animals did not have their bladders expressed manually at any time post injury because they retain a limited ability to micturate and this would interfere with the development of post-injury changes to the bladder.

Urodynamic analysis: Data for a single micturition cycle was gathered at the beginning of each recording session by noting the volume of saline infused into the empty bladder to elicit the first voiding event (Volume Threshold). The volume of saline voided was collected, measured and subtracted from the infused volume to give the volume of saline remaining inside the bladder (Residual Volume). Voiding efficiency was calculated as the percentage of the infused volume that was successfully voided.

Recording sessions lasted 20 mins per animal. The inter-contraction interval (ICI) was calculated by averaging the length of time between the end of one bladder contraction and the beginning of the next for each 20 min period. Bladder compliance, which described the relationship between change in bladder volume and change in bladder pressure, was calculated using the equation $\Delta V/\Delta P$, where ΔV is the volume of saline infused into the bladder during each ICI and ΔP is the difference between the baseline pressure and the intravesical pressure (IVP) at the moment a contraction begins. A high $\Delta V/\Delta P$ value indicates poor compliance during which high IVPs were recorded at

110

low volumes and in the absence of detrusor muscle activity. Physiologically normal animals show compliance values closer to zero. To analyze sphincter EMG activity, the waveform data was integrated by rectifying it to provide an interpretable waveform that can be easily compared between groups. The Acq*Knowledge*® software collects the absolute value of the input data prior to summing, and a plot of the waveform's mean obtained that envelope over 20 samples. The average filling phase EMG amplitude is expressed as a percentage of the average voiding phase EMG amplitude. The frequency of the phasic bursts characteristic of the EUS of the rat was measured in Hz or bursts per second, during voiding phase of the micturition cycle.

Physical analysis of bladder: Following transcardial perfusion, a lower abdominal incision was made and the bladder was dissected out, blotted dry and wet weights were recorded.

ASSESSMENT OF PAIN

Rats from the four injury/treatment groups (Sham/Vehicle, Sham/Artemin, DRC/Vehicle and DRC/Artemin) were tested for their response to a mechanically evoked stimulus 7 days post-surgery (the midpoint of the treatment schedule) and 30 days post-surgery (the final time point in the present study). Rats from each group (n=5 per group) were placed in the testing chambers on top of a wire mesh and acclimated 20 minutes prior to testing. A 26g Von Frey filament was used to probe the lower abdomen, in the suprapubic abdominal region (hypogastric and lower umbilical regions) between the mammillary lines. Each rat was probed 20 times at 5 minutes intervals on each test day.

Biting at the probe and/or licking the probed location was recorded as a noxious (painful) response to the mechanical stimulus. If there was no response the stimulus was considered non-noxious. The reactions to each mechanical stimulus were expressed as a percentage of the total number of stimuli in each test group.

STATISTICAL ANALYSIS

Statistical analysis of densitometric, urodynamic and morphological data was performed using Two-Way (comparisons between group of rats) analysis of variance (ANOVA) with repeated measures on time factor followed by the Tukey test for multiple comparisons, using the Sigmastat program (Ver. 3.1). An alpha level of significance was set at 0.05 for all statistical tests. Data are expressed as means $\pm$ standard error (means $\pm$ SE).

RESULTS

PRIMARY AFFERENT IMMUNOCYTOCHEMISTRY, HISTOCHEMISTRY AND ANTEROGRADE TRACING

Bilateral dorsal root crush (DRC) at the L6 and S1 spinal level resulted in significant acute and chronic decreases in CGRP-IR in the superficial laminae and the sacral parasympathetic nucleus (SPN) (Fig4.1a, DRC/Veh) compared to sham. Systemic artemin treatment resulted in a significant increase in CGRP-IR in superficial laminae, lateral collateral pathway (LCP) and SPN by 30 days post-surgery (Fig4.1a, DRC/Artn) compared to vehicle treated DRC animals. There was a 4-fold significant decrease in the density of CGRP-IR in the superficial laminae, down to 54.17 ± 3.37 in DRC animals

compared to 224.61 ± 7.27 in sham animals (p<0.05). CGRP-IR density remained significantly low in the DRC/Veh group throughout the post-surgical period. Systemic artemin treatment of DRC animals produced a significant increase in the density of CGRP-IR in the superficial laminae at 14 and 30 days post-surgery compared to DRC/Veh (Tukey post hoc test, p<0.05 and p<0.001 respectively). CGRP density increased significantly from 56.11 ± 12.58 at 7 days, to 87.91 ± 6.26 and 89.82 ± 5.65 at days 14 and 30 post-surgery respectively, a value that is approximately 52% of sham. Systemic artemin administration resulted in a significant increase in the density of CGRP-IR at the SPN as a result of time post injury (Fig 4.1c; p<0.05, F=4.814 by Two way ANOVA). There was a significant increase in CGRP-IR at the SPN of artemin treated animals relative to vehicle treated animals 30 days post surgery (Tukey post hoc test, p<0.05). Systemic artemin administration had no effect on the density of CGRP-IR in sham animals. There was no significant difference between Sham/Vehicle and Sham/ARTN at any time point post-surgery.

In sections taken from sham animals, IB4-bound reaction product was visualized in lamina II of the dorsal horn, along the LCP and in the SPN (Fig 4.2a, Sham). Bilateral DRC at the L6 and S1 spinal level resulted in a marked acute and chronic reduction in IB4-bound reaction product in lamina II (Fig 4.2a, DRC/Veh) compared to sham. In the artemin treated group, there was a significant increased IB4-bound reaction product in lateral portions of lamina II and on the SPN 30 days post injury (Fig 4.2a, DRC/Artn) compared to DRC/Veh (p<0.05). DRC injury resulted in a significant 4- to 7-fold

113

decrease in IB4-bound reaction product, from a mean sham value of 142.5 ± 11.95 to a DRC/Vehicle of 15.29 ± 1.72 and a DRC/ARTN level of 12.63 ± 0.47 at 14 days post-surgery. Systemic artemin treatment resulted in an increase in IB4 staining in the DRC/ARTN group by 30 days post-surgery, significantly higher than that of the DRC/Vehicle group (Tukey post hoc test, $p < 0.05$). Systemic artemin resulted in a 20% increase in the density of IB4-bound reaction product. The density of IB4-bound reaction product continued to decrease in the DRC/Vehicle group throughout the post-surgical period. Administering artemin to sham animals did not produce a significant difference in IB4-bound reaction product between Sham/Vehicle and Sham/ARTN groups. Systemic artemin administration had no significant effect on the density of IB4-bound reaction product at the SPN.

There was no significant effect of systemic artemin treatment on the density of VGLUT1-IR in DRC animals (data not shown). Unilateral DRC results in a significant reduction of GFP-filled collaterals in spinal cord white or gray matter ipsilateral to the injury (Fig 4.3b) compared to sham and contralateral to the injury. Systemic artemin treatment following unilateral DRC resulted in a significant increase in GFP-filled afferents the dorsal horn and dorsal column (Fig 4.3 c + d; $p < 0.05$). The artemin treated group had an average of 14.6 ± 1.48 GFP-filled collateral cross-sections in the dorsal horn 30 days post-surgery compared to zero in the vehicle treated group.

Representative urodynamic recordings, shown in Figure 2, illustrate micturition cycles of a sham animal (Fig 4.4a), a DRC/Vehicle animal (Fig 4.4b) and a DRC/Artn animal (Fig. 4.4c) 30 days post-surgery over 2.5 minutes of a 20 minute recording period of continuous saline infusion. There were no statistically significant differences in urodynamic recordings from animals in the sham/vehicle compared to sham/Artn groups. In sham animals (Fig 4.4a) during the filling phase, intravesical bladder pressure did not increase with increasing volume (< 10 mmHg) until a voiding contraction was initiated. Low level tonic EUS EMG activity (< 0.01 Volts) was maintained until voiding initiated high amplitude EMG phasic bursting. After voiding, intravesical pressure fell back to baseline and EMG activity reduced to a low amplitude baseline level. At a constant infusion rate, such cycles of filling and voiding occurred approximately once every 2.5 to 3 min in the uninjured animal.

In the DRC/Vehicle group (Fig 4.4b) during the filling phase, intravesical bladder pressure increased with increasing volume (up to 20 mmHg) relative to baseline pressure and higher amplitude EUS EMG activity than sham animals was recorded (>0.05 Volts) throughout the post-surgical period. In the DRC/Artn group (Fig 4.4c) during the filling phase, intravesical bladder pressure increased with increasing volume also, but the dysfunctional EUS EMG activity was significantly reduced.

Bladder Outcome Measures: Injury resulted in a significant reduction in bladder compliance in both DRC/Veh and DRC/Artn groups compared to sham (two way ANOVA, $p < 0.001$, $F = 11.53$). The average compliance of sham animals was 0.327

115

mL/mmHg ± 0.11 compared to an average post-injury compliance of 0.105 mL/mmHg ± 0.0246 (Fig 4.5a). There is no significant difference between the Sh/Veh group and the Sh/Artn group, and there no significant difference between the DRC/Veh group and the DRC/Artn group. DRC injury resulted in a significant trend towards longer ICIs with time post injury (two way ANOVA, $p<0.001$, F=11.43). The average DRC ICI increased from 106.03 sec ± 20.84 at 3 days post surgery to 287.98 sec ± 62.205 at 30 days post-surgery (Fig 4.5b). There is no significant difference between the Sh/Veh group and the Sh/Artn group, and there no significant difference between the DRC/Veh group and the DRC/Artn group.

External Urethal Sphincter Outcome Measures: DRC injury resulted in high amplitude EUS EMG activity during the filling phase of the micturition cycle (Fig 4.4b, Fig 4.6a) compared to baseline. The average filling phase EMG amplitude of rats in Sh/Veh and Sh/Artn groups was between 42.65% ± 10.17% and 56.35% ± 6.32% of their voiding phase EMG amplitude throughout the whole experimental period. The average filling phase EMG amplitudes at 3 days after DRC injury in the DRC/Veh and DRC/Artn groups were 96.78% ± 13.18 and 116.92% ± 34.17 of the voiding phase EMG respectively. By 30 days post-surgery the filling-to-voiding ratio of DRC rats treated with artemin was not significantly different to Sh/Veh or Sh/Artn and was significantly lower than that of DRC/Veh rats ($p=0.002$; Tukey post hoc test) which remained elevated at 112.98% ± 9.53.

Single Cystometry. The average residual volume in the DRC groups 3 days post-surgery was 1.5 mL ± 0.48 mL, compared to 0.12 mL ± 0.04 mL in the sham groups (Fig. 4.7a). The DRC/Veh group maintained a significantly increased post void residual volume compared to sham groups throughout the experimental period, with a residual volume of 1.62 mL ± 0.29 mL at 30 days post-surgery, which was significantly different compared to the residual volume of DRC/Artn rats 30 days post-surgery, at 0.26 mL ± 0.08 mL ($p<0.05$, Tukey post hoc test). By 30 days post-surgery, the average threshold volume of DRC/Veh rats was significantly greater than that of the other three groups ($p<0.05$ in all cases by Tukey post hoc test) (Fig 4.7b). Treating DRC rats with artemin significantly reduced the average threshold volume so that it was not significantly different to the sham groups by 30 days post-surgery. The efficiency of a bladder voiding in the DRC/Artn group increased to 85% by thirty days post-surgery compared to 45% in the DRC/Veh group (Table 1).

Physical Analysis of the Bladder: The average bladder weight of the DRC/Veh group (0.172g ± 0.021) was significantly increased compared to the average bladder weight in the sham groups (0.118g ± 0.012; two way ANOVA, $p<0.05$, F=0.472) The reduction in the average bladder weight of DRC/ARTN rats demonstrated a significant effect of time post-surgery (two way ANOVA, $p<0.006$, F=5.647), dropping to sham weight by 14 days post-surgery. The bladder weight of the DRC/Veh group was significantly greater than the bladder weight of the DRC/Artn group 14 days post surgery ($p<0.05$, Tukey post hoc test).

CHONDROITIN SULFATE PROTEOGLYCAN EXPRESSION IN THE DREZ

Neurocan: In spinal cord sections taken from sham animals, neurocan immunoreaction product (neurocan-IR) was restricted to the perineuronal nets of interneuronal cell soma and dendrites in the gray matter (Fig 4.9b Sham). Bilateral dorsal root crush (DRC) at the L6 and S1 spinal level resulted in significantly increased neurocan-IR in the dorsal column and the dorsal root entry zone (DREZ) (Fig 4.9b DRC). Neurocan-IR extended more distally into the dorsal root in the DRC groups compared to the sham groups (Fig 4.9a). There was a time dependent expression profile of neurocan-IR in the DREZ following DRC in the DRC/Veh and DRC/Artn groups. There was a 6-fold increase in neurocan-IR 3 days post-surgery. Neurocan-IR density peaked 7 days post surgery (7-fold greater than sham) and decreased to 3-fold greater than sham at both 14 and 30 days post-surgery.

NG2: NG2–IR density increased in the DREZ following bilateral DRC and the glia limitans extended distally into the injured root (Fig 4.10b DRC). Following DRC there was a 64% increase in NG2-IR density in the DREZ of the DRC/Veh and DRC/Artn groups. There was no significant change in neurocan-IR with time post injury or as a result of systemic artemin treatment (Fig 4.10a).

Phosphacan: Following DRC there is a marked increase in phosphacan-IR density in both the DREZ and dorsal column. Phosphacan-positive glia limitans extended distally into the injured root (Fig 4.11b DRC). There was a delay in the phosphacan-IR density increase in the DRC/ARTN group. Three days post-surgery there was a

118

significant 2-fold increase in DREZ phosphacan-IR density in DRC/Vehicle rats, compared to the DRC/ARTN group (p<0.001, Tukey post hoc test). Phosphacan-IR density in the DREZ peaked in the DRC/ARTN group 7 days post-surgery and was significantly greater than the DRC/Veh group 14 days post-surgery (p<0.001, Tukey post hoc test). By 30 days phosphacan-IR density in the DREZ of both the DRC/Vehicle and the DRC/ARTN groups was not significantly different to the Sham Vehicle or the Sham ARTN groups. Both DRC groups had similar expression profiles, however systemic artemin treatment resulted in a shift to the right, later in the post-surgical period. Artemin administration had no significant effect on phosphacan expression in sham animals.

PAIN ASSESSMENT

At 7 days post-surgery (Fig 4.12a), the Sh/Artn group and DRC/Veh group displayed significant hyposensitivity to mechanical probing, in that the response to a 26g Von Frey filament was 22% and 17% of the total test stimuli, respectively (p<0.01). The DRC/Artn group showed a noxious response to 57.5% of the Von Frey mechanical stimuli. Thirty days post-surgery (Fig 4.12b), the Sh/Artn group showed a hypersensitive response to 13% of the stimuli, 7 percentage points less than at 7 days. The DRC/Veh group showed a noxious response to 34% of the mechanical stimuli, 9 percentage points more than at 7 days. The DRC/Artn group showed a significant noxious response to mechanical probing of the abdomen 30 days post-surgery, 13 percentage points more than at 7 days.

DISCUSSION

In this study we report that systemic artemin treatment resulted in a significant increase in the density of CGRP immunoreaction product (CGRP-IR) and IB4 histochemistry in the dorsal horn superficial laminae of the projection territory left deafferented as a result of a bilateral dorsal root crush injury (DRC) of L6 and S1. There was also a significant increase in CGRP-IR and IB4 histochemistry in the sacral parasympathetic nucleus (SPN), when compared to vehicle treated rats. Tracing studies revealed a significant increase in the amount of GFP in the projection territory of larger myelinated afferents following DRC with artemin treatment compared to DRC with vehicle. Artemin treatment promoted improvements in lower urinary tract function, including significant reductions in dysfunctional external urethral sphincter (EUS) electromyographic (EMG) activity, and normalization of bladder threshold volumes and residual volumes. Artemin treatment had no significant effect on the post-injury increase in neurocan and NG2 in the dorsal root entry zone (DREZ). However, the expression profile of phosphacan in the DREZ was significantly delayed relative to the vehicle treated rats. Treating sham animals with artemin resulted in significant hyposensitivity to evoked mechanical stimuli applied to the abdomen that increased with time post-surgery, and treating DRC animals with artemin resulted in progressively increasing hypersensitivity to the same stimuli. We interpret the pattern of primary afferent projection territory reinnervation and improved lower urinary tract function as being a consequence of regeneration of the central branches of DRG neurons across the DREZ.

In the present study, we used a similar injury model and the same treatment regime reported by Wang and colleagues who described growth of multiple classes of nerve fibers through the DREZ with restoration of forelimb function following unilateral DRC of the C4-T2 dorsal roots (Wang *et al.* 2008). In the present study, there was a significant increase in CGRP-IR in lamina I at 14 and 30 days after the DRC surgery and the laminar density of IB4-bound afferent terminals increased significantly 30 days post-surgery. Our anterograde tracing study provided evidence of GFP-filled afferents in the medial dorsal horn and a significant increase in rostrocaudally oriented collaterals in the dorsal column ipsilateral to the DRC in rats treated with artemin. We interpret this increase to be evidence of primary afferent regeneration across the DREZ and not a result of primary afferents spared during the crush injury.

While we interpret the changes that occur following systemic artemin treatment as being a consequence of regeneration across the DREZ, we cannot rule out the possibility that a small number of axons survived the crush injury and that significant collateral sprouting of primary afferents occurs from adjacent uninjured spinal segments rostral and caudal to the injury site under the influence of artemin. Artemin treatment did not produce any increase in CGRP-IR or IB4 histochemistry in sham animals nor was there any density increase in the DRC/Artn group within the first 7 days post-surgery suggesting that sprouting from adjacent segments or spared axons did not occur. Regeneration of central axons is estimated to occur at a rate of 2mm per day (Oblinger &

121

Lasek 1984, Wujek & Lasek 1983) which is consistent with the timescale of increased immunoreaction product density and functional improvement. In our tracer study, the only sources of GFP are the L6 and S1 dorsal root ganglia. Following DRC and vehicle treatment, no GFP was detected ipsilateral to the injury but with artemin, GFP increased in the dorsal horn and dorsal column, suggesting regeneration across the DREZ and not sprouting.

Both CGRP-IR and IB4 histochemistry (peptidergic and non-peptidergic unmyelinated C- and thinly myelinated Aδ-fibers) increased in the lateral collateral pathway (LCP) and SPN, and GFP-filled fibers were found in the medial dorsal horn in the DRC group after artemin treatment. The LCP is the central projection of bladder afferent fibers, exiting Lissauer's tract and extending ventrally to the SPN containing autonomic interneurons and preganglionic parasympathetic motor neurons (Morgan *et al.* 1981, Nadelhaft & Booth 1984). GFRα3 (the artemin receptor) is expressed by both peptidergic and non-petidergic fine fibers (Bennett *et al.* 2006) and GFRα3-positive fibers are found in lamina I with a few fibers in lamina II, the LCP and SPN, and in a medial band extending to the midline of the lumbosacral spinal cord (Forrest & Keast 2008). Considering the pattern of reinnervation that we report closely matches the distinctive pattern of GRFα3 and bladder afferent distribution in the spinal cord, there is a neuroarchitectural basis for artemin mediated signaling in regeneration that led to improved lower urinary tract function.

ARTEMIN TREATMENT RESULTED IN IMPROVED LOWER URINARY TRACT FUNCTION

Urodynamic recordings from the bladder and EUS revealed significant improvements in EUS function and normalization of bladder threshold and residual volumes on a timescale consistent with the level of afferent regeneration produced by systemic artemin treatment. In this study, we measured inter-contraction intervals (ICIs), bladder compliance, EUS EMG amplitude, residual volume, threshold volume, voiding efficiency and bladder weight. For ICI and compliance we reported no change with artemin treatment. In contrast, systemic artemin treatment significantly reduced threshold volume and normalized voiding efficiency by reducing the post-void residual volume, a characteristic symptom of neurogenic bladder dysfunction (Podnar *et al.* 2006, Barrington 1941, Fowler 1999). Systemic artemin treatment also reduced the amplitude of the filling phase EUS EMG activity. High amplitude EMG activity during the filling phase is characteristic of dysfunction (Rooney & Hulsebosch 2010). Bladder weight was significantly reduced in the artemin treated group. However, the bladders of artemin treated animals still resemble those of vehicle treated animals in translucence and shape. When the bladder wall's muscular and structural integrity is severely perturbed by two to three weeks of over distension and muscle hypertrophy and hyperplasia (Andersson & Arner 2004), normal compliance and ICI will take some time to return to normal. On the whole, the improvement in EUS EMG activity and reductions in threshold and residual volume appear indicative of functional reinnervation of spinal cord and repair of broken reflex arcs.

Artemin treatment had no effect on the post-injury increase in neurocan-IR or NG2-IR in the DREZ. Neurocan is a secreted CSPG that undergoes increased expression by reactive astrocytes and prevents growth cone extension by binding neuronal cell adhesion molecules (N-CAMs) and neuron-glia cell adhesion molecules (Ng-CAMs) (McKeon *et al.* 1999, Friedlander *et al.* 1994). NG2 can be secreted or membrane bound and is most commonly associated with a recently described a fourth glial population, called NG2-glia (Butt *et al.* 2002, Nishiyama *et al.* 1995). NG2-glia also become reactive and increase NG2 expression following injury (Jones *et al.* 2002, Zhang *et al.* 2001).

Artemin treatment resulted in a delay in the expression of phosphacan in the DREZ. Phosphacan, synthesized by glial cells, is the noncatalytic secreted isoform of receptor-type protein tyrosine phosphatase β (RPTPβ) (Maurel *et al.* 1994). It could be argued that the expression profile shift that occurred due to Artn treatment in this study was a result of inhibited production of one isoform in favor of another. The secreted phosphacan inhibits growth by binding to CAMs on neuronal growth cones, thus preventing cell adhesion in the DREZ (Milev *et al.* 1994). Therefore, if RPTPβ was preferentially expressed, a more favorable regenerative environment could be created in the glial scar of the DREZ. Alternatively, a temporal delay in the expression of any component of the ECM would inevitably change the extracellular environment that an axon growth cone encounters, perhaps rendering it growth permissive. Recent work done in mice reported that there was no increase in phosphacan mRNA in the DREZ following dorsal root injury (Waselle *et al.* 2009), suggest that the majority of the immunoproduct

we found in the DREZ following DRC was phosphacan secreted from neighboring glial cells or cells that migrated to the DREZ. It must be noted that the density of phosphacan positive staining peaked in both the Artn group and the vehicle group 7 days post-surgery before any signs of afferent regeneration into and within the spinal cord were seen. Regardless of which isoform was present in the DREZ, such a high concentration of N-CAM- and Ng-CAM-binding receptors could be enough to halt neurite extension.

HOW DOES ARTEMIN STIMULATE PRIMARY AFFERENT REGENERATION ACROSS THE DREZ? Artemin is one of four members of the GDNF family of ligands (GFLs), and in the present study consists of a 113 amino acid recombinant form of human artemin. The artemin receptor is the GDNF family receptor-α3 (GFRα3) and is almost exclusively expressed by primary afferent DRG neurons (Baloh *et al.* 1998). Like the rest of the GFLs, as a homodimer, artemin binds to two non-signaling GPI-anchored GFRα3 coreceptors and this complex then dimerizes two molecules of the transmembrane protein RET (Durbec *et al.* 1996, Treanor *et al.* 1996, Trupp *et al.* 1996, Worby *et al.* 1996). Formation of the RET dimer induces transphosphorylation of their intracellular tyrosine kinase domains (Airaksinen *et al.* 1999) that initiates many understudied intracellular signal transduction pathways (Hauck *et al.* 2006, Zhou *et al.* 2009).

It is thought that artemin induced regeneration across the DREZ by increasing the intrinsic regenerative capacity of primary afferent neurons. Recently it was reported that transgene-mediated artemin supported the extension of neurites of primary DRG neurons in culture, and allowed these cells to overcome myelin inhibition of neurite extension

(Zhou et al. 2009). The GFRα3 mediated signaling mechanism involves cyclic adenosine monophosphate (cAMP) induced activation of protein kinase A (PKA) to phosphorylate cAMP response element binding protein (CREB) and increase expression of arginase I (Zhou et al. 2009). More recent work by the same group showed that the addition of artemin to the medium of DRG neurons plated on CNS myelin prevented the myelin induced increase in neuronal Nogo-A (Peng *et al.* 2010). CSPGs inhibit regeneration in part by stimulating Rho-GTPases, which induces growth cone collapse (Mizuno *et al.* 2004). Therefore artemin induced increases in endogenous cAMP levels and activation of PKA suppresses Rho activity and activity of its downstream target Rho-associated coiled kinase (ROCK) and promotes regeneration (Borisoff *et al.* 2003, Brabeck *et al.* 2004, Domeniconi & Filbin 2005, Tanaka *et al.* 2007). Since artemin has little impact on reactive gliosis at the DREZ, artemin may allow regenerating axons to overcome inhibition at the DREZ, by increasing the inate regenerative capacity of afferent neurons, rather than reducing the presence of growth inhibitory substances.

PAIN ASSESSMENT

Caution must always be used when using neurotrophic factors because of the risk of adverse side effects such as hyperalgesia (Malin *et al.* 2006, Vellani *et al.* 2006, Amaya *et al.* 2004). We found that systemic artemin treatment made the DRC group hypersensitive to evoked mechanical stimuli around the deafferented myotome. Conversely, artemin resulted in hyposensitivity in the sham group, which was unexpected.

126

Neurogenic bladder dysfunction has a devastating effect on the quality of life of those who have suffered spinal cord or cauda equina injuries; therefore, efforts to restore voluntary control of micturition are vitally important. In summary, this study demonstrates that artemin shows promise for clinical use. It is relatively specific to the population of primary afferent neurons, it does not appear to result in aberrant sprouting since it has only a minor effect on the content of the extracellular matrix and it can exert its effect by systemic administration. However, future studies must examine closely the potential side effects of artemin's systemic use.
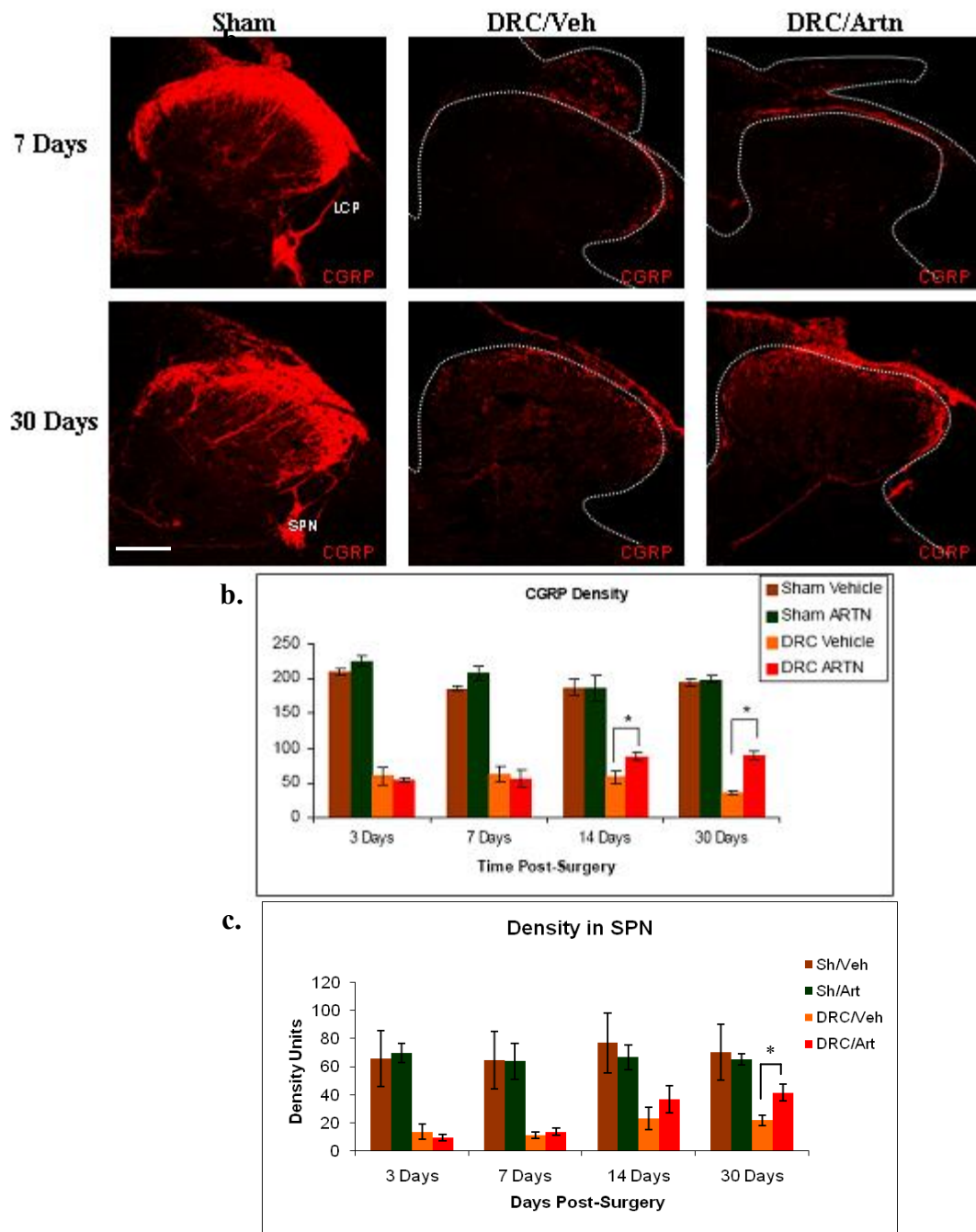
Figure 14 Dorsal horn and SPN CGRP density following systemic artemin administration.
Shown in a are confocal immunofluoresent micrographs of the dorsal horn from sections of the L6-S1 spinal cord immunoreacted for CGRP taken from rats 7 and 30 days following sham surgery (left column), bilateral dorsal root crush at L6 and S1 injected with vehicle (DRC/Veh; middle column) and bilateral dorsal root crush injected with artemin (DRC/Artn; right column). The dashed white line indicates the dorsal horn gray matter boundary and spinal cord perimeter with rootlet attached. The density of CGRP immunoreactions product (CGRP-IR) staining in laminae I and II is demonstrated graphically in **b** and the

128

density of CGRP-IR staining in the sacral parasympathetic nucleus(SPN) is demonstrated graphically in **c** for all four experimental groups: 1) Sham surgery injected with saline vehicle (Sham Vehicle), 2) Sham surgery injected with artemin (Sham ARTN), 3) bilateral dorsal root crush at L6 and S1 injected with vehicle (DRC Vehicle) and 4) bilateral dorsal root crush injected with artemin (DRC ARTN) at each of the four time points (3, 7, 14 and 28 days) post-surgery. There is a significant difference between the DRC Vehicle and DRC ARTN groups (two way ANOVA, p=0.01, F=7.718) with significant separation at 14 and 30 days post-surgery. * indicates significance p<0.05 in both cases by Tukey post hoc analysis. There is no significant difference between sham groups and there is no change in CGRP-IR density with time post-surgery. *Error bars = Standard Error of the mean. Scale bar = 200 μm.* Density of immunoreaction product is expressed in immunodensity units.
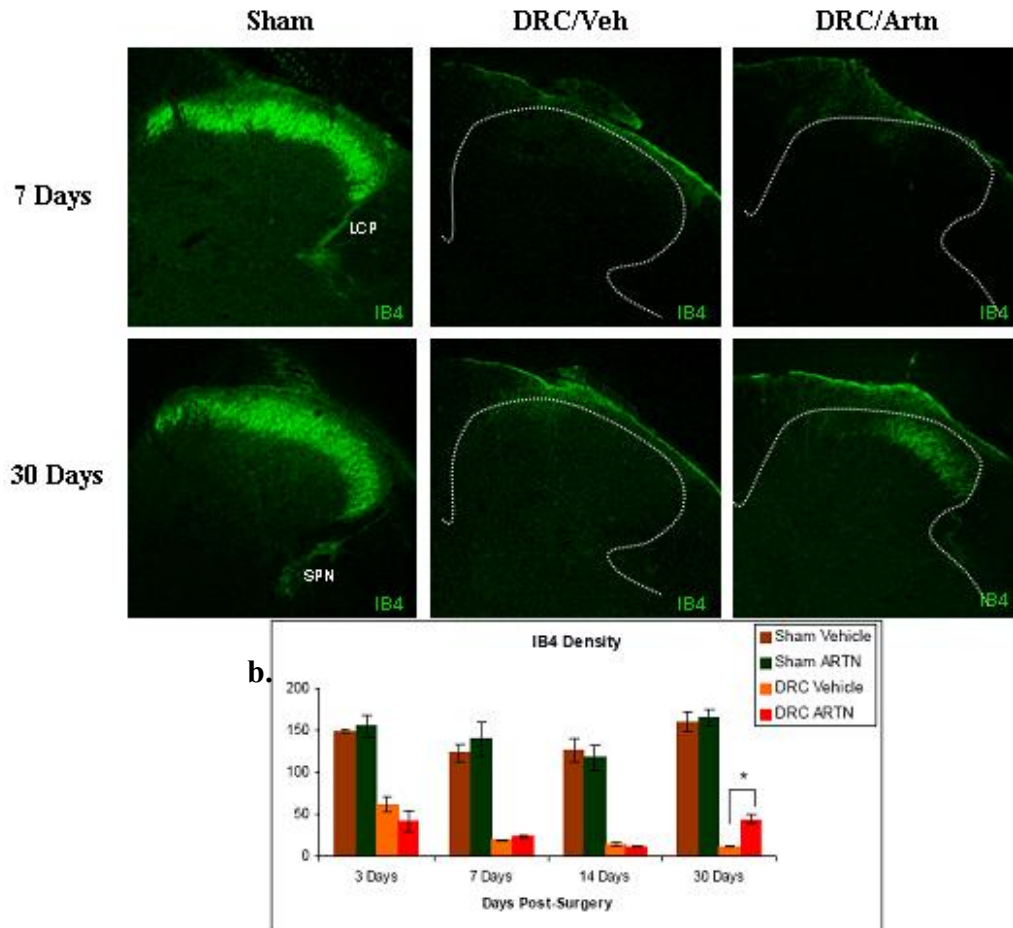
Figure 15 Dorsal horn IB4 density following systemic artemin administration.
Shown in a are confocal immunofluoresent micrographs of the dorsal horn from sections of the L6-S1 spinal cord reacted for IB4 taken from rats 7 and 30 days following sham surgery (left column), bilateral dorsal root crush at L6 and S1 injected with vehicle (DRC/Veh; middle column) and bilateral dorsal root crush injected with artemin (DRC/Artn; right column). The dashed white line indicates the dorsal horn gray matter boundary. The density of IB4 staining in laminae II is demonstrated graphically in b for all four experimental groups, at all four post-surgical time points in this study. Injury significantly reduced IB4 staining, compared to sham groups in lamina II (two way ANOVA, p<0.001, F=100.42). Tukey post hoc analysis at day 30 reveals a significant increase in the density of IB4 staining in spinal dorsal horn of injured animals treated with artemin (* indicates a significant difference between DRC Vehicle and DRC

ARTN, p<0.001). There is no significant difference between sham groups and there is no change in IB4 histochemical density with time post-surgery. *Error bars = Standard Error of the mean. Scale bar = 200 μm.* Lateral collateral pathway (LCP); sacral parasympathetic nucleus (SPN). Density of reaction product is expressed in immunodensity units.

Sham

Unilateral DRC/Vehicle

c. **Unilateral DRC/Artemin**

d. **High Mag. of Boxed Area**

e. **Dorsal Column Collateral Cross-sections**
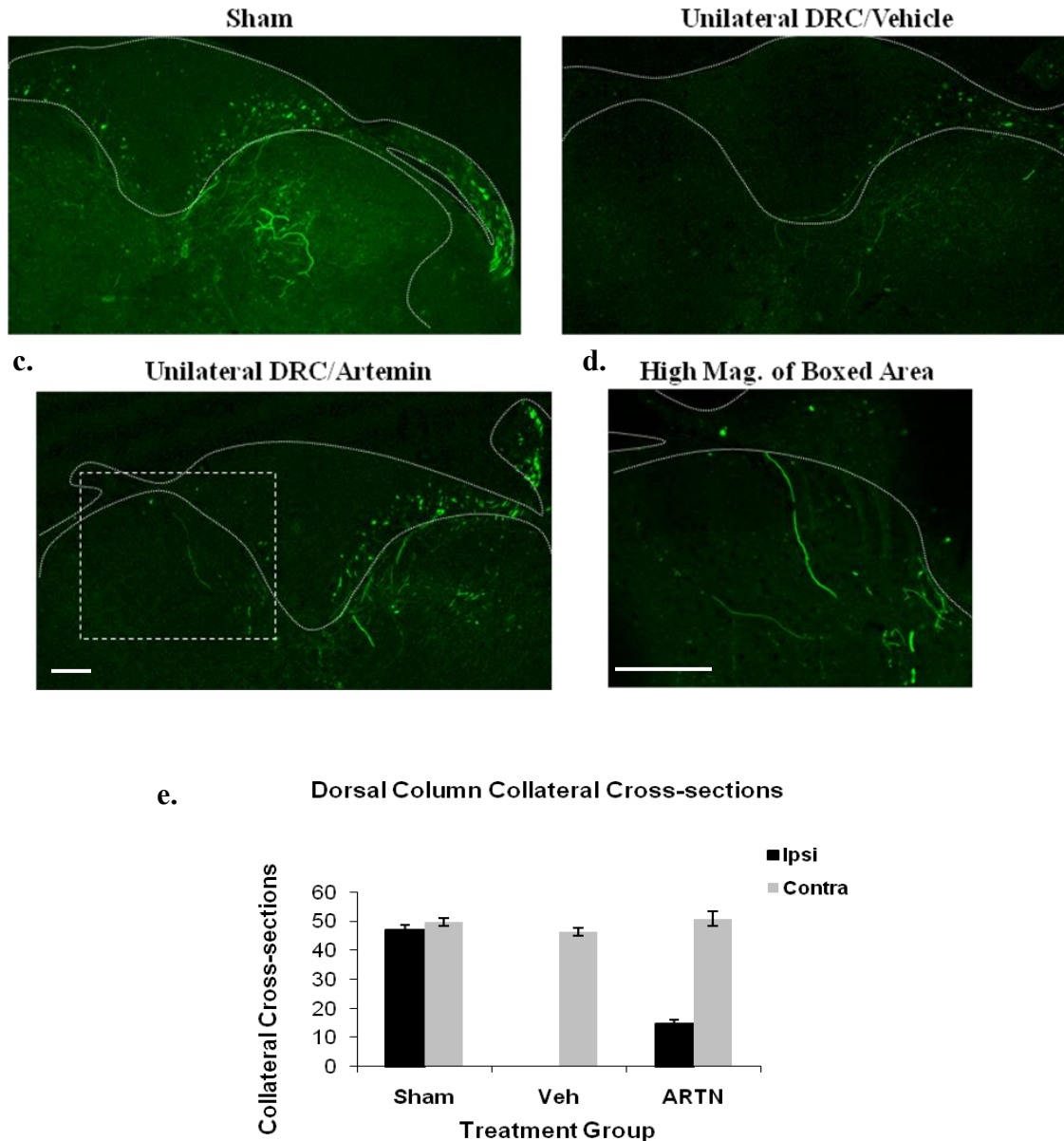
Figure 16 Anterograde AAV-GFP tracing following systemic artemin administration.
Confocal immunofluorescent micrographs of the dorsal spinal cord 30 days after bilateral injection of AAV-GFP into the L6 and S1 dorsal root ganglia are shown. The gray line indicates the dorsal horn gray matter boundary and spinal cord perimeter with rootlet attached. **a** shows a spinal cord section from a sham operated animals. GFP is located in the dorsal column, medial dorsal horn and deeper laminae left and right, as well as the attached rootlet. **b** shows a section from an animal injected bilaterally with AAV-GFP

130

and given a unilateral dorsal root crush (DRC) and treated with vehicle. GFP is present contralateral but not ipsilateral to the injury. **c** shows a section from an animal bilaterally injected with AAV-GFP, unilaterally injured and treated with artemin. GFP is found ipsilateral to the injury in both the dorsal column and dorsal horn, as can be seen under high magnification in **d**. **e)** graphically presents the average number of GFP filled collateral cross-sections in the dorsal columns ipsilateral and contralateral to a unilateral dorsal root crush in sham animals, unilaterally injured animals treated with vehicle (Veh) and unilaterally injured animals treated with artemin (ARTN). Artemin treatment resulted in an increase of GFP in the dorsal column (interpreted as filled collateral cross-sections) ipsilateral to the site of DRC injury. *Error bars = Standard Error of the mean. Scale bar = 200 μm*
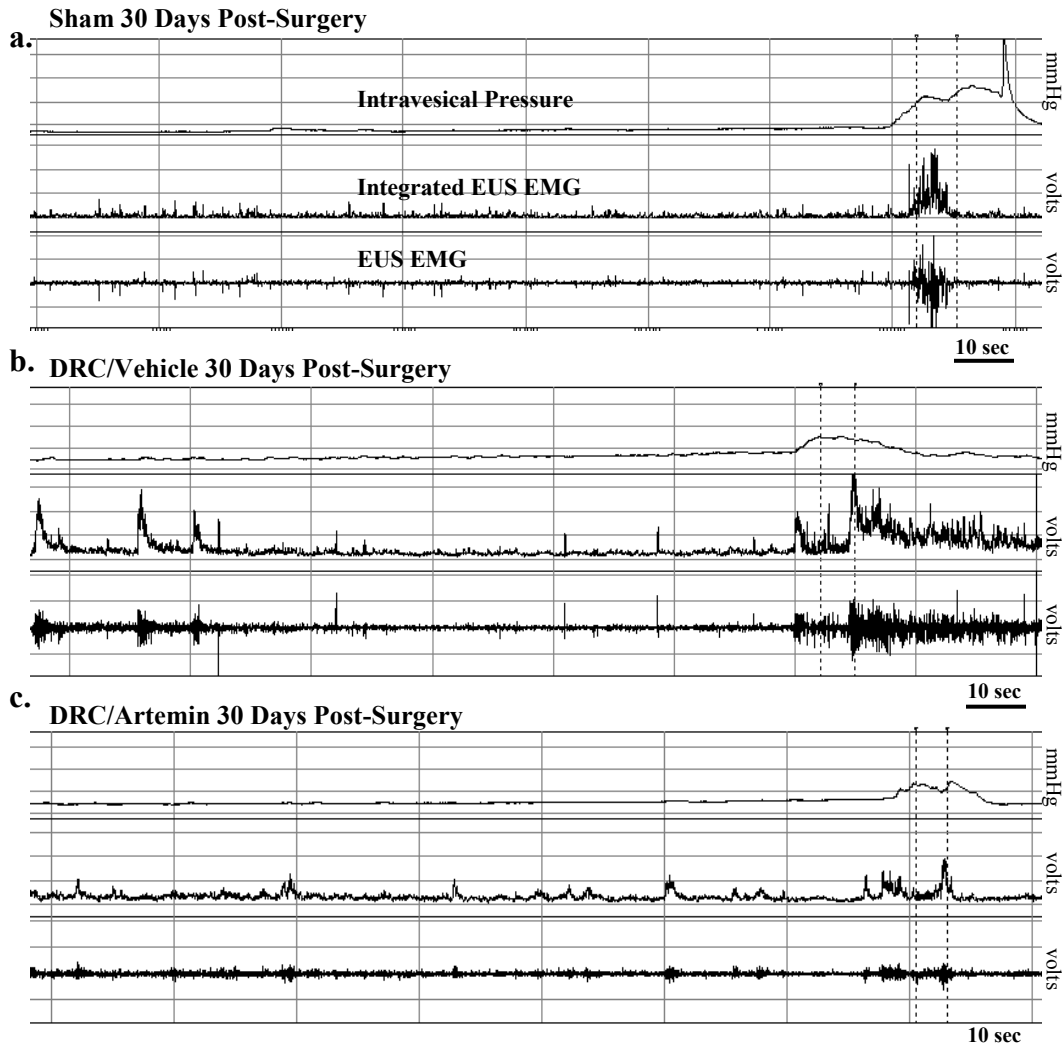
Figure 17 Sample urodynamic recording following systemic artemin administration.
Sample urodynamic recordings from an uninjured animal **(a)**, an animal 30 days after a bilateral dorsal root crush (DRC) injury at spinal level L6 and S1 and treated with vehicle **(b),** and from an animal 30 days after DRC and treated with Artemin **(c)**. Each panel displays 3 traces: the top is intravesical pressure (IVP) measured in millimeters of mercury, on the bottom is external urethral sphincter (EUS) electromyography (EMG) raw data recording in volts and in the center is the integrated EUS EMG during 3 minutes of a 20

131

minute recording period. The first vertical dashed line indicates the beginning of saline voiding and the second dashed line indicates the end of voiding. In **a** during the filling phase of the micturition cycle IVP remained low and flat and the amplitude of EUS EMG activity is low in uninjured animals until voiding occurred. During voiding, as liquid is allowed pass through the urethra, sphincter muscle activity increases. By contrast in **b**, there is a gradual increase in IVP as the volume increased. A lot of non-voiding EUS EMG tonic activity was present during the filling phase and for an extended period following voiding. By comparison in **c,** the animal treated with artemin, exhibited a flatter filling phase pressure profile and less non-voiding EMG tonic activity.

b.
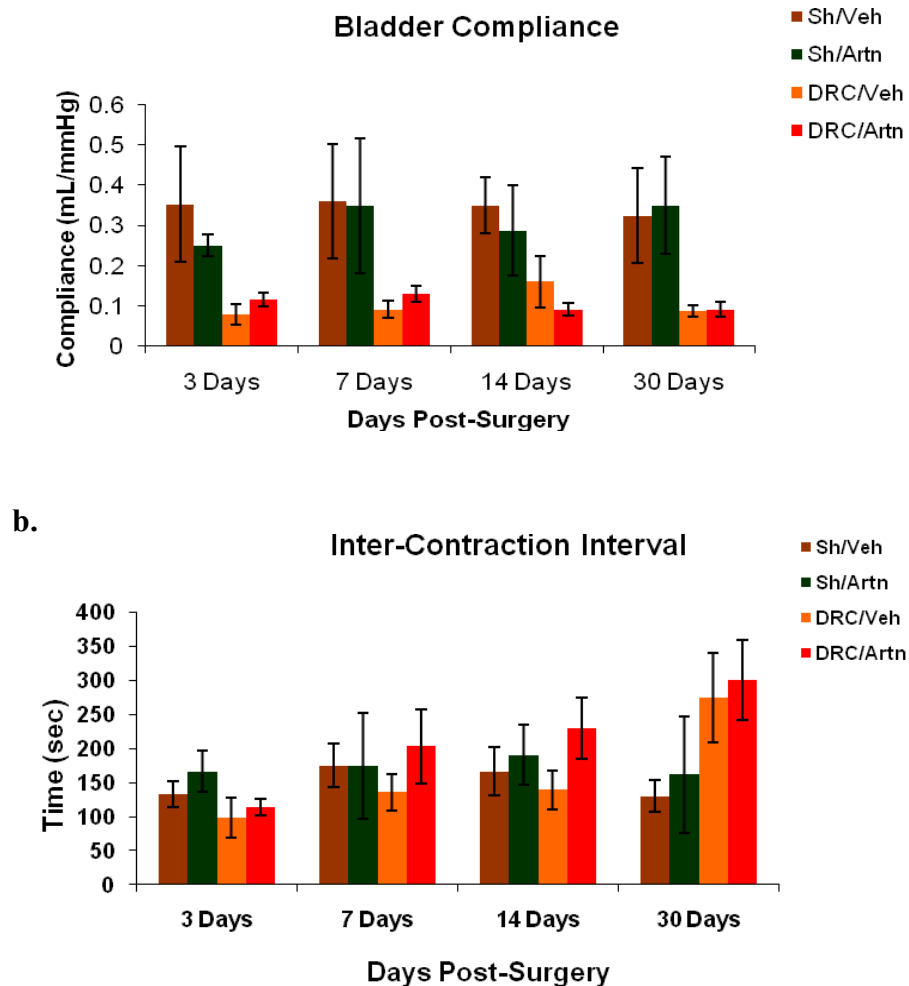
Figure 18 Bladder compliance and inter-contraction interval following systemic artemin administration.
Two outcome measures of bladder function are shown in these figures for all four experimental groups: 1) Sham surgery injected with saline vehicle (Sh/Veh), 2) Sham surgery injected with artemin (Sh/Artn), 3) bilateral dorsal root crush at L6 and S1 injected with vehicle (DRC/Veh) and 4) bilateral dorsal root crush injected with artemin (DRC/Artn) at each of the four time points (3, 7, 14 and 28 days) post-surgery. **a** shows bladder compliance ($\Delta V/\Delta P$) measured in milliliters per millimeter of mercury (mL/mmHg). Injury status resulted in statistically significant separation between the sham and DRC groups (Two way ANOVA, $p<0.001$) however, treating DRC animals with artemin did not improve compliance when compared with those given vehicle. **b** shows the average inter contraction intervals (ICIs) measured in seconds, in all four

injury/treatment groups at all four post-surgical time points in this study. Treating animals with artemin did not result in any statistically significant separation between groups.

a. **Filling Phase**
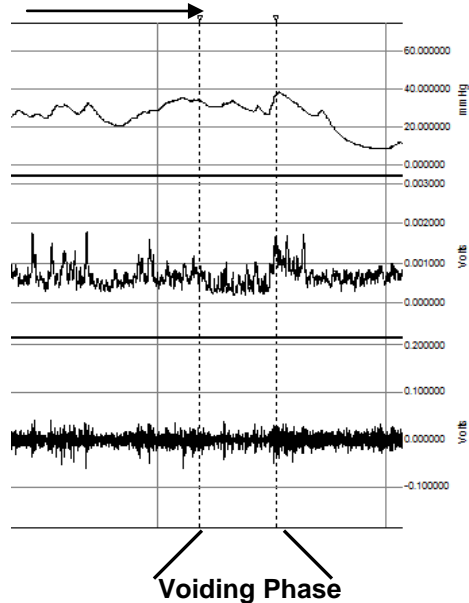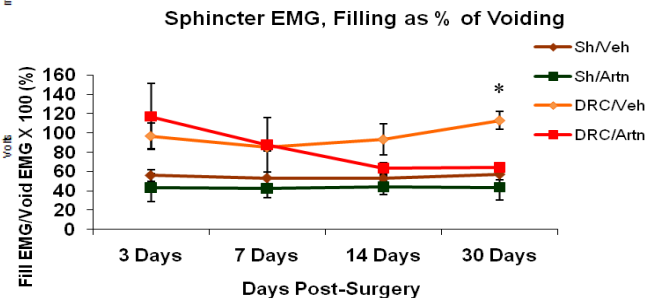
Voiding Phase

Figure 19 The ratio of filling:voiding phase EUS EMG following systemic artemin administration.
A sample urodynamic recording taken from an animal 30 days following bilateral dorsal root crush injury, given vehicle (DRC/Veh) to demonstrate the filling phase and voiding phase; and quantitative analysis of external urethral sphincter electromyography (EUS EMG). a shows intravesical bladder pressure on the top, integrated EUS EMG in the center and the raw EMG trace on the bottom. The first vertical dashed line indicates the end of a filling phase and the beginning of a voiding phase. The dashed line on the right indicates the end of the voiding phase and the beginning of the next filling phase. Injured animals displayed dysfunctional high amplitude EMG activity during the filling phase. b The average filling phase EMG amplitude is expressed as a percentage of the average voiding phase EMG in all four groups 1) Sham surgery with vehicle (brown diamonds), 2) Sham surgery with artemin (green squares), 3) bilateral dorsal root crush with vehicle (orange diamonds) and 4) bilateral dorsal root crush with artemin (re squares) at all four post-surgical time points in this study. 100% indicates a 1:1 ratio. Artemin treatment of DRC animals (DRC/Artn; Red squares) successfully reduced the ratio of their filling phase: voiding phase EUS EMG to sham levels by thirty days post-surgery. The average filling phase EMG of the DRC/Veh group is a significantly larger percentage of voiding phase EMG compared to Sh/Veh, Sh/Artn and DRC/Artn. * indicates significance p<0.05 in all cases by Tukey post hoc analysis.

a.

Residual Volume

b.
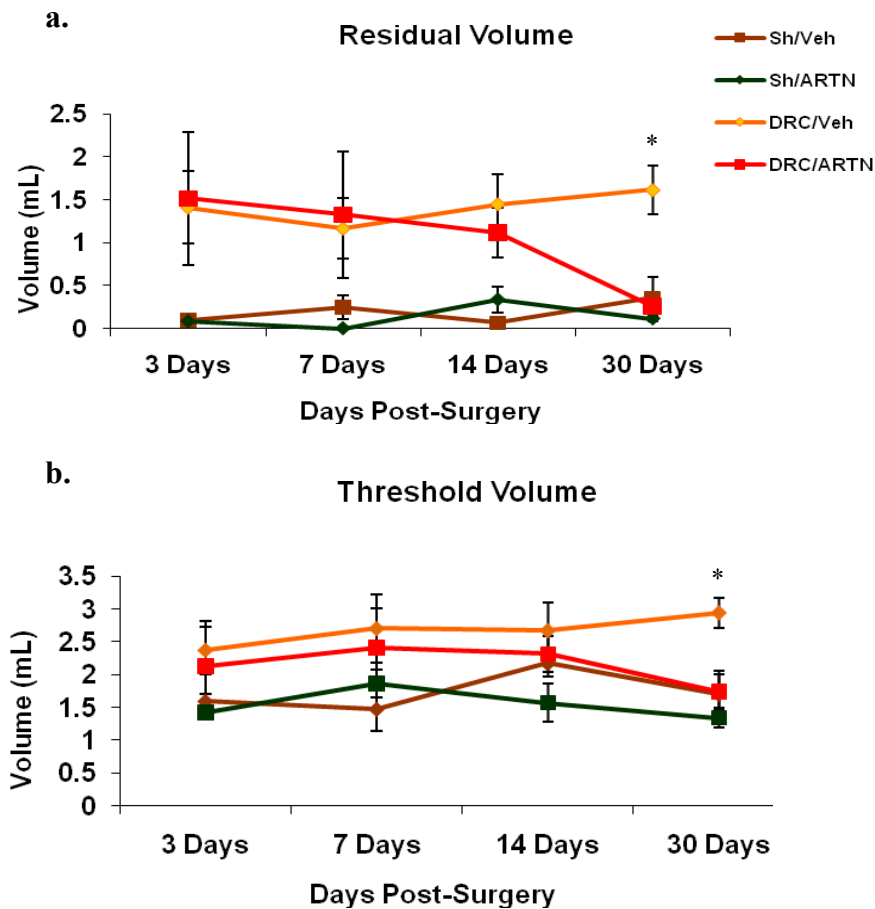
Threshold Volume

Figure 20 Bladder residual and threshold volumes following systemic artemin administration.
Two outcome measures of bladder function are shown in these figures for all four experimental groups: 1) Sham surgery injected with saline vehicle (Sh/Veh), 2) Sham surgery injected with artemin (Sh/Artn), 3) bilateral dorsal root crush at L6 and S1 injected with vehicle (DRC/Veh) and 4) bilateral dorsal root crush injected with artemin (DRC/Artn) at each of the four time points (3, 7, 14 and 28 days) post-surgery. **a** shows the average residual volume of the bladder, which was recorded as the volume of infused saline remaining in the bladder after the first voiding event of each recording session. DRC injury resulted in large post-void residual volumes. Treatment of injured animals with artemin (DRC/Artn; Red squares) reduced the average residual volume to sham levels by 30 days post-surgery. The average residual volume of injured animals given vehicle (DRC/Veh) was significantly larger compared to Sh/Veh, Sh/Artn and DRC/Artn. * indicates significance p<0.05 in all cases by Tukey post hoc analysis. **b** shows the average threshold volume, recorded as the volume of saline infused into the bladder to elicit the first voiding event of each recording session. Treatment of injured animals with artemin (DRC/Artn; Red squares) reduced the average threshold volume to sham levels by 30 days post-surgery. The average threshold volume of injured animals given vehicle (DRC/Veh) was significantly larger by 30 days compared to Sh/Veh, Sh/Artn and DRC/Artn. * indicates significance p<0.05 in all cases by Tukey post hoc analysis.

134

| Voiding Efficiency				
	3 Days	7 Days	14 Days	30 Days
Sh/Veh	94%	83%	97%	80%
Sh/ARTN	94%	100%	78%	91%
DRC/Veh	41%	57%	46%	45%
DRC/ARTN	29%	45%	55%	85%

Table 4.1 Voiding Efficiency.
Using the data represented in Figure 7 we tabulated the percentage of infused saline that was successfully voided at the beginning of each recording session in each group at all four post-surgical time points. The voiding efficiency of injured animals treated with artemin improved to 85% at the final time point whereas the efficiency of those treated with vehicle remained low.
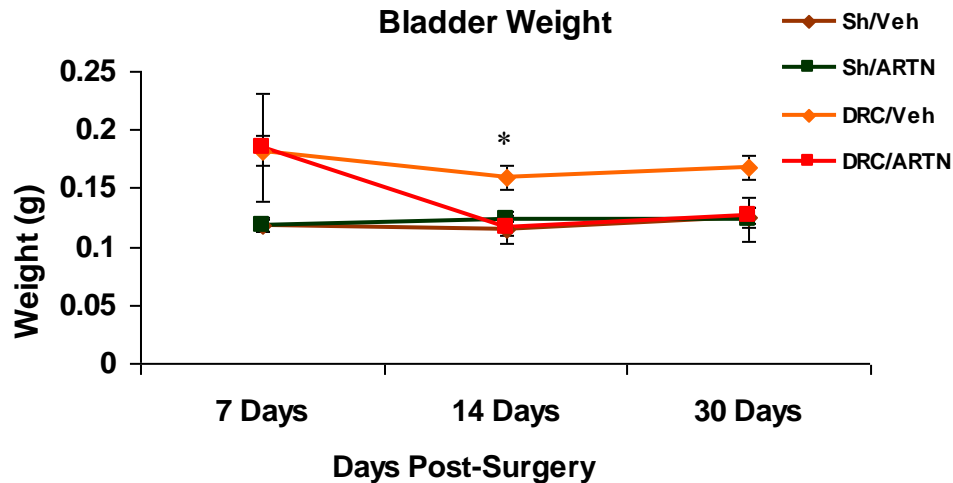
Figure 21 Bladder weight following systemic artemin administration.
Demonstrated graphically is the average weight (in grams) of bladders from animals in all four groups 7, 14 and 30 days post-surgery. The bladder was removed, blotted dry and weighed following animal perfusion. The weight of bladders taken from injured animals was greater than sham animals. While artemin treatment appeared to decrease the bladder weight of DRC/ARTN, there is no statistical significance at any time point. There is a statistically significant effect of time post-surgery detected in the DRC/Artn group (two way ANOVA; $p < 0.006$, F=5.647).
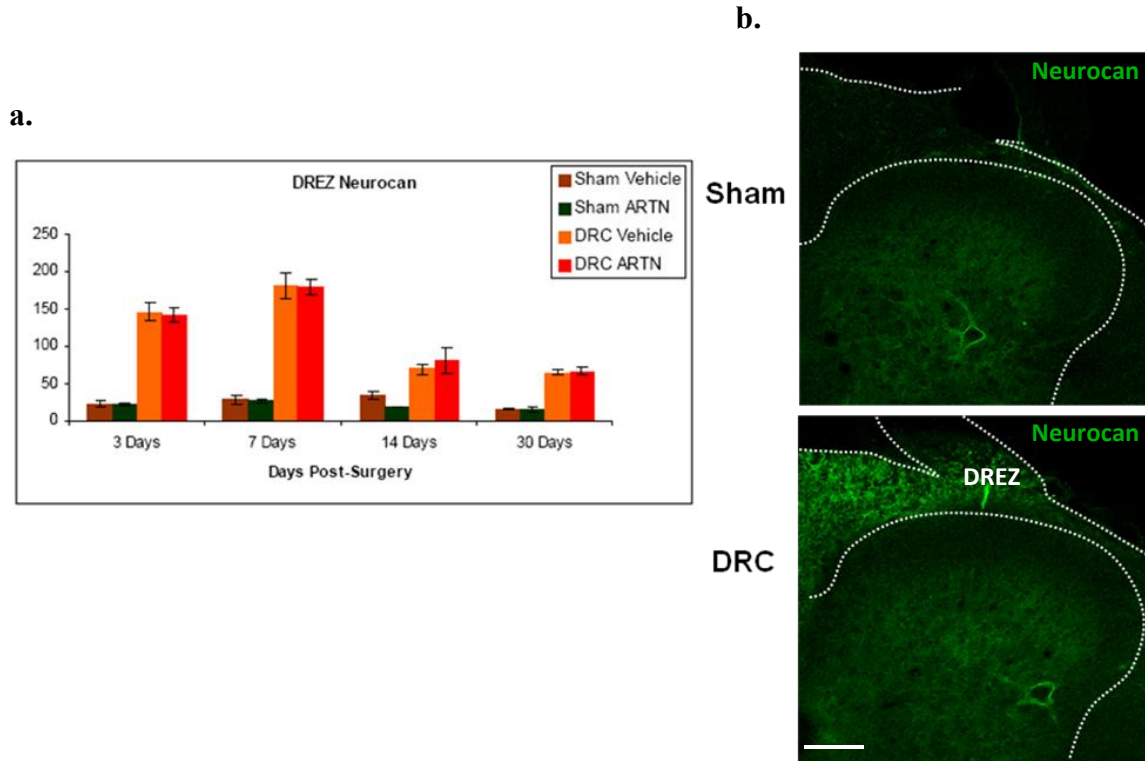
Figure 22 Dorsal horn neurocan following systemic artemin administration.
The density of dorsal root entry zone (DREZ) neurocan immunoreactions product (neurocan-IR) in the four experimental groups at all four time points is demonstrated graphically in **a.** Bilateral dorsal root crush (DRC) resulted in a marked increase in the density neurocan-IR in the DREZ, peaking at 7 days post-surgery in a statistically significant time-dependant manner (two way ANOVA, $p<0.001$, F=46.976). There was no significant difference between either of the sham treatment groups (Brown and Green) or either of the DRC treatment groups (Orange and Red); thus, artemin treatment does not influence the expression of neurocan in the DREZ. Shown in **b** are confocal immunofluoresent micrographs of the dorsal horn from sections from the L6-S1 spinal cord immunoreacted for neurocan. These are representative sections taken from rats 7 days following sham surgery (top) or a bilateral dorsal root crush (bottom) demonstrating the localization of neurocan in the spinal cord. The dashed white line indicates the dorsal horn gray matter boundary and spinal cord perimeter and any attached rootlets (the attached rootlet in the DRC section became disoriented during tissue handling). In the unlesioned lumbosacral spinal cord, neurocan-IR is present most noticeably in the perineuronal net that surrounds the soma and dendrites of a large interneuron deep in the lateral dorsal horn. Dorsal root crush results in a marked increase in neurocan-IR in the dorsal root entry zone (DREZ) and dorsal column. *Error bars = Standard Error of the Mean. Scale bar = 200 μm.* Density of immunoreaction product is expressed in immunodensity units.

136

a.

b.
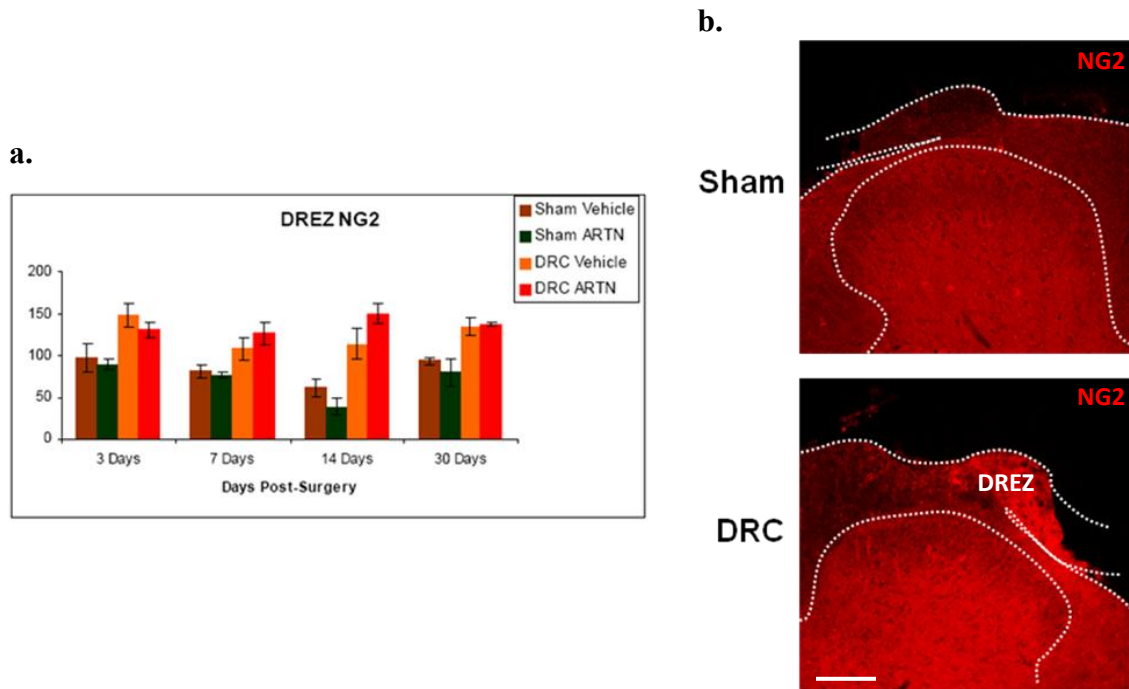
Figure 23 Dorsal horn NG2 following systemic artemin administration.
The density of dorsal root entry zone (DREZ) NG2 immunoreaction product (NG2-IR) in the four experimental groups at all four time points is demonstrated graphically in **a.** Bilateral dorsal root crush (DRC) resulted in a marked increase in the density NG-IR in the DREZ. NG2 staining remains elevated throughout the full post-surgical period and does not change in any significant time-dependant manner. There was no significant difference between either of the sham treatment groups (Brown and Green) or either of the DRC treatment groups (Orange and Red); thus, artemin treatment does not influence the expression of NG2 in the DREZ. Shown in **b** are confocal immunofluoresent micrographs displaying the dorsal horn of sections from the L6-S1 spinal cord labeled with NG2. These are representative sections taken from rats 7 days following sham surgery (top) or a bilateral dorsal root crush (bottom) in order to demonstrate the localization of NG2 in the spinal cord with and without DRC injury. The dashed white line indicates the dorsal horn gray matter boundary and spinal cord perimeter and any attached rootlets. In the unlesioned lumbosacral spinal cord, NG2-IR staining occurs diffusely throughout the white and gray matter. Dorsal root crush results in a marked increase in NG2-IR in the dorsal root entry zone (DREZ) and dorsal column. *Error bars = Standard Error of the Mean. Scale bar = 200 μm.* Density of immunoreaction product is expressed in immunodensity units.
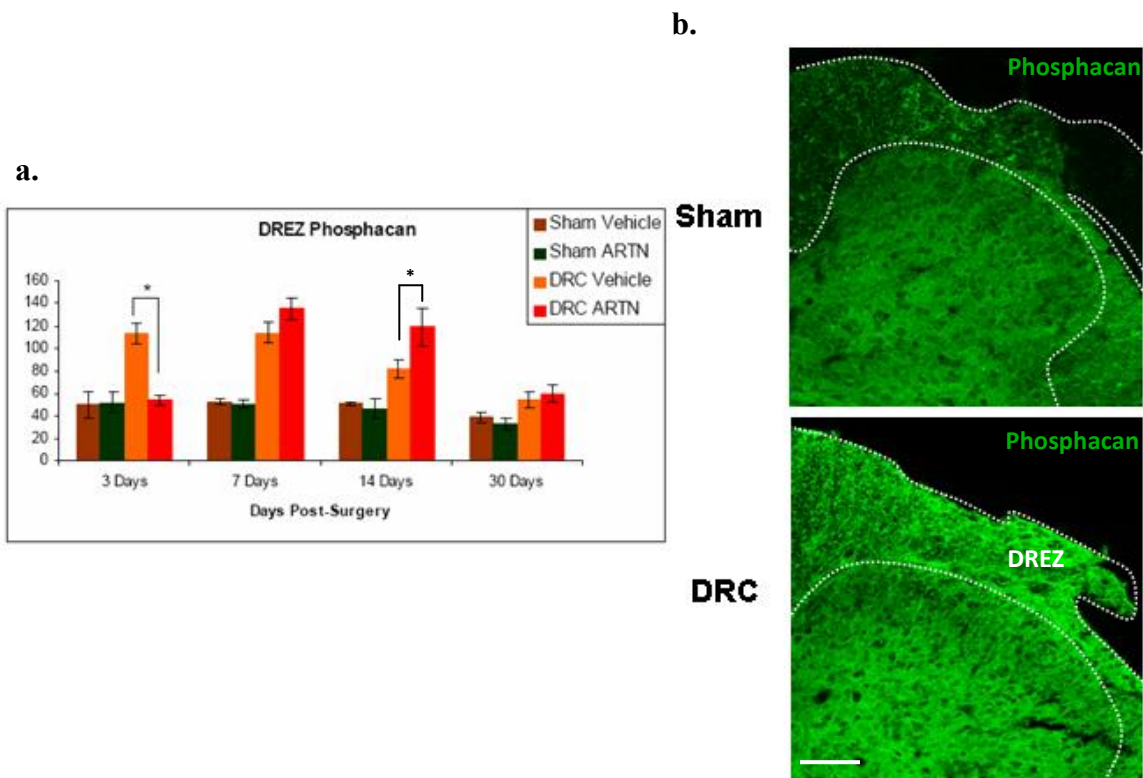
b.

a.

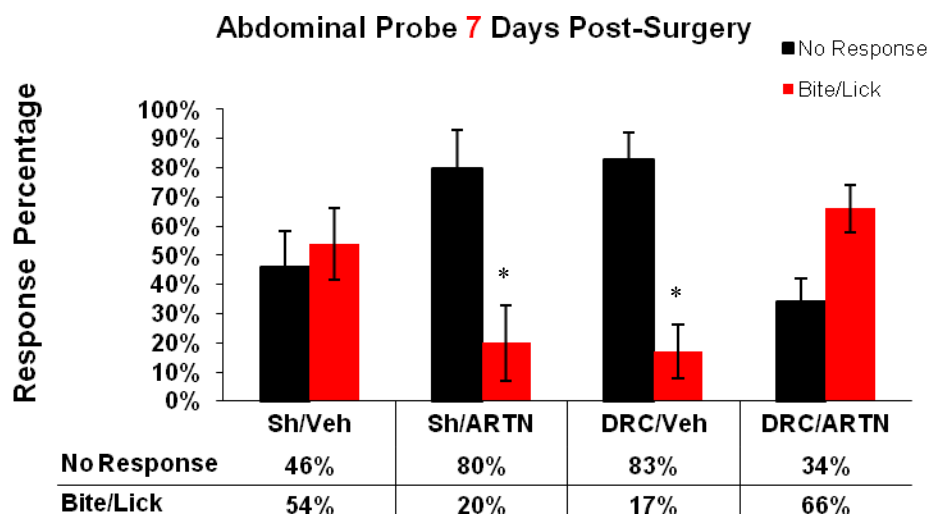**Figure 24 Doral horn phosphacan following systemic artemin administration.**
The density of dorsal root entry zone (DREZ) phosphacan immunoreaction product (phosphacan-IR) in the four experimental groups at all four time points is demonstrated graphically in **11a.** Bilateral dorsal root crush (DRC) resulted in a marked increase in the density of phosphacan-IR in the DREZ, peaking at 7 days post-surgery in a statistically significant time-dependant manner (two way ANOVA, $p < 0.001$, $F = 13.889$). Artemin treatment of DRC animals resulted in a delay in the expression of phosphacan in the DREZ. There is a statistically significant difference between the DRC Vehicle and DRC ARTN groups at 3 and 14 days post-surgery (* indicates a significance in both cases, $p < 0.01$). Shown in **11b** are confocal immunofluoresent micrographs of the dorsal horn from sections of the L6-S1 spinal cord immunoreacted for phosphacan. These are representative sections taken from rats 7 days following sham surgery (top) or a bilateral dorsal root crush (bottom) in order to demonstrate the localization of phosphacan in the spinal cord with and without DRC injury. The dashed white lines indicate the approximate outline of the dorsal horn gray matter, spinal cord and any attached rootlets. In the unlesioned lumbosacral spinal cord, phosphacan-IR staining is found diffusely throughout the white and gray matter. Dorsal root crush results in a marked increase in phosphacan in the dorsal root entry zone (DREZ) and dorsal column. *Error bars = Standard Error of the Mean. Scale bar = 200 μm.* Density of immunoreaction product is expressed in immunodensity units.

a.

Abdominal Probe **7** Days Post-Surgery

	Sh/Veh	Sh/ARTN	DRC/Veh	DRC/ARTN
No Response	46%	80%	83%	34%
Bite/Lick	54%	20%	17%	66%

b.

Abdominal Probe **30** Days Post-Surgery

	Sh/Veh	Sh/ARTN	DRC/Veh	DRC/ARTN
No Response	62%	88%	85%	27%
Bite/Lick	38%	13%	15%	73%
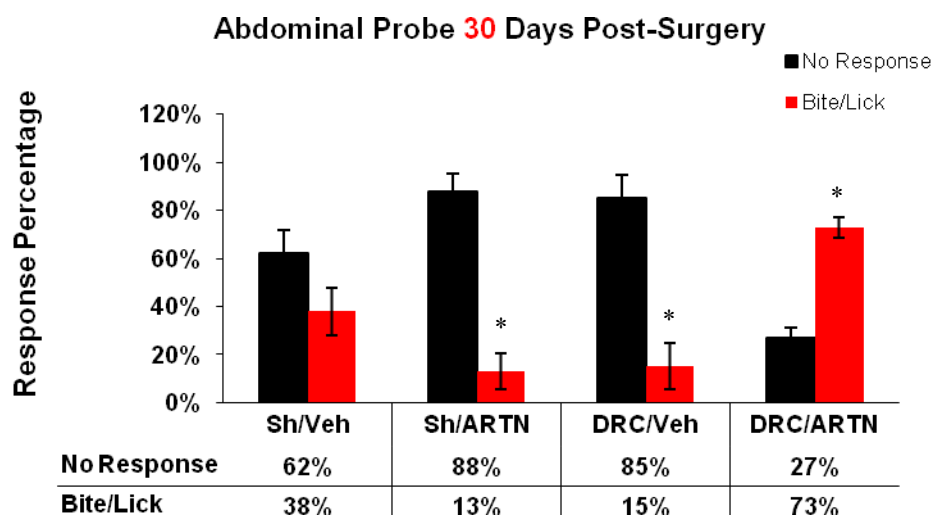
Figure 4.125 Pain assessment following systemic artemin administration.
Assessing the pain state of experimental rats by recording responses to abdominal probing. The relative percentage of non-noxious (No Response)-to-noxious (Bite/Lick) responses to an evoked mechanical stimulus applied to the abdomen of rats in each injury/treatment group are reported on post-surgical days 7 **(a)** and 30 **(b)**. The percentage values are given in the table below the X axes.

139

CHAPTER 5: SUMMARY AND CONCLUSIONS

In my first set of experiments, we demonstrated that crushing the dorsal roots as part of a rat cauda equina injury model resulted in differential acute and chronic disruptions in bladder function. The initial elimination of afferent input to the CNS resulted in a hypoactive bladder that stores more fluid than normal and paradoxically, becomes hyperactive at later time points. The external urethral sphincter was dysfunctional throughout and the malfunctioning bladder increased in weight and volume over time. While many techniques for assessing functional recovery following nervous system injury (e.g. BBB locomotor test) involve the subjective observations of the investigator, the use of this type of objective recording technique provides data immune to anthropocentric interpretation.

In our second set of experiment, we described how dorsal root crush injury, as a model of dorsal rhizotomy/deafferentation, results in the decreased presence of three different labels of primary afferents in the dorsal horn, similar to observations after multiple complete dorsal root transections. We also demonstrated that the CSPGs, neurocan, NG2 and phosphacan showed both short-term and long-term increases in immunoreactivity in the DREZ and DC following injury that reflects the development and maintenance of an inhibitory environment. Thus, we were able to show that in the lumbosacral spinal cord it is possible to produce an effective rhizotomy and stimulate astroglial responses by crushing the L6 and S1 dorsal roots on a par with that seen following complete transection. Not only does the crush model act as a more clinically

140

relevant model of cauda equina injury, it preserves the connection between the DRG and spinal cord, thereby providing a potential pathway for successful regeneration of dorsal root axons given appropriate therapeutic interventions.

When this body of work began, the mechanism by which artemin promoted regeneration across the DREZ was unknown. It was only in that last 12 months that mechanistic clues to how artemin enables axonal regeneration through a normally axon-growth-inhibitory environment became known. Our work revealed an effect of artemin on the temporal expression profile of phosphacan, as well as promoting functional regeneration of primary afferents across the DREZ. In light of our work and recent reports, we will discuss, based on an extensive review of the literature, the potential influence artemin has on both phosphacan expression and axonal regeneration.

Phosphacan, synthesized by glial cells, is the noncatalytic secreted isoform of receptor-type protein tyrosine phosphatase β (RPTPβ), lacking the transmembrane domain and two intracellular catalytic phosphatase domains of RPTPβ (Maurel *et al.* 1994). It could be argued that the expression profile shift that occurred due to artemin treatment in this study was a result of inhibited production of one isoform in favor of another. The secreted phosphacan inhibits growth by binding to CAMs on neuronal growth cones, thus preventing cell adhesion in the DREZ (Milev et al. 1994). Therefore, if RPTPβ was preferentially expressed, a more favorable regenerative environment could be created in the glial scar of the DREZ after N-CAM and Ng-CAM binding due to increased dephosphorylation of specific intracellular signaling proteins and alterations in

141

glial cell function. Alternatively, a temporal delay in the expression of any component of the ECM would inevitably change the extracellular environment that an axon growth cone encounters, perhaps rendering it growth permissive.

Recent work done in mice reported that there was no increase in phosphacan mRNA in the DREZ following dorsal root injury (Waselle *et al.* 2009). If RPTPβ mRNA is indistinguishable from phosphacan mRNA, this would suggest that, assuming our animal models are comparable, the majority of the immunoproduct we report as increasing in the DREZ post injury is phosphacan, the secreted isofom, and not RPTPβ, the membrane bound isoform. Phosphacan polypeptide has a much wider distribution than the corresponding mRNA, consistent with its secretion from glial cells (Snyder *et al.* 1996). Therefore, if cells within the DREZ demonstrate a minimal increase in phosphacan production after dorsal root injury, the majority must be secreted from neighboring glial cells or cells that migrated to the DREZ. It must be noted that the density of phosphacan positive staining peaked in both the artemin group and the vehicle group 7 days before any signs of afferent regeneration into and within the spinal cord were seen. Regardless of which isoform was present in the DREZ, such a high concentration of N-CAM- and Ng-CAM-binding receptors could be enough to halt neurite extension.

Artemin is one of four members of the GDNF family of ligands (GFLs) and in the present study consisted of a 113 amino acid recombinant form of human artemin. The artemin receptor is GDNF family receptor-α3 (GFRα3) and is almost exclusively

expressed by primary afferent DRG neurons (Baloh *et al.* 1998). Like the rest of the GFLs, as a homodimer, artemin binds to two non-signaling GPI-anchored GFRα3 coreceptors and this complex then dimerizes two molecules of the transmembrane protein RET (Durbec *et al.* 1996, Treanor *et al.* 1996, Trupp *et al.* 1996, Worby *et al.* 1996). Formation of the RET dimer induces transphosphorylation of their intracellular tyrosine kinase domains (Airaksinen *et al.* 1999) that initiates many intracellular signal transduction pathways (Hauck *et al.* 2006, Zhou *et al.* 2009). Membrane bound heparan sulfate glycosaminoglycans (HSPGs) facilitate GDNF-GFRα1-RET signaling by promoting the dimerizaton process (Barnett *et al.* 2002, Tanaka *et al.* 2002); in fact, without HSPGs GDNF-induced axonal growth does not occur (Barnett et al. 2002). Artemin also has a HSPG binding domain and the addition of exogenous heparin sulfate enhanced RET activation, suggesting a similar mechanism (Silvian *et al.* 2006). HSPGs are also thought to modulate RET-independent GFL signaling that activates Src and Met tyrosine kinases (Sariola & Saarma 2003). HSPGs bind N-CAM in mediating this RET-independent pathway and N-CAM has also been reported to act as an alternative signaling receptor for GFLs in its own right, promoting axon extension (Paratcha *et al.* 2003). Consequently, if artemin proves to have the same close signaling relationship with N-CAM as GDNF, systemic artemin administration may be resulting in the binding of artemin to a considerable proportion of N-CAM molecules on the surface of the regenerating growth cone, stimulating axon extension. Also, through competition and

143

steric hindrance, artemin might be blocking the binding of CSPGs like neurocan and phosphacan to N-CAM, thus promoting growth across the DREZ instead of inhibition.

An alternative or possibly complementary mechanism for artemin induced regeneration across the DREZ results from increasing the intrinsic regenerative capacity of primary afferent neurons. Recently it was reported that transgene-mediated Artemin supported the extension of neurites of primary DRG neurons in culture, and allowed these cells to overcome myelin inhibition of neurite extension (Zhou et al. 2009). The signaling mechanism involved cyclic adenosine monophosphate (cAMP) induced activation of protein kinase A (PKA) to phosphorylate cAMP response element binding protein (CREB) and increase expression of arginase I(Zhou et al. 2009). More recent work by the same group showed that the addition of artemin to the medium of DRG neurons plated on CNS myelin prevented the myelin induced increase in neuronal Nogo-A (Peng *et al.* 2010). Increasing neuronal cAMP levels is a key element dictating the regenerative capacity of neurons (Qiu *et al.* 2002). Growth cone extension is encouraged by the addition of cAMP to culture media (Song *et al.* 1998). Chemoattraction can be halted if a cAMP competitor or inhibitor of PKA is added to culture medium (Ming *et al.* 1997). Conditioning lesions of peripheral nerves that promote regeneration within the CNS (Neumann & Woolf 1999) result in increased neuronal cAMP (Qiu *et al.* 2005). Exposure to growth inhibitors like MAG lowers cAMP but exposure to neurotrophins reverses this (Cai *et al.* 1999). Myelin and CSPGs inhibit regeneration in part by stimulating Rho-GTPases, which induces growth cone collapse (Mizuno *et al.* 2004). Increasing

144

endogenous cAMP levels suppresses Rho activity and activity of its downstream target Rho-associated coiled kinase (ROCK) and promotes regeneration (Borisoff *et al.* 2003, Brabeck *et al.* 2004, Domeniconi & Filbin 2005, Tanaka *et al.* 2007). This is convincing evidence that artemin mediated regeneration involves increasing the regenerative capacity of injured primary afferents so that they overcome the inhibitory barrier rather than break the barrier down.

Thus, artemin shows promise for clinical use. It is relatively specific to the population of primary afferent neurons, it does not appear to result in aberrant sprouting since it has only a minor effect on the content of the extracellular matrix and it can exert its effect by systemic administration. However, future studies must examine closely the potential side effects of artemin's systemic use. The results of this research not only provide a deeper understanding of the sensory control of lower urinary tract function and give hope to those suffering from cauda equina injury, but it also provides a solution to the problem of axon regeneration through the DREZ. The loss of adequate bladder function after injury to the CNS remains largely unrecognized by the general public and even by the research community. The goal of our research is to advance this field of study and help to improve the quality of the day-to-day lives of those who suffer from neurogenic bladder dysfunction.

REFERENCES

Airaksinen, M. S., Titievsky, A. and Saarma, M. (1999) GDNF family neurotrophic factor signaling: four masters, one servant? *Mol Cell Neurosci,* **13,** 313-325.

Al-Qattan, M. M. (2003) Obstetric brachial plexus palsy associated with breech delivery. *Ann Plast Surg,* **51,** 257-264; discussion 265.

Alvarez, F. J., Villalba, R. M., Zerda, R. and Schneider, S. P. (2004) Vesicular glutamate transporters in the spinal cord, with special reference to sensory primary afferent synapses. *J Comp Neurol,* **472,** 257-280.

Amaya, F., Shimosato, G., Nagano, M., Ueda, M., Hashimoto, S., Tanaka, Y., Suzuki, H. and Tanaka, M. (2004) NGF and GDNF differentially regulate TRPV1 expression that contributes to development of inflammatory thermal hyperalgesia. *Eur J Neurosci,* **20,** 2303-2310.

Anderson, K. D. (2004) Targeting recovery: priorities of the spinal cord-injured population. *J Neurotrauma,* **21,** 1371-1383.

Andersson, K. E. (2002) Bladder activation: afferent mechanisms. *Urology,* **59** (Suppl 1), 41-50.

Andersson, K. E. and Arner, A. (2004) Urinary bladder contraction and relaxation: physiology and pathophysiology. *Physiol Rev,* **84,** 935-986.

Andrews, M. R., Czvitkovich, S., Dassie, E., Vogelaar, C. F., Faissner, A., Blits, B., Gage, F. H., ffrench-Constant, C. and Fawcett, J. W. (2009) Alpha9 integrin promotes neurite outgrowth on tenascin-C and enhances sensory axon regeneration. *J Neurosci,* **29,** 5546-5557.

Aoki, Y., Ohtori, S., Takahashi, K., Ino, H., Douya, H., Ozawa, T., Saito, T. and Moriya, H. (2005) Expression and co-expression of VR1, CGRP, and IB4-binding glycoprotein in dorsal root ganglion neurons in rats: differences between the disc afferents and the cutaneous afferents. *Spine,* **30,** 1496-1500.

Apodaca, G. (2004) The uroepithelium: not just a passive barrier. *Traffic,* **5,** 117-128.

Apodaca, G., Kiss, S., Ruiz, W., Meyers, S., Zeidel, M. and Birder, L. (2003) Disruption of bladder epithelium barrier function after spinal cord injury. *Am J Physiol Renal Physiol,* **284,** F966-976.

Asher, R. A., Morgenstern, D. A., Fidler, P. S., Adcock, K. H., Oohira, A., Braistead J. E., Levine, J. M., Margolis, R. U., Rogers, J. H. and Fawcett, J. W. (2000) Neurocan is upregulated in injured brain and in cytokine-treated astrocytes. *J Neurosci,* **20,** 2427-2438.

Averill, S., McMahon, S. B., Clary, D. O., Reichardt, L. F. and Priestley, J. V. (1995) Immunocytochemical localization of trkA receptors in chemically identified subgroups of adult rat sensory neurons. *Eur J Neurosci,* **7,** 1484-1494.

146

Bahns, E., Ernsberger, U., Janig, W. and Nelke, A. (1986) Functional characteristics of lumbar visceral afferent fibres from the urinary bladder and the urethra in the cat. *Pflugers Arch,* **407,** 510-518.

Baker, M. W. and Macagno, E. R. (2000) The role of a LAR-like receptor tyrosine phosphatase in growth cone collapse and mutual-avoidance by sibling processes. *J Neurobiol,* **44,** 194-203.

Baloh, R. H., Tansey, M. G., Lampe, P. A., Fahmer, T. J., Enomoto, H., Simburger, K. S., Leitner, M. L., Araki, T., Johnson, E. M. and Milbrandt, J. (1998) Artemin, a novel member of the GDNF ligand family, supports peripheral and central neurons and signals through the GFRalpha3-RET receptor complex. *Neuron,* **21,** 1291-1302.

Bandtlow, C. E. and Zimmermann, D. R. (2000) Proteoglycans in the developing brain: new conceptual insights for old proteins. *Physiol Rev,* **80,** 1267-1290.

Barnett, M. W., Fisher, C. E., Perona-Wright, G. and Davies, J. A. (2002) Signalling by glial cell line-derived neurotrophic factor (GDNF) requires heparan sulphate glycosaminoglycan. *J Cell Sci,* **115,** 4495-4503.

Baron, R. and Janig, W. (1991) Afferent and sympathetic neurons projecting into lumbar visceral nerves of the male rat. *J Comp Neurol,* **314,** 429-436.

Barrington, F. J. F. (1941) The component reflexes of micturition in the cat. Part III. *Brain,* **64,** 239-243.

Bartsch, U., Bandtlow, C. E., Schnell, L. et al. (1995) Lack of evidence that myelin-associated glycoprotein is a major inhibitor of axonal regeneration in the CNS. *Neuron,* **15,** 1375-1381.

Beckel, J. M., Kanai, A., Lee, S. J., de Groat, W. C. and Birder, L. A. (2006) Expression of functional nicotinic acetylcholine receptors in rat urinary bladder epithelial cells. *Am J Physiol Renal Physiol,* **290,** F103-110.

Becker, T., Anliker, B., Becker, C. G., Taylor, J., Schachner, M., Meyer, R. L. and Bartsch, U. (2000) Tenascin-R inhibits regrowth of optic fibers in vitro and persists in the optic nerve of mice after injury. *Glia,* **29,** 330-346.

Beggah, A. T., Dours-Zimmermann, M. T., Barras, F. M., Brosius, A., Zimmermann, D. R. and Zurn, A. D. (2005) Lesion-induced differential expression and cell association of Neurocan, Brevican, Versican V1 and V2 in the mouse dorsal root entry zone. *Neuroscience,* **133,** 749-762.

Belyantseva, I. A. and Lewin, G. R. (1999) Stability and plasticity of primary afferent projections following nerve regeneration and central degeneration. *Eur J Neurosci,* **11,** 457-468.

Benevento, B. T. and Sipski, M. L. (2002) Neurogenic bladder, neurogenic bowel, and sexual dysfunction in people with spinal cord injury. *Phys Ther,* **82,** 601-612.

Bennett, D. L., Boucher, T. J., Michael, G. J. et al. (2006) Artemin has potent neurotrophic actions on injured C-fibres. *J Peripher Nerv Syst,* **11,** 330-345.

Berggren, T. and Uvelius, B. (1996) Acute effects of unilateral pelvic ganglionectomy on urinary bladder function in vivo in the male rat. *Scand J Urol Nephrol,* **30,** 179-184.

Beric, A. and Light, J. K. (1992) Function of the conus medullaris and cauda equina in the early period following spinal cord injury and the relationship to recovery of detrusor function. *J Urol,* **148,** 1845-1848.

Berry, M. (1982) Post-injury myelin-breakdown products inhibit axonal growth: an hypothesis to explain the failure of axonal regeneration in the mammalian central nervous system. *Bibl Anat***,** 1-11.

Bespalov, M. M. and Saarma, M. (2007) GDNF family receptor complexes are emerging drug targets. *Trends Pharmacol Sci,* **28,** 68-74.

Birder, L. A. (2006) Role of the urothelium in urinary bladder dysfunction following spinal cord injury. *Prog Brain Res,* **152,** 135-146.

Birder, L. A., Kanai, A. J., de Groat, W. C. et al. (2001) Vanilloid receptor expression suggests a sensory role for urinary bladder epithelial cells. *Proc Natl Acad Sci U S A,* **98,** 13396-13401.

Birder, L. A., Nakamura, Y., Kiss, S. et al. (2002a) Altered urinary bladder function in mice lacking the vanilloid receptor TRPV1. *Nat Neurosci,* **5,** 856-860.

Birder, L. A., Nealen, M. L., Kiss, S., de Groat, W. C., Caterina, M. J., Wang, E., Apodaca, G. and Kanai, A. J. (2002b) Beta-adrenoceptor agonists stimulate endothelial nitric oxide synthase in rat urinary bladder urothelial cells. *J Neurosci,* **22,** 8063-8070.

Birder, L. A., Wolf-Johnston, A. S., Chib, M. K., Buffington, C. A., Roppolo, J. R. and Hanna-Mitchell, A. T. Beyond neurons: Involvement of urothelial and glial cells in bladder function. *Neurourol Urodyn,* **29,** 88-96.

Blaivas, J. G., Sinha, H. P., Zayed, A. A. and Labib, K. B. (1981) Detrusor-external sphincter dyssynergia: a detailed electromyographic study. *J Urol,* **125,** 545-548.

Bodner, D. R., Delamarter, R. B., Bohlman, H. H., Witcher, M., Biro, C. and Resnick, M. I. (1990) Urologic changes after cauda equina compression in dogs. *J Urol,* **143,** 186-190.

Borisoff, J. F., Chan, C. C., Hiebert, G. W., Oschipok, L., Robertson, G. S., Zamboni, R., Steeves, J. D. and Tetzlaff, W. (2003) Suppression of Rho-kinase activity promotes axonal growth on inhibitory CNS substrates. *Mol Cell Neurosci,* **22,** 405-416.

Bors, E. H. and Blinn, K. A. (1957) Spinal reflex activity from the vesical mucosa in paraplegic patients. *AMA Arch Neurol Psychiatry,* **78,** 339-354.

Bovolenta, P., Wandosell, F. and Nieto-Sampedro, M. (1992) CNS glial scar tissue: a source of molecules which inhibit central neurite outgrowth. *Prog Brain Res,* **94,** 367-379.

Bovolenta, P., Wandosell, F. and Nieto-Sampedro, M. (1993) Neurite outgrowth inhibitors associated with glial cells and glial cell lines. *Neuroreport,* **5,** 345-348.

Brabeck, C., Beschorner, R., Conrad, S., Mittelbronn, M., Bekure, K., Meyermann, R., Schluesener, H. J. and Schwab, J. M. (2004) Lesional expression of RhoA and RhoB following traumatic brain injury in humans. *J Neurotrauma,* **21,** 697-706.

Bradbury, E. J., Moon, L. D., Popat, R. J., King, V. R., Bennett, G. S., Patel, P. N., Fawcett, J. W. and McMahon, S. B. (2002) Chondroitinase ABC promotes functional recovery after spinal cord injury. *Nature,* **416,** 636-640.

Bregman, B. S., Kunkel-Bagden, E., Schnell, L., Dai, H. N., Gao, D. and Schwab, M. E. (1995) Recovery from spinal cord injury mediated by antibodies to neurite growth inhibitors. *Nature,* **378,** 498-501.

Brown, A. G. (1982) The dorsal horn of the spinal cord. *Q J Exp Physiol,* **67,** 193-212.

Brown, A. G., Fyffe, R. E., Rose, P. K. and Snow, P. J. (1981) Spinal cord collaterals from axons of type II slowly adapting units in the cat. *J Physiol,* **316,** 469-480.

Brown, A. G. and Noble, R. (1982) Connexions between hair follicle afferent fibres and spinocervical tract neurones in the cat: the synthesis of receptive fields. *J Physiol,* **323,** 77-91.

Brumovsky, P., Hygge-Blakeman, K., Villar, M. J., Watanabe, M., Wiesenfeld-Hallin, Z. and Hokfelt, T. (2006) Phenotyping of sensory and sympathetic ganglion neurons of a galanin-overexpressing mouse--possible implications for pain processing. *J Chem Neuroanat,* **31,** 243-262.

Brumovsky, P., Watanabe, M. and Hokfelt, T. (2007) Expression of the vesicular glutamate transporters-1 and -2 in adult mouse dorsal root ganglia and spinal cord and their regulation by nerve injury. *Neuroscience,* **147,** 469-490.

Bu, J., Akhtar, N. and Nishiyama, A. (2001) Transient expression of the NG2 proteoglycan by a subpopulation of activated macrophages in an excitotoxic hippocampal lesion. *Glia,* **34,** 296-310.

Bucy, P. C., Huggins, C. and Buchanan, D. N. (1937) Sympathetic innervation of the external sphincter of the human bladder. *Amer J Dis Child,* **54,** 1012-1018

Bunge, R. P., Puckett, W. R. and Hiester, E. D. (1997) Observations on the pathology of several types of human spinal cord injury, with emphasis on the astrocyte response to penetrating injuries. *Adv Neurol,* **72,** 305-315.

Burnstock, G. (2001) Purine-mediated signalling in pain and visceral perception. *Trends Pharmacol Sci,* **22,** 182-188.

Bush, T. G., Puvanachandra, N., Horner, C. H., Polito, A., Ostenfeld, T., Svendsen, C. N., Mucke, L., Johnson, M. H. and Sofroniew, M. V. (1999) Leukocyte infiltration, neuronal degeneration, and neurite outgrowth after ablation of scar-forming, reactive astrocytes in adult transgenic mice. *Neuron,* **23,** 297-308.

Butt, A. M., Hamilton, N., Hubbard, P., Pugh, M. and Ibrahim, M. (2005) Synantocytes: the fifth element. *J Anat,* **207,** 695-706.

Butt, A. M., Kiff, J., Hubbard, P. and Berry, M. (2002) Synantocytes: new functions for novel NG2 expressing glia. *J Neurocytol,* **31,** 551-565.

Cafferty, W. B., Bradbury, E. J., Lidierth, M., Jones, M., Duffy, P. J., Pezet, S. and McMahon, S. B. (2008) Chondroitinase ABC-mediated plasticity of spinal sensory function. *J Neurosci,* **28,** 11998-12009.

Cai, D., Shen, Y., De Bellard, M., Tang, S. and Filbin, M. T. (1999) Prior exposure to neurotrophins blocks inhibition of axonal regeneration by MAG and myelin via a cAMP-dependent mechanism. *Neuron,* **22,** 89-101.

Canoll, P. D., Petanceska, S., Schlessinger, J. and Musacchio, J. M. (1996) Three forms of RPTP-beta are differentially expressed during gliogenesis in the developing rat brain and during glial cell differentiation in culture. *J Neurosci Res,* **44,** 199-215.

Carlstedt, T. (1983) Regrowth of anastomosed ventral root nerve fibers in the dorsal root of rats. *Brain Res,* **272,** 162-165.

Carlstedt, T. (1985a) Dorsal root innervation of spinal cord neurons after dorsal root implantation into the spinal cord of adult rats. *Neurosci Lett,* **55,** 343-348.

Carlstedt, T. (1985b) Regenerating axons form nerve terminals at astrocytes. *Brain Res,* **347,** 188-191.

Carlstedt, T. (1988) Reinnervation of the mammalian spinal cord after neonatal dorsal root crush. *J Neurocytol,* **17,** 335-350.

Carlstedt, T. (1997) Nerve fibre regeneration across the peripheral-central transitional zone. *J Anat,* **190 (Pt 1),** 51-56.

Carlstedt, T. (2000) Approaches permitting and enhancing motoneuron regeneration after spinal cord, ventral root, plexus and peripheral nerve injuries. *Curr Opin Neurol,* **13,** 683-686.

Carlstedt, T., Cullheim, S., Risling, M. and Ulfhake, B. (1988) Mammalian root-spinal cord regeneration. *Prog Brain Res,* **78,** 225-229.

Carlstedt, T., Cullheim, S., Risling, M. and Ulfhake, B. (1989) Nerve fibre regeneration across the PNS-CNS interface at the root-spinal cord junction. *Brain Res Bull,* **22,** 93-102.

Carlstedt, T., Dalsgaard, C. J. and Molander, C. (1987) Regrowth of lesioned dorsal root nerve fibers into the spinal cord of neonatal rats. *Neurosci Lett,* **74,** 14-18.

Carlstedt, T., Linda, H., Cullheim, S. and Risling, M. (1986) Reinnervation of hind limb muscles after ventral root avulsion and implantation in the lumbar spinal cord of the adult rat. *Acta Physiol Scand,* **128,** 645-646.

Carmeliet, P. (2003) Blood vessels and nerves: common signals, pathways and diseases. *Nat Rev Genet,* **4,** 710-720.

Caroni, P. and Schwab, M. E. (1988a) Antibody against myelin-associated inhibitor of neurite growth neutralizes nonpermissive substrate properties of CNS white matter. *Neuron,* **1,** 85-96.

Caroni, P. and Schwab, M. E. (1988b) Two membrane protein fractions from rat central myelin with inhibitory properties for neurite growth and fibroblast spreading. *J Cell Biol,* **106,** 1281-1288.

Carpenter, F. G. (1951) Histological changes in the parasympathetically denervated feline bladder. . *Amer J Physiol,* **166,** 692-698.

Cheek, W. R., Anchondo, H., Raso, E. and Scott, B. (1973) Neurogenic bladder and the lumbar spine. *Urology, 2,* 30-33.

Chen, M. S., Huber, A. B., van der Haar, M. E., Frank, M., Schnell, L., Spillmann, A. A., Christ, F. and Schwab, M. E. (2000) Nogo-A is a myelin-associated neurite outgrowth inhibitor and an antigen for monoclonal antibody IN-1. *Nature, 403,* 434-439.

Christensen, M. D. and Hulsebosch, C. E. (1997) Spinal cord injury and anti-NGF treatment results in changes in CGRP density and distribution in the dorsal horn in the rat. *Exp Neurol, 147,* 463-475.

Clark, W. E. L. (1943) The insertion of peripheral nerve stumps in the brain. II The insertion of peripheral nerve stumps into the brain. *Br Med Bull, 1*.

Clifton, G. L., Coggeshall, R. E., Vance, W. H. and Willis, W. D. (1976) Receptive fields of unmyelinated ventral root afferent fibres in the cat. *J Physiol, 256,* 573-600.

Cockayne, D. A., Hamilton, S. G., Zhu, Q. M. et al. (2000) Urinary bladder hyporeflexia and reduced pain-related behaviour in P2X3-deficient mice. *Nature, 407,* 1011-1015.

Coggeshall, R. E., Coulter, J. D. and Willis, W. D., Jr. (1974) Unmyelinated axons in the ventral roots of the cat lumbosacral enlargement. *J Comp Neurol, 153,* 39-58.

David, S. and Aguayo, A. J. (1981) Axonal elongation into peripheral nervous system "bridges" after central nervous system injury in adult rats. *Science, 214,* 931-933.

Dawson, M. R., Levine, J. M. and Reynolds, R. (2000) NG2-expressing cells in the central nervous system: are they oligodendroglial progenitors? *J Neurosci Res, 61,* 471-479.

Dawson, M. R., Polito, A., Levine, J. M. and Reynolds, R. (2003) NG2-expressing glial progenitor cells: an abundant and widespread population of cycling cells in the adult rat CNS. *Mol Cell Neurosci, 24,* 476-488.

de Groat, W. C. (1976) Mechanisms underlying recurrent inhibition in the sacral parasympathetic outflow to the urinary bladder. *J Physiol, 257,* 503-513.

de Groat, W. C. (1993) Anatomy and physiology of the lower urinary tract. *Urol Clin North Am, 20,* 383-401.

de Groat, W. C. (1995) Mechanisms underlying the recovery of lower urinary tract function following spinal cord injury. *Paraplegia, 33,* 493-505.

de Groat, W. C. (1997) A neurologic basis for the overactive bladder. *Urology, 50,* 36-52; discussion 53-36.

de Groat, W. C. (2006) Integrative control of the lower urinary tract: preclinical perspective. *Br J Pharmacol, 147 Suppl 2,* S25-40.

De Groat, W. C. and Booth, A. M. (1993) Nervous control of the urogenital system. In: *Autonomic Nervous System,* (C. A. Maggi ed.), Vol. 3, pp. 291-347. Harwood Academic Publishers, London, UK.

De Groat, W. C. and Steers, W. D. (1990) Autonomic regulation of the urinary bladder and sex organs. In: *Central Regulation of Autonomic Functions,* (A. D. Loewy and K. M. Spyer eds.), pp. 310-333. Oxford University Press, London, UK.

Deen, H. G., Jr., Zimmerman, R. S., Swanson, S. K. and Larson, T. R. (1994) Assessment of bladder function after lumbar decompressive laminectomy for spinal stenosis: a prospective study. *J Neurosurg,* **80,** 971-974.

Domeniconi, M. and Filbin, M. T. (2005) Overcoming inhibitors in myelin to promote axonal regeneration. *J Neurol Sci,* **233,** 43-47.

Dou, C. L. and Levine, J. M. (1994) Inhibition of neurite growth by the NG2 chondroitin sulfate proteoglycan. *J Neurosci,* **14,** 7616-7628.

Doucette, R. (1991) PNS-CNS transitional zone of the first cranial nerve. *J Comp Neurol,* **312,** 451-466.

Duffy, P., Schmandke, A., Sigworth, J., Narumiya, S., Cafferty, W. B. and Strittmatter, S. M. (2009) Rho-associated kinase II (ROCKII) limits axonal growth after trauma within the adult mouse spinal cord. *J Neurosci,* **29,** 15266-15276.

Durbec, P. L., Larsson-Blomberg, L. B., Schuchardt, A., Costantini, F. and Pachnis, V. (1996) Common origin and developmental dependence on c-ret of subsets of enteric and sympathetic neuroblasts. *Development,* **122,** 349-358.

Elliott, T. R. (1907) Innervation of the bladder and urethra. *J Physiol,* **35,** 367-445.

Eng, L. F., Reier, P. J. and Houle, J. D. (1987) Astrocyte activation and fibrous gliosis: glial fibrillary acidic protein immunostaining of astrocytes following intraspinal cord grafting of fetal CNS tissue. *Prog Brain Res,* **71,** 439-455.

Ersoz, M. and Akyuz, M. (2004) Bladder-filling sensation in patients with spinal cord injury and the potential for sensation-dependent bladder emptying. *Spinal Cord,* **42,** 110-116.

Esko, J. D., Kimata, K. and Lindahl, U. (1999) Proteoglycans and Sulfated Glycoaminoglycans. In: *Essentials of Glycobiology*, (A. Varki, R. D. Cummings, J. D. Esko, H. H. Freeze, P. Stanley and G. Bertozzi eds.). Cold Spring Harbor Laboratory Press, Cold Spring Harbor, New York, NY

Esteban, I., Levanti, B., Garcia-Suarez, O., Germana, G., Ciriaco, E., Naves, F. J. and Vega, J. A. (1998) A neuronal subpopulation in the mammalian enteric nervous system expresses TrkA and TrkC neurotrophin receptor-like proteins. *Anat Rec,* **251,** 360-370.

Faissner, A., Clement, A., Lochter, A., Streit, A., Mandl, C. and Schachner, M. (1994) Isolation of a neural chondroitin sulfate proteoglycan with neurite outgrowth promoting properties. *J Cell Biol,* **126,** 783-799.

Fall, M., Lindstrom, S. and Mazieres, L. (1990) A bladder-to-bladder cooling reflex in the cat. *J Physiol,* **427,** 281-300.

Faulkner, J. R., Herrmann, J. E., Woo, M. J., Tansey, K. E., Doan, N. B. and Sofroniew, M. V. (2004) Reactive astrocytes protect tissue and preserve function after spinal cord injury. *J Neurosci,* **24,** 2143-2155.

Fawcett, J. W. and Asher, R. A. (1999) The glial scar and central nervous system repair. *Brain Res Bull,* **49,** 377-391.

Fawcett, J. W. and Keynes, R. J. (1990) Peripheral nerve regeneration. *Annu Rev Neurosci,* **13,** 43-60.

Ferguson, D. R., Kennedy, I. and Burton, T. J. (1997) ATP is released from rabbit urinary bladder epithelial cells by hydrostatic pressure changes--a possible sensory mechanism? *J Physiol,* **505 (Pt 2),** 503-511.

Fernandez, O. (2002) Mechanisms and current treatments of urogenital dysfunction in multiple sclerosis. *J Neurol,* **249,** 1-8.

Fife, D. and Kraus, J. (1986) Anatomic location of spinal cord injury. Relationship to the cause of injury. *Spine (Phila Pa 1976),* **11,** 2-5.

Filbin, M. T. (1995) Myelin-associated glycoprotein: a role in myelination and in the inhibition of axonal regeneration? *Curr Opin Neurobiol,* **5,** 588-595.

Fitch, M. T., Doller, C., Combs, C. K., Landreth, G. E. and Silver, J. (1999) Cellular and molecular mechanisms of glial scarring and progressive cavitation: in vivo and in vitro analysis of inflammation-induced secondary injury after CNS trauma. *J Neurosci,* **19,** 8182-8198.

Flood, H. D., Downie, J. W. and Awad, S. A. (1990) Urethral function after chronic cauda equina lesion in cats. II. The role of autonomically-innervated smooth and striated muscle in distal sphincter dysfunction. *J Urol,* **144,** 1029-1035.

Floyd, K., Hick, V. E. and Morrison, J. F. (1976) Mechanosensitive afferent units in the hypogastric nerve of the cat. *J Physiol,* **259,** 457-471.

Forrest, S. L. and Keast, J. R. (2008) Expression of receptors for glial cell line-derived neurotrophic factor family ligands in sacral spinal cord reveals separate targets of pelvic afferent fibers. *J Comp Neurol,* **506,** 989-1002.

Fouad, K., Klusman, I. and Schwab, M. E. (2004) Regenerating corticospinal fibers in the Marmoset (Callitrix jacchus) after spinal cord lesion and treatment with the anti-Nogo-A antibody IN-1. *Eur J Neurosci,* **20,** 2479-2482.

Fournier, A. E. and Strittmatter, S. M. (2001) Repulsive factors and axon regeneration in the CNS. *Curr Opin Neurobiol,* **11,** 89-94.

Fowler, C. J. (1999) Neurological disorders of micturition and their treatment. *Brain,* **122,** 1213-1231.

Fowler, C. J., Griffiths, D. and de Groat, W. C. (2008) The neural control of micturition. *Nat Rev Neurosci,* **9,** 453-466.

Fowler, C. J., Kirby, R. S., Harrison, M. J., Milroy, E. J. and Turner-Warwick, R. (1984) Individual motor unit analysis in the diagnosis of disorders of urethral sphincter innervation. *J Neurol Neurosurg Psychiatry,* **47,** 637-641.

Fraher, J. (2002) Axons and glial interfaces: ultrastructural studies. *J Anat,* **200,** 415-430.

Fraher, J. P. (1982) The ultrastructure of sheath cells in developing rat vomeronasal nerve. *J Anat,* **134,** 149-168.

Fraher, J. P. and Kaar, G. F. (1984) The transitional node of Ranvier at the junction of the central and peripheral nervous systems: an ultrastructural study of its development and mature form. *J Anat,* **139 (Pt 2),** 215-238.

Friedlander, D. R., Milev, P., Karthikeyan, L., Margolis, R. K., Margolis, R. U. and Grumet, M. (1994) The neuronal chondroitin sulfate proteoglycan neurocan binds

to the neural cell adhesion molecules Ng-CAM/L1/NILE and N-CAM, and inhibits neuronal adhesion and neurite outgrowth. *J Cell Biol,* **125,** 669-680.

Gabella, G. (1995) The structural relations between nerve fibres and muscle cells in the urinary bladder of the rat. *J Neurocytol,* **24,** 159-187.

Gabella, G. and Davis, C. (1998) Distribution of afferent axons in the bladder of rats. *J Neurocytol,* **27,** 141-155.

Gabella, G. and Uvelius, B. (1990) Urinary bladder of rat: fine structure of normal and hypertrophic musculature. *Cell Tissue Res,* **262,** 67-79.

Gardell, L. R., Wang, R., Ehrenfels, C. et al. (2003) Multiple actions of systemic artemin in experimental neuropathy. *Nat Med,* **9,** 1383-1389.

Garry, R. C., Roberts, T. D. and Todd, J. K. (1959) Reflexes involving the external urethral sphincter in the cat. *J Physiol,* **149,** 653-665.

Garwood, J., Rigato, F., Heck, N. and Faissner, A. (2001) Tenascin glycoproteins and the complementary ligand DSD-1-PG/ phosphacan--structuring the neural extracellular matrix during development and repair. *Restor Neurol Neurosci,* **19,** 51-64.

Garwood, J., Schnadelbach, O., Clement, A., Schutte, K., Bach, A. and Faissner, A. (1999) DSD-1-proteoglycan is the mouse homolog of phosphacan and displays opposing effects on neurite outgrowth dependent on neuronal lineage. *J Neurosci,* **19,** 3888-3899.

Geppetti, P., Nassini, R., Materazzi, S. and Benemei, S. (2008) The concept of neurogenic inflammation. *Br J Urol Int,* **101 Suppl 3,** 2-6.

German, K., Bedwani, J., Davies, J., Brading, A. F. and Stephenson, T. P. (1994) An assessment of the contribution of visco-elastic factors in the aetiology of poor compliance in the human neuropathic bladder. *Br J Urol,* **74,** 744-748.

Gerstenberg, T. C., Lykkegaard Nielsen, M. and Lindenberg, J. (1983) Spastic striated external sphincter syndrome imitating recurrent urinary tract infection in females. Effect of long-term alpha-adrenergic blockade with phenoxybenzamine. *Eur Urol,* **9,** 87-92.

Gibson, S. J., Polak, J. M., Bloom, S. R. et al. (1984) Calcitonin gene-related peptide immunoreactivity in the spinal cord of man and of eight other species. *J Neurosci,* **4,** 3101-3111.

Gilbert, R. J., McKeon, R. J., Darr, A., Calabro, A., Hascall, V. C. and Bellamkonda, R. V. (2005) CS-4,6 is differentially upregulated in glial scar and is a potent inhibitor of neurite extension. *Mol Cell Neurosci,* **29,** 545-558.

Gobel, S., Falls, W. M. and Humphrey, E. (1981) Morphology and synaptic connections of ultrafine primary axons in lamina I of the spinal dorsal horn: candidates for the terminal axonal arbors of primary neurons with unmyelinated (C) axons. *J Neurosci,* **1,** 1163-1179.

Goldberger, M. E. and Murray, M. (1974) Restitution of function and collateral sprouting in the cat spinal cord: the deafferented animal. *J Comp Neurol,* **158,** 37-53.

Goldstein, I. J. and Winter, H. G. (1999) The Griffonia simplicifolia I-B4 isolectin. A probe for alpha-D-galactosyl end groups. *Subcell Biochem,* **32,** 127-141.

Gosling, J. A. and Dixon, J. S. (1974) Sensory nerves in the mammalian urinary tract. An evaluation using light and electron microscopy. *J Anat,* **117,** 133-144.

Gosling, J. A. and Dixon, J. S. (1980) Structure of trabeculated detrusor smooth muscle in cases of prostatic hypertrophy. *Urol Int,* **35,** 351-355.

GrandPre, T., Li, S. and Strittmatter, S. M. (2002) Nogo-66 receptor antagonist peptide promotes axonal regeneration. *Nature,* **417,** 547-551.

GrandPre, T., Nakamura, F., Vartanian, T. and Strittmatter, S. M. (2000) Identification of the Nogo inhibitor of axon regeneration as a Reticulon protein. *Nature,* **403,** 439-444.

Gruber, C. M. (1933) The autonomic innervation of the genito-urinary tract. *Physiol Rev,* **13,** 497-609.

Grumet, M., Flaccus, A. and Margolis, R. U. (1993) Functional characterization of chondroitin sulfate proteoglycans of brain: interactions with neurons and neural cell adhesion molecules. *J Cell Biol,* **120,** 815-824.

Grumet, M., Milev, P., Sakurai, T., Karthikeyan, L., Bourdon, M., Margolis, R. K. and Margolis, R. U. (1994) Interactions with tenascin and differential effects on cell adhesion of neurocan and phosphacan, two major chondroitin sulfate proteoglycans of nervous tissue. *J Biol Chem,* **269,** 12142-12146.

Gu, H. Y., Chai, H., Zhang, J. Y., Yao, Z. B., Zhou, L. H., Wong, W. M., Bruce, I. and Wu, W. T. (2004) Survival, regeneration and functional recovery of motoneurons in adult rats by reimplantation of ventral root following spinal root avulsion. *Eur J Neurosci,* **19,** 2123-2131.

Guest, J. D., Hesse, D., Schnell, L., Schwab, M. E., Bunge, M. B. and Bunge, R. P. (1997) Influence of IN-1 antibody and acidic FGF-fibrin glue on the response of injured corticospinal tract axons to human Schwann cell grafts. *J Neurosci Res,* **50,** 888-905.

Haas, C. A., Rauch, U., Thon, N., Merten, T. and Deller, T. (1999) Entorhinal cortex lesion in adult rats induces the expression of the neuronal chondroitin sulfate proteoglycan neurocan in reactive astrocytes. *J Neurosci,* **19,** 9953-9963.

Habler, H. J., Janig, W. and Koltzenburg, M. (1990) Activation of unmyelinated afferent fibres by mechanical stimuli and inflammation of the urinary bladder in the cat. *J Physiol,* **425,** 545-562.

Hallin, R. G., Carlstedt, T., Nilsson-Remahl, I. and Risling, M. (1999) Spinal cord implantation of avulsed ventral roots in primates; correlation between restored motor function and morphology. *Exp Brain Res,* **124,** 304-310.

Hamill, O. P. and McBride, D. W., Jr. (1996) The pharmacology of mechanogated membrane ion channels. *Pharmacol Rev,* **48,** 231-252.

Hampton, D. W., Steeves, J. D., Fawcett, J. W. and Ramer, M. S. (2007) Spinally upregulated noggin suppresses axonal and dendritic plasticity following dorsal rhizotomy. *Exp Neurol,* **204,** 366-379.

Hancock, M. B. and Peveto, C. A. (1979) A preganglionic autonomic nucleus in the dorsal gray commissure of the lumbar spinal cord of the rat. *J Comp Neurol,* **183,** 65-72.

Hanna-Mitchell, A. T., Beckel, J. M., Barbadora, S., Kanai, A. J., de Groat, W. C. and Birder, L. A. (2007) Non-neuronal acetylcholine and urinary bladder urothelium. *Life Sci,* **80,** 2298-2302.

Hanna-Mitchell, A. T., O'Leary, D., Mobarak, M. S. et al. (2008) The impact of neurotrophin-3 on the dorsal root transitional zone following injury. *Spinal Cord,* **46,** 804-810.

Hannila, S. S. and Kawaja, M. D. (2005) Nerve growth factor-mediated collateral sprouting of central sensory axons into deafferentated regions of the dorsal horn is enhanced in the absence of the p75 neurotrophin receptor. *J Comp Neurol,* **486,** 331-343.

Harroch, S., Palmeri, M., Rosenbluth, J., Custer, A., Okigaki, M., Shrager, P., Blum, M., Buxbaum, J. D. and Schlessinger, J. (2000) No obvious abnormality in mice deficient in receptor protein tyrosine phosphatase beta. *Mol Cell Biol,* **20,** 7706-7715.

Harvey, P. A., Lee, D. H., Qian, F., Weinreb, P. H. and Frank, E. (2009) Blockade of Nogo receptor ligands promotes functional regeneration of sensory axons after dorsal root crush. *J Neurosci,* **29,** 6285-6295.

Harvey, P. A., Gong, B. J., Rossomondo, J. A. and Frank, E. (2010) Topographically specific regeneration of sensory axons in the spinal cord. *Proc Natl Acad Sci USA,* **107**, 11585-11590.

Hashimoto, M., Nitta, A., Fukumitsu, H., Nomoto, H., Shen, L. and Furukawa, S. (2005) Inflammation-induced GDNF improves locomotor function after spinal cord injury. *Neuroreport,* **16,** 99-102.

Hauck, S. M., Kinkl, N., Deeg, C. A., Swiatek-de Lange, M., Schoffmann, S. and Ueffing, M. (2006) GDNF family ligands trigger indirect neuroprotective signaling in retinal glial cells. *Mol Cell Biol,* **26,** 2746-2757.

Hellstrom, P., Kortelainen, P. and Kontturi, M. (1986) Late urodynamic findings after surgery for cauda equina syndrome caused by a prolapsed lumbar intervertebral disk. *J Urol,* **135,** 308-312.

Hirsch, S. and Bahr, M. (1999) Immunocytochemical characterization of reactive optic nerve astrocytes and meningeal cells. *Glia,* **26,** 36-46.

Hoang, T. X. and Havton, L. A. (2006) A single re-implanted ventral root exerts neurotropic effects over multiple spinal cord segments in the adult rat. *Exp Brain Res,* **169,** 208-217.

Hoang, T. X., Nieto, J. H., Dobkin, B. H., Tillakaratne, N. J. and Havton, L. A. (2006a) Acute implantation of an avulsed lumbosacral ventral root into the rat conus medullaris promotes neuroprotection and graft reinnervation by autonomic and motor neurons. *Neuroscience,* **138,** 1149-1160.

156

Hoang, T. X., Pikov, V. and Havton, L. A. (2006b) Functional reinnervation of the rat lower urinary tract after cauda equina injury and repair. *J Neurosci,* **26,** 8672-8679.

Honma, Y., Araki, T., Gianino, S., Bruce, A., Heuckeroth, R., Johnson, E. and Milbrandt, J. (2002) Artemin is a vascular-derived neurotropic factor for developing sympathetic neurons. *Neuron,* **35,** 267-282.

Horn, K. P., Busch, S. A., Hawthorne, A. L., van Rooijen, N. and Silver, J. (2008) Another barrier to regeneration in the CNS: activated macrophages induce extensive retraction of dystrophic axons through direct physical interactions. *J Neurosci,* **28,** 9330-9341.

Horner, P. J. and Gage, F. H. (2000) Regenerating the damaged central nervous system. *Nature,* **407,** 963-970.

Houle, J. D., Tom, V. J., Mayes, D., Wagoner, G., Phillips, N. and Silver, J. (2006) Combining an autologous peripheral nervous system "bridge" and matrix modification by chondroitinase allows robust, functional regeneration beyond a hemisection lesion of the adult rat spinal cord. *J Neurosci,* **26,** 7405-7415.

Hulsebosch, C. E. and Coggeshall, R. E. (1982) An analysis of the axon populations in the nerves to the pelvic viscera in the rat. *J Comp Neurol,* **211,** 1-10.

Hwang, S. J., Oh, J. M. and Valtschanoff, J. G. (2005) The majority of bladder sensory afferents to the rat lumbosacral spinal cord are both IB4- and CGRP-positive. *Brain Res,* **1062,** 86-91.

Iggo, A. (1955) Tension receptors in the stomach and the urinary bladder. *J Physiol,* **128,** 593-607.

Inatani, M., Tanihara, H., Oohira, A., Honjo, M., Kido, N. and Honda, Y. (2000) Upregulated expression of neurocan, a nervous tissue specific proteoglycan, in transient retinal ischemia. *Invest Ophthalmol Vis Sci,* **41,** 2748-2754.

Ingersoll, E. H. and Jones, L. L. (1958) Effects upon the urinary bladder of unilateral stimulation of pelvic nerves in the dog. *Anat Rec,* **130,** 605-615.

Iozzo, R. V. and Murdoch, A. D. (1996) Proteoglycans of the extracellular environment: clues from the gene and protein side offer novel perspectives in molecular diversity and function. *FASEB J,* **10,** 598-614.

Ivacko, J. A., Sun, R. and Silverstein, F. S. (1996) Hypoxic-ischemic brain injury induces an acute microglial reaction in perinatal rats. *Pediatr Res,* **39,** 39-47.

Jackson, A. (2008) www.spinalcord.uab.edu.

Janig, W. and Morrison, J. F. (1986) Functional properties of spinal visceral afferents supplying abdominal and pelvic organs, with special emphasis on visceral nociception. *Prog Brain Res,* **67,** 87-114.

Janig, W., Schmidt, M., Schnitzler, A. and Wesselmann, U. (1991) Differentiation of sympathetic neurones projecting in the hypogastric nerves in terms of their discharge patterns in cats. *J Physiol,* **437,** 157-179.

Jones, D. L. and Moore, T. (1973) The types of neuropathic bladder dysfunction associated with prolapsed lumbar intervertebral discs. *Br J Urol,* **45,** 39-43.

Jones, F. S. and Jones, P. L. (2000) The tenascin family of ECM glycoproteins: structure, function, and regulation during embryonic development and tissue remodeling. *Dev Dyn,* **218,** 235-259.

Jones, L. L., Yamaguchi, Y., Stallcup, W. B. and Tuszynski, M. H. (2002) NG2 is a major chondroitin sulfate proteoglycan produced after spinal cord injury and is expressed by macrophages and oligodendrocyte progenitors. *J Neurosci,* **22,** 2792-2803.

Jung, S. Y., Fraser, M. O., Ozawa, H., Yokoyama, O., Yoshiyama, M., De Groat, W. C. and Chancellor, M. B. (1999) Urethral afferent nerve activity affects the micturition reflex; implication for the relationship between stress incontinence and detrusor instability. *J Urol,* **162,** 204-212.

Kaplan, S. A., Chancellor, M. B. and Blaivas, J. G. (1991) Bladder and sphincter behavior in patients with spinal cord lesions. *J Urol,* **146,** 113-117.

Kennedy, J. G., Soffe, K. E., McGrath, A., Stephens, M. M., Walsh, M. G. and McManus, F. (1999) Predictors of outcome in cauda equina syndrome. *Eur Spine J,* **8,** 317-322.

Kim, J. E., Liu, B. P., Park, J. H. and Strittmatter, S. M. (2004) Nogo-66 receptor prevents raphespinal and rubrospinal axon regeneration and limits functional recovery from spinal cord injury. *Neuron,* **44,** 439-451.

Kitchener, P. D., Wilson, P. and Snow, P. J. (1993) Selective labelling of primary sensory afferent terminals in lamina II of the dorsal horn by injection of Bandeiraea simplicifolia isolectin B4 into peripheral nerves. *Neuroscience,* **54,** 545-551.

Kluck, P. (1980) The autonomic innervation of the human urinary bladder, bladder neck and urethra: a histochemical study. *Anat Rec,* **198,** 439-447.

Kostuik, J. P., Harrington, I., Alexander, D., Rand, W. and Evans, D. (1986) Cauda equina syndrome and lumbar disc herniation. *J Bone Joint Surg Am,* **68,** 386-391.

Kotzbauer, P. T., Lampe, P. A., Heuckeroth, R. O., Golden, J. P., Creedon, D. J., Johnson, E. M., Jr. and Milbrandt, J. (1996) Neurturin, a relative of glial-cell-line-derived neurotrophic factor. *Nature,* **384,** 467-470.

Kozlova, E. N., Rosario, C. M., Stromberg, I., Bygdeman, M. and Aldskogius, H. (1995) Peripherally grafted human foetal dorsal root ganglion cells extend axons into the spinal cord of adult host rats by circumventing dorsal root entry zone astrocytes. *Neuroreport,* **6,** 269-272.

Kozlova, E. N., Seiger, A. and Aldskogius, H. (1997) Human dorsal root ganglion neurons from embryonic donors extend axons into the host rat spinal cord along laminin-rich peripheral surroundings of the dorsal root transitional zone. *J Neurocytol,* **26,** 811-822.

Kreutzberg, G. W. (1996) Microglia: a sensor for pathological events in the CNS. *Trends Neurosci,* **19,** 312-318.

Kruse, M. N., Belton, A. L. and de Groat, W. C. (1993) Changes in bladder and external urethral sphincter function after spinal cord injury in the rat. *Am J Physiol,* **264,** R1157-1163.

Kruse, M. N., Mallory, B. S., Noto, H., Roppolo, J. R. and de Groat, W. C. (1991) Properties of the descending limb of the spinobulbospinal micturition reflex pathway in the cat. *Brain Res,* **556,** 6-12.

Kuru, M. (1965) Nervous Control of Micturition. *Physiol Rev,* **45,** 425-494.

Kuru, M., Koyama, Y. and Kurati, T. (1960) The bulbar vesico-relaxer center and the bulbo-sacral connections arising from it. A study of the function of the ventral reticulo-spinal tract. *J Comp Neurol,* **115,** 15-25.

Kuru, M., Koyama, Y. and Ozaki, H. (1963) Part of the brain stem controlling the tone of external urethral sphincter. *Proc. Jap. Acad. ,* **39,** 530-533.

Kwon, S. K., Woo, J., Kim, S. Y., Kim, H. and Kim, E. (2010) Trans-synaptic adhesions between netrin-G ligand-3 (NGL-3) and receptor tyrosine phosphatases lar, PTP(de Groat), and PTP(Kwon *et al.*) via specific domains regulate excitatory synapse formation. *J Biol Chem*.

LaMotte, C. C. and Kapadia, S. E. (1993) Deafferentation-induced terminal field expansion of myelinated saphenous afferents in the adult rat dorsal horn and the nucleus gracilis following pronase injection of the sciatic nerve. *J Comp Neurol,* **330,** 83-94.

Langworthy, O. R. and Kolb, L. C. (1933) The encephalic control of tone in musculature of the urinary bladder. *Brain,* **56,** 371-381.

Levine, B., Moore, K. A., Titus, J. M. and Fowler, D. (2002) A comparison of carboxyhemoglobin saturation values in postmortem heart blood and peripheral blood specimens. *J Forensic Sci,* **47,** 1388-1390.

Li, H., Leung, T. C., Hoffman, S., Balsamo, J. and Lilien, J. (2000) Coordinate regulation of cadherin and integrin function by the chondroitin sulfate proteoglycan neurocan. *J Cell Biol,* **149,** 1275-1288.

Li, J. L., Fujiyama, F., Kaneko, T. and Mizuno, N. (2003) Expression of vesicular glutamate transporters, VGluT1 and VGluT2, in axon terminals of nociceptive primary afferent fibers in the superficial layers of the medullary and spinal dorsal horns of the rat. *J Comp Neurol,* **457,** 236-249.

Light, A. R. and Perl, E. R. (1979) Reexamination of the dorsal root projection to the spinal dorsal horn including observations on the differential termination of coarse and fine fibers. *J Comp Neurol,* **186,** 117-131.

Liu, C. N. and Chambers, W. W. (1958) Intraspinal sprouting of dorsal root axons; development of new collaterals and preterminals following partial denervation of the spinal cord in the cat. *AMA Arch Neurol Psychiatry,* **79,** 46-61.

Liu, L., Rudin, M. and Kozlova, E. N. (2000) Glial cell proliferation in the spinal cord after dorsal rhizotomy or sciatic nerve transection in the adult rat. *Exp Brain Res,* **131,** 64-73.

Liuzzi, F. J. and Lasek, R. J. (1987) Astrocytes block axonal regeneration in mammals by activating the physiological stop pathway. *Science,* **237,** 642-645.

Loeb, G. E. (1976) Ventral root projections of myelinated dorsal root ganglion cells in the cat. *Brain Res,* **106,** 159-165.

Maeda, N. and Noda, M. (1998) Involvement of receptor-like protein tyrosine phosphatase zeta/RPTPbeta and its ligand pleiotrophin/heparin-binding growth-associated molecule (HB-GAM) in neuronal migration. *J Cell Biol,* **142,** 203-216.

Malin, S. A., Molliver, D. C., Koerber, H. R., Cornuet, P., Frye, R., Albers, K. M. and Davis, B. M. (2006) Glial cell line-derived neurotrophic factor family members sensitize nociceptors in vitro and produce thermal hyperalgesia in vivo. *J Neurosci,* **26,** 8588-8599.

Malkowicz, S. B., Atta, M. A., Elbadawi, A., Wein, A. J. and Levin, R. M. (1985) The effect of parasympathetic decentralization on the feline urinary bladder. *J Urol,* **133,** 521-523.

Margolis, R. K., Margolis, R. U., Preti, C. and Lai, D. (1975) Distribution and metabolism of glycoproteins and glycosaminoglycans in subcellular fractions of brain. *Biochemistry,* **14,** 4797-4804.

Martin, S., Levine, A. K., Chen, Z. J., Ughrin, Y. and Levine, J. M. (2001) Deposition of the NG2 proteoglycan at nodes of Ranvier in the peripheral nervous system. *J Neurosci,* **21,** 8119-8128.

Massague, J. and Chen, Y. G. (2000) Controlling TGF-beta signaling. *Genes Dev,* **14,** 627-644.

Massey, J. M., Hubscher, C. H., Wagoner, M. R., Decker, J. A., Amps, J., Silver, J. and Onifer, S. M. (2006) Chondroitinase ABC digestion of the perineuronal net promotes functional collateral sprouting in the cuneate nucleus after cervical spinal cord injury. *J Neurosci,* **26,** 4406-4414.

Matsui, F., Watanabe, E. and Oohira, A. (1994) Immunological identification of two proteoglycan fragments derived from neurocan, a brain-specific chondroitin sulfate proteoglycan. *Neurochem Int,* **25,** 425-431.

Matsui, M., Motomura, D., Fujikawa, T., Jiang, J., Takahashi, S., Manabe, T. and Taketo, M. M. (2002) Mice lacking M2 and M3 muscarinic acetylcholine receptors are devoid of cholinergic smooth muscle contractions but still viable. *J Neurosci,* **22,** 10627-10632.

Matsuura, S. and Downie, J. W. (2000) Effect of anesthetics on reflex micturition in the chronic cannula-implanted rat. *Neurourol Urodyn,* **19,** 87-99.

Maurel, P., Rauch, U., Flad, M., Margolis, R. K. and Margolis, R. U. (1994) Phosphacan, a chondroitin sulfate proteoglycan of brain that interacts with neurons and neural cell-adhesion molecules, is an extracellular variant of a receptor-type protein tyrosine phosphatase. *Proc Natl Acad Sci U S A,* **91,** 2512-2516.

McGlone, F. and Reilly, D. (2009) The cutaneous sensory system. *Neurosci Biobehav Rev,* **34,** 148-159.

McIlvried, L. A., Albers, K. and Gold, M. S. (2009) Distribution of Artemin and GFRalpha3 Labeled Nerve Fibers in the Dura Mater of Rat. *Headache*. **50**, 442-450.

McKeon, R. J., Hoke, A. and Silver, J. (1995) Injury-induced proteoglycans inhibit the potential for laminin-mediated axon growth on astrocytic scars. *Exp Neurol,* **136,** 32-43.

McKeon, R. J., Jurynec, M. J. and Buck, C. R. (1999) The chondroitin sulfate proteoglycans neurocan and phosphacan are expressed by reactive astrocytes in the chronic CNS glial scar. *J Neurosci,* **19,** 10778-10788.

McKeon, R. J., Schreiber, R. C., Rudge, J. S. and Silver, J. (1991) Reduction of neurite outgrowth in a model of glial scarring following CNS injury is correlated with the expression of inhibitory molecules on reactive astrocytes. *J Neurosci,* **11,** 3398-3411.

McKerracher, L., David, S., Jackson, D. L., Kottis, V., Dunn, R. J. and Braun, P. E. (1994) Identification of myelin-associated glycoprotein as a major myelin-derived inhibitor of neurite growth. *Neuron,* **13,** 805-811.

McMahon, S. B. and Kett-White, R. (1991) Sprouting of peripherally regenerating primary sensory neurones in the adult central nervous system. *J Comp Neurol,* **304,** 307-315.

McNeill, D. L., Carlton, S. M., Coggeshall, R. E. and Hulsebosch, C. E. (1990) Denervation-induced intraspinal synaptogenesis of calcitonin gene-related peptide containing primary afferent terminals. *J Comp Neurol,* **296,** 263-268.

McNeill, D. L., Carlton, S. M. and Hulsebosch, C. E. (1991) Intraspinal sprouting of calcitonin gene-related peptide containing primary afferents after deafferentation in the rat. *Exp Neurol,* **114,** 321-329.

McNeill, D. L. and Hulsebosch, C. E. (1987) Intraspinal sprouting of rat primary afferents after deafferentation. *Neurosci Lett,* **81,** 57-62.

McPhail, L. T., Borisoff, J. F., Tsang, B., Hwi, L. P., Kwiecien, J. M. and Ramer, M. S. (2007) Protracted myelin clearance hinders central primary afferent regeneration following dorsal rhizotomy and delayed neurotrophin-3 treatment. *Neurosci Lett,* **411,** 206-211.

Meyer-Puttlitz, B., Milev, P., Junker, E., Zimmer, I., Margolis, R. U. and Margolis, R. K. (1995) Chondroitin sulfate and chondroitin/keratan sulfate proteoglycans of nervous tissue: developmental changes of neurocan and phosphacan. *J Neurochem,* **65,** 2327-2337.

Meyer, P. R., Jr., Cybulski, G. R., Rusin, J. J. and Haak, M. H. (1991) Spinal cord injury. *Neurol Clin,* **9,** 625-661.

Middleton, J. W. and Keast, J. R. (2004) Artificial autonomic reflexes: using functional electrical stimulation to mimic bladder reflexes after injury or disease. *Auton Neurosci,* **113,** 3-15.

Milbrandt, J., de Sauvage, F. J., Fahrner, T. J. et al. (1998) Persephin, a novel neurotrophic factor related to GDNF and neurturin. *Neuron,* **20,** 245-253.

Milev, P., Fischer, D., Haring, M., Schulthess, T., Margolis, R. K., Chiquet-Ehrismann, R. and Margolis, R. U. (1997) The fibrinogen-like globe of tenascin-C mediates

its interactions with neurocan and phosphacan/protein-tyrosine phosphatase-zeta/beta. *J Biol Chem,* **272,** 15501-15509.

Milev, P., Friedlander, D. R., Sakurai, T., Karthikeyan, L., Flad, M., Margolis, R. K., Grumet, M. and Margolis, R. U. (1994) Interactions of the chondroitin sulfate proteoglycan phosphacan, the extracellular domain of a receptor-type protein tyrosine phosphatase, with neurons, glia, and neural cell adhesion molecules. *J Cell Biol,* **127,** 1703-1715.

Milev, P., Maurel, P., Haring, M., Margolis, R. K. and Margolis, R. U. (1996) TAG-1/axonin-1 is a high-affinity ligand of neurocan, phosphacan/protein-tyrosine phosphatase-zeta/beta, and N-CAM. *J Biol Chem,* **271,** 15716-15723.

Mimata, H., Satoh, F., Tanigawa, T., Nomura, Y. and Ogata, J. (1993) Changes of rat urinary bladder during acute phase of spinal cord injury. *Urol Int,* **51,** 89-93.

Ming, G. L., Song, H. J., Berninger, B., Holt, C. E., Tessier-Lavigne, M. and Poo, M. M. (1997) cAMP-dependent growth cone guidance by netrin-1. *Neuron,* **19,** 1225-1235.

Misgeld, T. and Kerschensteiner, M. (2006) In vivo imaging of the diseased nervous system. *Nat Rev Neurosci,* **7,** 449-463.

Misgeld, T., Nikic, I. and Kerschensteiner, M. (2007) In vivo imaging of single axons in the mouse spinal cord. *Nat Protoc,* **2,** 263-268.

Mizuno, T., Yamashita, T. and Tohyama, M. (2004) Chimaerins act downstream from neurotrophins in overcoming the inhibition of neurite outgrowth produced by myelin-associated glycoprotein. *J Neurochem,* **91,** 395-403.

Morgan, C., Nadelhaft, I. and de Groat, W. C. (1981) The distribution of visceral primary afferents from the pelvic nerve to Lissauer's tract and the spinal gray matter and its relationship to the sacral parasympathetic nucleus. *J Comp Neurol,* **201,** 415-440.

Mosdal, C., Iversen, P. and Iversen-Hansen, R. (1979) Bladder neuropathy in lumbar disc disease. *Acta Neurochir (Wien),* **46,** 281-286.

Moseley, R. L. (1936) Preganglionic connections of intramural ganglia of urinary bladder. *Proc Soc Exp Biol,* **34,** 728-730.

Moss, H. E., Tansey, E. M., Milner, P., Lincoln, J. and Burnstock, G. (1990) Neuropeptide immunoreactivity and choline acetyltransferase activity in the mouse urinary bladder following inoculation with Semliki Forest Virus. *J Auton Nerv Syst,* **31,** 47-56.

Moss, N. G., Harrington, W. W. and Tucker, M. S. (1997) Pressure, volume, and chemosensitivity in afferent innervation of urinary bladder in rats. *Am J Physiol,* **272,** R695-703.

Muellner, S. R. (1958) The voluntary control of micturition in man. *J Urol,* **80,** 473-478.

Mukhopadhyay, G., Doherty, P., Walsh, F. S., Crocker, P. R. and Filbin, M. T. (1994) A novel role for myelin-associated glycoprotein as an inhibitor of axonal regeneration. *Neuron,* **13,** 757-767.

162

Murakumo, M., Ushiki, T., Abe, K., Matsumura, K., Shinno, Y. and Koyanagi, T. (1995) Three-dimensional arrangement of collagen and elastin fibers in the human urinary bladder: a scanning electron microscopic study. *J Urol,* **154,** 251-256.

Nadelhaft, I. and Booth, A. M. (1984) The location and morphology of preganglionic neurons and the distribution of visceral afferents from the rat pelvic nerve: a horseradish peroxidase study. *J Comp Neurol,* **226,** 238-245.

Nadelhaft, I. and Vera, P. L. (1996) Neurons in the rat brain and spinal cord labeled after pseudorabies virus injected into the external urethral sphincter. *J Comp Neurol,* **375,** 502-517.

Nash, H. H., Borke, R. C. and Anders, J. J. (2002) Ensheathing cells and methylprednisolone promote axonal regeneration and functional recovery in the lesioned adult rat spinal cord. *J Neurosci,* **22,** 7111-7120.

Nathan, P. W. (1956) Sensations associated with micturition. *Br J Urol,* **28,** 126-131.

Neumann, S., Braz, J. M., Skinner, K., Llewellyn-Smith, I. J. and Basbaum, A. I. (2008) Innocuous, not noxious, input activates PKCgamma interneurons of the spinal dorsal horn via myelinated afferent fibers. *J Neurosci,* **28,** 7936-7944.

Neumann, S. and Woolf, C. J. (1999) Regeneration of dorsal column fibers into and beyond the lesion site following adult spinal cord injury. *Neuron,* **23,** 83-91.

Nielsen, B., de Nully, M., Schmidt, K. and Hansen, R. I. (1980) A urodynamic study of cauda equina syndrome due to lumbar disc herniation. *Urol Int,* **35,** 167-170.

Nishino, J., Mochida, K., Ohfuji, Y. et al. (1999) GFR alpha3, a component of the artemin receptor, is required for migration and survival of the superior cervical ganglion. *Neuron,* **23,** 725-736.

Nishiyama, A., Lin, X. H. and Stallcup, W. B. (1995) Generation of truncated forms of the NG2 proteoglycan by cell surface proteolysis. *Mol Biol Cell,* **6,** 1819-1832.

Nishiyama, A., Watanabe, M., Yang, Z. and Bu, J. (2002) Identity, distribution, and development of polydendrocytes: NG2-expressing glial cells. *J Neurocytol,* **31,** 437-455.

Novak, U. and Kaye, A. H. (2000) Extracellular matrix and the brain: components and function. *J Clin Neurosci,* **7,** 280-290.

Oblinger, M. M. and Lasek, R. J. (1984) A conditioning lesion of the peripheral axons of dorsal root ganglion cells accelerates regeneration of only their peripheral axons. *J Neurosci,* **4,** 1736-1744.

Ohta, Y., Iwasaki, Y., Abe, H. and Kato, M. (1991) Activation of spinal neurons by afferent fibers in the ventral roots of rats. *Neurosci Lett,* **130,** 137-139.

Okragly, A. J., Niles, A. L., Saban, R., Schmidt, D., Hoffman, R. L., Warner, T. F., Moon, T. D., Uehling, D. T. and Haak-Frendscho, M. (1999) Elevated tryptase, nerve growth factor, neurotrophin-3 and glial cell line-derived neurotrophic factor levels in the urine of interstitial cystitis and bladder cancer patients. *J Urol,* **161,** 438-441; discussion 441-432.

Oliveira, A. L., Hydling, F., Olsson, E. et al. (2003) Cellular localization of three vesicular glutamate transporter mRNAs and proteins in rat spinal cord and dorsal root ganglia. *Synapse,* **50,** 117-129.

Pannek, J., Hilfiker, R., Goecking, K. and Bersch, U. (2009) Preoperative urodynamic assessment in patients with spinal cord lesions undergoing sphincterotomy: is success predictable? *Urol Int,* **83,** 386-391.

Paratcha, G., Ledda, F. and Ibanez, C. F. (2003) The neural cell adhesion molecule NCAM is an alternative signaling receptor for GDNF family ligands. *Cell,* **113,** 867-879.

Pardridge, W. M. (2002) Drug and gene delivery to the brain: the vascular route. *Neuron,* **36,** 555-558.

Pascual, J. I., Gudino-Cabrera, G., Insausti, R. and Nieto-Sampedro, M. (2002) Spinal implants of olfactory ensheathing cells promote axon regeneration and bladder activity after bilateral lumbosacral dorsal rhizotomy in the adult rat. *J Urol,* **167,** 1522-1526.

Pavlakis, A. J., Siroky, M. B., Goldstein, I. and Krane, R. J. (1983) Neurourologic findings in conus medullaris and cauda equina injury. *Arch Neurol,* **40,** 570-573.

Peles, E., Nativ, M., Campbell, P. L. et al. (1995) The carbonic anhydrase domain of receptor tyrosine phosphatase beta is a functional ligand for the axonal cell recognition molecule contactin. *Cell,* **82,** 251-260.

Peng, X., Zhou, Z., Hu, J., Fink, D. J. and Mata, M. (2010) Soluble Nogo receptor down-regulates expression of neuronal Nogo-A to enhance axonal regeneration. *J Biol Chem,* **285,** 2783-2795.

Peters, A. (2004) A fourth type of neuroglial cell in the adult central nervous system. *J Neurocytol,* **33,** 345-357.

Petruska, J. C., Napaporn, J., Johnson, R. D. and Cooper, B. Y. (2002) Chemical responsiveness and histochemical phenotype of electrophysiologically classified cells of the adult rat dorsal root ganglion. *Neuroscience,* **115,** 15-30.

Petruska, J. C., Napaporn, J., Johnson, R. D., Gu, J. G. and Cooper, B. Y. (2000) Subclassified acutely dissociated cells of rat DRG: histochemistry and patterns of capsaicin-, proton-, and ATP-activated currents. *J Neurophysiol,* **84,** 2365-2379.

Pikov, V., Gillis, R. A., Jasmin, L. and Wrathall, J. R. (1998) Assessment of lower urinary tract functional deficit in rats with contusive spinal cord injury. *J Neurotrauma,* **15,** 375-386.

Pindzola, R. R., Doller, C. and Silver, J. (1993) Putative inhibitory extracellular matrix molecules at the dorsal root entry zone of the spinal cord during development and after root and sciatic nerve lesions. *Dev Biol,* **156,** 34-48.

Pizzorusso, T., Medini, P., Landi, S., Baldini, S., Berardi, N. and Maffei, L. (2006) Structural and functional recovery from early monocular deprivation in adult rats. *Proc Natl Acad Sci U S A,* **103,** 8517-8522.

Podnar, S., Trsinar, B. and Vodusek, D. B. (2006) Bladder dysfunction in patients with cauda equina lesions. *Neurourol Urodyn,* **25,** 23-31.

Potter, P. J. (2006) Disordered control of the urinary bladder after human spinal cord injury: what are the problems? *Prog Brain Res,* **152,** 51-57.

Priestley, J. V., Ramer, M. S., King, V. R., McMahon, S. B. and Brown, R. A. (2002) Stimulating regeneration in the damaged spinal cord. *J Physiol Paris,* **96,** 123-133.

Prinjha, R., Moore, S. E., Vinson, M., Blake, S., Morrow, R., Christie, G., Michalovich, D., Simmons, D. L. and Walsh, F. S. (2000) Inhibitor of neurite outgrowth in humans. *Nature,* **403,** 383-384.

Properzi, F. and Fawcett, J. W. (2004) Proteoglycans and brain repair. *News Physiol Sci,* **19,** 33-38.

Qiu, J., Cafferty, W. B., McMahon, S. B. and Thompson, S. W. (2005) Conditioning injury-induced spinal axon regeneration requires signal transducer and activator of transcription 3 activation. *J Neurosci,* **25,** 1645-1653.

Qiu, J., Cai, D. and Filbin, M. T. (2002) A role for cAMP in regeneration during development and after injury. *Prog Brain Res,* **137,** 381-387.

Quaglia, X., Beggah, A. T., Seidenbecher, C. and Zurn, A. D. (2008) Delayed priming promotes CNS regeneration post-rhizotomy in Neurocan and Brevican-deficient mice. *Brain,* **131,** 240-249.

Ramer, L. M., Richter, M. W., Roskams, A. J., Tetzlaff, W. and Ramer, M. S. (2004) Peripherally-derived olfactory ensheathing cells do not promote primary afferent regeneration following dorsal root injury. *Glia,* **47,** 189-206.

Ramer, M. S., Priestley, J. V. and McMahon, S. B. (2000) Functional regeneration of sensory axons into the adult spinal cord. *Nature,* **403,** 312-316.

Ramon y Cajal, S. (1928) *Degeneration and regeneration of the nervous system.* Oxford University Press, London, UK.

Rathjen, F. G. (1991) Neural cell contact and axonal growth. *Curr Opin Cell Biol,* **3,** 992-1000.

Rauch, U. (2004) Extracellular matrix components associated with remodeling processes in brain. *Cell Mol Life Sci,* **61,** 2031-2045.

Rethelyi, M. (1977) Preterminal and terminal axon arborizations in the substantia gelatinosa of cat's spinal cord. *J Comp Neurol,* **172,** 511-521.

Rethelyi, M., Horvath-Oszwald, E. and Boros, C. (2008) Caudal end of the rat spinal dorsal horn. *Neurosci Lett,* **445,** 153-157.

Rezajooi, K., Pavlides, M., Winterbottom, J., Stallcup, W. B., Hamlyn, P. J., Lieberman, A. R. and Anderson, P. N. (2004) NG2 proteoglycan expression in the peripheral nervous system: upregulation following injury and comparison with CNS lesions. *Mol Cell Neurosci,* **25,** 572-584.

Richardson, P. M., McGuinness, U. M. and Aguayo, A. J. (1980) Axons from CNS neurons regenerate into PNS grafts. *Nature,* **284,** 264-265.

Rivers, L. E., Young, K. M., Rizzi, M., Jamen, F., Psachoulia, K., Wade, A., Kessaris, N. and Richardson, W. D. (2008) PDGFRA/NG2 glia generate myelinating

oligodendrocytes and piriform projection neurons in adult mice. *Nat Neurosci,* **11,** 1392-1401.

Rong, W., Spyer, K. M. and Burnstock, G. (2002) Activation and sensitisation of low and high threshold afferent fibres mediated by P2X receptors in the mouse urinary bladder. *J Physiol,* **541,** 591-600.

Rooney, B. A. and Hulsebosch, C. E. (2010) Characterizing bladder and external urethral sphincter dysfunction using a model of cauda euina injury. *Exp Neurol; in press.*

Rosenblad, C., Gronborg, M., Hansen, C. et al. (2000) In vivo protection of nigral dopamine neurons by lentiviral gene transfer of the novel GDNF-family member neublastin/artemin. *Mol Cell Neurosci,* **15,** 199-214.

Rosenzweig, E. S. and McDonald, J. W. (2004) Rodent models for treatment of spinal cord injury: research trends and progress toward useful repair. *Curr Opin Neurol,* **17,** 121-131.

Rossiter, J. P. and Fraher, J. P. (1990) Intermingling of central and peripheral nervous tissues in rat dorsolateral vagal rootlet transitional zones. *J Neurocytol,* **19,** 385-407.

Runyan, S. A., Roy, R. R., Zhong, H. and Phelps, P. E. (2007) L1 cell adhesion molecule is not required for small-diameter primary afferent sprouting after deafferentation. *Neuroscience,* **150,** 959-969.

Ruoslahti, E. (1996) Brain extracellular matrix. *Glycobiology,* **6,** 489-492.

Rutka, J. T., Apodaca, G., Stern, R. and Rosenblum, M. (1988) The extracellular matrix of the central and peripheral nervous systems: structure and function. *J Neurosurg,* **69,** 155-170.

Sakurai, T., Friedlander, D. R. and Grumet, M. (1996) Expression of polypeptide variants of receptor-type protein tyrosine phosphatase beta: the secreted form, phosphacan, increases dramatically during embryonic development and modulates glial cell behavior in vitro. *J Neurosci Res,* **43,** 694-706.

Sanes, J. R. (1989) Extracellular matrix molecules that influence neural development. *Annu Rev Neurosci,* **12,** 491-516.

Sariola, H. and Saarma, M. (2003) Novel functions and signalling pathways for GDNF. *J Cell Sci,* **116,** 3855-3862.

Sato, S., Hayashi, R. H. and Garfield, R. E. (1989) Mechanical responses of the rat uterus, cervix, and bladder to stimulation of hypogastric and pelvic nerves in vivo. *Biol Reprod,* **40,** 209-219.

Savitsky, E. and Votey, S. (1997) Emergency department approach to acute thoracolumbar spine injury. *J Emerg Med,* **15,** 49-60.

Schmalfeldt, M., Bandtlow, C. E., Dours-Zimmermann, M. T., Winterhalter, K. H. and Zimmermann, D. R. (2000) Brain derived versican V2 is a potent inhibitor of axonal growth. *J Cell Sci,* **113,** 807-816.

Schmutzler, B. S., Roy, S. and Hingtgen, C. M. (2009) Glial cell line-derived neurotrophic factor family ligands enhance capsaicin-stimulated release of

166

calcitonin gene-related peptide from sensory neurons. *Neuroscience,* **161,** 148-156.

Schnadelbach, O., Mandl, C. and Faissner, A. (1998) Expression of DSD-1-PG in primary neural and glial-derived cell line cultures, upregulation by TGF-beta, and implications for cell-substrate interactions of the glial cell line Oli-neu. *Glia,* **23,** 99-119.

Schnell, L. and Schwab, M. E. (1990) Axonal regeneration in the rat spinal cord produced by an antibody against myelin-associated neurite growth inhibitors. *Nature,* **343,** 269-272.

Schwab, M. E. (1996a) Bridging the gap in spinal cord regeneration. *Nat Med,* **2,** 976-977.

Schwab, M. E. (1996b) Molecules inhibiting neurite growth: a minireview. *Neurochem Res,* **21,** 755-761.

Schwab, M. E. and Brosamle, C. (1997) Regeneration of lesioned corticospinal tract fibers in the adult rat spinal cord under experimental conditions. *Spinal Cord,* **35,** 469-473.

Sengupta, J. N. and Gebhart, G. F. (1994) Mechanosensitive properties of pelvic nerve afferent fibers innervating the urinary bladder of the rat. *J Neurophysiol,* **72,** 2420-2430.

Shen, Y., Tenney, A. P., Busch, S. A., Horn, K. P., Cuascut, F. X., Liu, K., He, Z., Silver, J. and Flanagan, J. G. (2009) PTPsigma is a receptor for chondroitin sulfate proteoglycan, an inhibitor of neural regeneration. *Science,* **326,** 592-596.

Shibata, A., Wright, M. V., David, S., McKerracher, L., Braun, P. E. and Kater, S. B. (1998) Unique responses of differentiating neuronal growth cones to inhibitory cues presented by oligodendrocytes. *J Cell Biol,* **142,** 191-202.

Shin, J. C., Park, C. I., Kim, H. J. and Lee, I. Y. (2002) Significance of low compliance bladder in cauda equina injury. *Spinal Cord,* **40,** 650-655.

Shu, X. Q. and Mendell, L. M. (1999) Neurotrophins and hyperalgesia. *Proc Natl Acad Sci U S A,* **96,** 7693-7696.

Silver, J. and Miller, J. H. (2004) Regeneration beyond the glial scar. *Nat Rev Neurosci,* **5,** 146-156.

Silverman, J. D. and Kruger, L. (1990) Selective neuronal glycoconjugate expression in sensory and autonomic ganglia: relation of lectin reactivity to peptide and enzyme markers. *J Neurocytol,* **19,** 789-801.

Silvian, L., Jin, P., Carmillo, P. et al. (2006) Artemin crystal structure reveals insights into heparan sulfate binding. *Biochemistry,* **45,** 6801-6812.

Simonen, M., Pedersen, V., Weinmann, O. et al. (2003) Systemic deletion of the myelin-associated outgrowth inhibitor Nogo-A improves regenerative and plastic responses after spinal cord injury. *Neuron,* **38,** 201-211.

Snow, D. M., Lemmon, V., Carrino, D. A., Caplan, A. I. and Silver, J. (1990) Sulfated proteoglycans in astroglial barriers inhibit neurite outgrowth in vitro. *Exp Neurol,* **109,** 111-130.

Snyder, S. E., Li, J., Schauwecker, P. E., McNeill, T. H. and Salton, S. R. (1996) Comparison of RPTP zeta/beta, phosphacan, and trkB mRNA expression in the developing and adult rat nervous system and induction of RPTP zeta/beta and phosphacan mRNA following brain injury. *Brain Res Mol Brain Res,* **40,** 79-96.

Somogyi, G. T., Zernova, G. V., Yoshiyama, M., Yamamoto, T. and de Groat, W. C. (1998) Frequency dependence of muscarinic facilitation of transmitter release in urinary bladder strips from neurally intact or chronic spinal cord transected rats. *Br J Pharmacol,* **125,** 241-246.

Song, H., Ming, G., He, Z., Lehmann, M., McKerracher, L., Tessier-Lavigne, M. and Poo, M. (1998) Conversion of neuronal growth cone responses from repulsion to attraction by cyclic nucleotides. *Science,* **281,** 1515-1518.

Spicer, A. P., Joo, A. and Bowling, R. A., Jr. (2003) A hyaluronan binding link protein gene family whose members are physically linked adjacent to chondroitin sulfate proteoglycan core protein genes: the missing links. *J Biol Chem,* **278,** 21083-21091.

Spicer, A. P. and Tien, J. Y. (2004) Hyaluronan and morphogenesis. *Birth Defects Res C Embryo Today,* **72,** 89-108.

Spillmann, A. A., Amberger, V. R. and Schwab, M. E. (1997) High molecular weight protein of human central nervous system myelin inhibits neurite outgrowth: an effect which can be neutralized by the monoclonal antibody IN-1. *Eur J Neurosci,* **9,** 549-555.

Starkey, M. L., Davies, M., Yip, P. K., Carter, L. M., Wong, D. J., McMahon, S. B. and Bradbury, E. J. (2009) Expression of the regeneration-associated protein SPRR1A in primary sensory neurons and spinal cord of the adult mouse following peripheral and central injury. *J Comp Neurol,* **513,** 51-68.

Steers, W. D., Ciambotti, J., Etzel, B., Erdman, S. and de Groat, W. C. (1991) Alterations in afferent pathways from the urinary bladder of the rat in response to partial urethral obstruction. *J Comp Neurol,* **310,** 401-410.

Steinmetz, M. P., Horn, K. P., Tom, V. J., Miller, J. H., Busch, S. A., Nair, D., Silver, D. J. and Silver, J. (2005) Chronic enhancement of the intrinsic growth capacity of sensory neurons combined with the degradation of inhibitory proteoglycans allows functional regeneration of sensory axons through the dorsal root entry zone in the mammalian spinal cord. *J Neurosci,* **25,** 8066-8076.

Stichel, C. C. and Muller, H. W. (1998) The CNS lesion scar: new vistas on an old regeneration barrier. *Cell Tissue Res,* **294**, 1-9.

Streit, W. J. and Kreutzberg, G. W. (1987) Lectin binding by resting and reactive microglia. *J Neurocytol,* **16,** 249-260.

Susset, J. G., Peters, N. D., Cohen, S. I. and Ghoniem, G. M. (1982) Early detection of neurogenic bladder dysfunction caused by protruded lumbar disk. *Urology,* **20,** 461-463.

Talaat, M. (1937a) Afferent impulses in nerves supplying urinary bladder. *J Physiol,* **89,** 1-13.

Talaat, M. (1937b) Afferent impulses in the nerves supplying the urinary bladder. *J Physiol,* **89,** 1-13.

Tanaka, M., Xiao, H. and Kiuchi, K. (2002) Heparin facilitates glial cell line-derived neurotrophic factor signal transduction. *Neuroreport,* **13,** 1913-1916.

Tanaka, S., Ishii, K., Kasai, K., Yoon, S. O. and Saeki, Y. (2007) Neural expression of G protein-coupled receptors GPR3, GPR6, and GPR12 up-regulates cyclic AMP levels and promotes neurite outgrowth. *J Biol Chem,* **282,** 10506-10515.

Tang, X., Davies, J. E. and Davies, S. J. (2003) Changes in distribution, cell associations, and protein expression levels of NG2, neurocan, phosphacan, brevican, versican V2, and tenascin-C during acute to chronic maturation of spinal cord scar tissue. *J Neurosci Res,* **71,** 427-444.

Tang, X. Q., Heron, P., Mashburn, C. and Smith, G. M. (2007) Targeting sensory axon regeneration in adult spinal cord. *J Neurosci,* **27,** 6068-6078.

Tatagiba, M., Brosamle, C. and Schwab, M. E. (1997) Regeneration of injured axons in the adult mammalian central nervous system. *Neurosurgery,* **40,** 541-546; discussion 546-547.

Tester, N. J. and Howland, D. R. (2008) Chondroitinase ABC improves basic and skilled locomotion in spinal cord injured cats. *Exp Neurol,* **209,** 483-496.

Thor, K. B., Morgan, C., Nadelhaft, I., Houston, M. and De Groat, W. C. (1989) Organization of afferent and efferent pathways in the pudendal nerve of the female cat. *J Comp Neurol,* **288,** 263-279.

Todd, A. J., Hughes, D. I., Polgar, E., Nagy, G. G., Mackie, M., Ottersen, O. P. and Maxwell, D. J. (2003) The expression of vesicular glutamate transporters VGLUT1 and VGLUT2 in neurochemically defined axonal populations in the rat spinal cord with emphasis on the dorsal horn. *Eur J Neurosci,* **17,** 13-27.

Tom, V. J., Steinmetz, M. P., Miller, J. H., Doller, C. M. and Silver, J. (2004) Studies on the development and behavior of the dystrophic growth cone, the hallmark of regeneration failure, in an in vitro model of the glial scar and after spinal cord injury. *J Neurosci,* **24,** 6531-6539.

Toole, B. P. (2000) Hyaluronan is not just a goo! *J Clin Invest,* **106,** 335-336.

Treanor, J. J., Goodman, L., de Sauvage, F. et al. (1996) Characterization of a multicomponent receptor for GDNF. *Nature,* **382,** 80-83.

Trupp, M., Arenas, E., Fainzilber, M. et al. (1996) Functional receptor for GDNF encoded by the c-ret proto-oncogene. *Nature,* **381,** 785-789.

Uvelius, B. and Mattiasson, A. (1984) Collagen content in the rat urinary bladder subjected to infravesical outflow obstruction. *J Urol,* **132,** 587-590.

Varoqui, H., Schafer, M. K., Zhu, H., Weihe, E. and Erickson, J. D. (2002) Identification of the differentiation-associated Na+/PI transporter as a novel vesicular glutamate transporter expressed in a distinct set of glutamatergic synapses. *J Neurosci,* **22,** 142-155.

Vellani, V., Colucci, M., Lattanzi, R., Giannini, E., Negri, L., Melchiorri, P. and McNaughton, P. A. (2006) Sensitization of transient receptor potential vanilloid 1 by the prokineticin receptor agonist Bv8. *J Neurosci,* **26,** 5109-5116.

Vera, P. L. and Nadelhaft, I. (1992) Afferent and sympathetic innervation of the dome and the base of the urinary bladder of the female rat. *Brain Res Bull,* **29,** 651-658.

Vignes, J. R., Bauchet, L. and Ohanna, F. (2007) Dorsal rhizotomy combined with anterior sacral root stimulation for neurogenic bladder. *Acta Neurochir Suppl,* **97,** 323-331.

von Boyen, G. B., Steinkamp, M., Reinshagen, M., Schafer, K. H., Adler, G. and Kirsch, J. (2004) Proinflammatory cytokines increase glial fibrillary acidic protein expression in enteric glia. *Gut,* **53,** 222-228.

Voris, H. C. and Landes, H. E. (1940) Cystometric studies in cases of neurologic disease. *Arch Neurol Psychiatry,* **44,** 104-117.

Walton, K. M. and Dixon, J. E. (1993) Protein tyrosine phosphatases. *Annu Rev Biochem,* **62,** 101-120.

Wang, G. J., Deng, H. Y., Maier, C. M., Sun, G. H. and Yenari, M. A. (2002) Mild hypothermia reduces ICAM-1 expression, neutrophil infiltration and microglia/monocyte accumulation following experimental stroke. *Neuroscience,* **114,** 1081-1090.

Wang, R., King, T., Ossipov, M. H. et al. (2008) Persistent restoration of sensory function by immediate or delayed systemic artemin after dorsal root injury. *Nat Neurosci,* **11,** 488-496.

Wang, S. C. and Ranson, S. W. (1939) Autonomic responses to electrical stimulation of the lower brain stem. . *Journal of Comparative Neurology,* **71,** 437-455.

Waselle, L., Quaglia, X. and Zurn, A. D. (2009) Differential proteoglycan expression in two spinal cord regions after dorsal root injury. *Mol Cell Neurosci,* **42,** 315-327.

Wein, A. J. (2005) The urothelium in overactive bladder: passive bystander or active participant? *J Urol,* **173,** 2199-2200.

Wen, J. and Morrison, J. F. (1995) The effects of high urinary potassium concentration on pelvic nerve mechanoreceptors and 'silent' afferents from the rat bladder. *Adv Exp Med Biol,* **385,** 237-239.

Wigley, R. and Butt, A. M. (2009) Integration of NG2-glia (synantocytes) into the neuroglial network. *Neuron Glia Biol***,** 1-8.

Willis, W. D. and Coggeshall, R. E. (1991) *Sensory mechanisms of the spinal cord*. Plenum Press, New York and London.

Windle, W. F. and Chambers, W. W. (1950) Regeneration in the spinal cord of the cat and dog. *J Comp Neurol,* **93,** 241-257.

Wintergerst, E. S., Faissner, A. and Celio, M. R. (1996) The proteoglycan DSD-1-PG occurs in perineuronal nets around parvalbumin-immunoreactive interneurons of the rat cerebral cortex. *Int J Dev Neurosci,* **14,** 249-255.

Wiseman, O. J., Brady, C. M., Hussain, I. F., Dasgupta, P., Watt, H., Fowler, C. J. and Landon, D. N. (2002) The ultrastructure of bladder lamina propria nerves in healthy subjects and patients with detrusor hyperreflexia. *J Urol,* **168,** 2040-2045.

Wong, L. F., Yip, P. K., Battaglia, A. et al. (2006) Retinoic acid receptor beta2 promotes functional regeneration of sensory axons in the spinal cord. *Nat Neurosci,* **9,** 243-250.

Worby, C. A., Vega, Q. C., Zhao, Y., Chao, H. H., Seasholtz, A. F. and Dixon, J. E. (1996) Glial cell line-derived neurotrophic factor signals through the RET receptor and activates mitogen-activated protein kinase. *J Biol Chem,* **271,** 23619-23622.

Wu, A., Lauschke, J. L., Morris, R. and Waite, P. M. (2009) Characterization of rat forepaw function in two models of cervical dorsal root injury. *J Neurotrauma,* **26,** 17-29.

Wu, D. (2005) Neuroprotection in experimental stroke with targeted neurotrophins. *NeuroRx,* **2,** 120-128.

Wujek, J. R. and Lasek, R. J. (1983) Correlation of axonal regeneration and slow component B in two branches of a single axon. *J Neurosci,* **3,** 243-251.

Wyndaele, J. J. (1991) Investigation of the afferent nerves of the lower urinary tract in patients with 'complete' and 'incomplete' spinal cord injury. *Paraplegia,* **29,** 490-494.

Wyndaele, J. J. (1997) Correlation between clinical neurological data and urodynamic function in spinal cord injured patients. *Spinal Cord,* **35,** 213-216.

Yamaguchi, Y. (2000) Lecticans: organizers of the brain extracellular matrix. *Cell Mol Life Sci,* **57,** 276-289.

Yan, H., Newgreen, D. F. and Young, H. M. (2003) Developmental changes in neurite outgrowth responses of dorsal root and sympathetic ganglia to GDNF, neurturin, and artemin. *Dev Dyn,* **227,** 395-401.

Yoshimura, N. and de Groat, W. C. (1997) Neural control of the lower urinary tract. *Int J Urol,* **4,** 111-125.

Yoshimura, N., Erdman, S. L., Snider, M. W. and de Groat, W. C. (1998) Effects of spinal cord injury on neurofilament immunoreactivity and capsaicin sensitivity in rat dorsal root ganglion neurons innervating the urinary bladder. *Neuroscience,* **83,** 633-643.

Yoshiyama, M., Nezu, F. M., Yokoyama, O., de Groat, W. C. and Chancellor, M. B. (1999) Changes in micturition after spinal cord injury in conscious rats. *Urology,* **54,** 929-933.

Young, H. M., Anderson, R. B. and Anderson, C. R. (2004) Guidance cues involved in the development of the peripheral autonomic nervous system. *Auton Neurosci,* **112,** 1-14.

Yrjanheikki, J., Keinanen, R., Pellikka, M., Hokfelt, T. and Koistinaho, J. (1998) Tetracyclines inhibit microglial activation and are neuroprotective in global brain ischemia. *Proc Natl Acad Sci U S A,* **95,** 15769-15774.

Zagorodnyuk, V. P., Costa, M. and Brookes, S. J. (2006) Major classes of sensory neurons to the urinary bladder. *Auton Neurosci,* **126-127,** 390-397.

Zhang, Y., Ghadiri-Sani, M., Zhang, X., Richardson, P. M., Yeh, J. and Bo, X. (2007) Induced expression of polysialic acid in the spinal cord promotes regeneration of sensory axons. *Mol Cell Neurosci,* **35,** 109-119.

Zhang, Y., Tohyama, K., Winterbottom, J. K., Haque, N. S., Schachner, M., Lieberman, A. R. and Anderson, P. N. (2001) Correlation between putative inhibitory molecules at the dorsal root entry zone and failure of dorsal root axonal regeneration. *Mol Cell Neurosci,* **17,** 444-459.

Zhou, Z., Peng, X., Fink, D. J. and Mata, M. (2009) HSV-mediated transfer of artemin overcomes myelin inhibition to improve outcome after spinal cord injury. *Mol Ther,* **17,** 1173-1179.

Zhu, X., Bergles, D. E. and Nishiyama, A. (2008) NG2 cells generate both oligodendrocytes and gray matter astrocytes. *Development,* **135,** 145-157.

Zinck, N. D., Rafuse, V. F. and Downie, J. W. (2007) Sprouting of CGRP primary afferents in lumbosacral spinal cord precedes emergence of bladder activity after spinal injury. *Exp Neurol,* **204,** 777-790.

VITA

Brian Anthony was born on the 27th of July 1979 in Drogheda, County Louth,

Ireland to Anthony and Bríd Rooney.

Education

Leaving Certificate, St Mary's Diocesan School, Drogheda, County Louth, Ireland

B.A. Moderatorship in Zoology from the University of Dublin, Trinity College, Dublin,

Ireland.

Publications:

Articles in peer-reviewed journals

Rooney B.A., Crown E.D., Hulsebosch C.E. and McAdoo D.J. Preemptive analgesia with lidocaine prevents Failed Back Surgery Syndrome. Exp Neurol. 204(2):589-96, 2007. Epub 2006 Dec 20.

Rooney B.A. and Hulsebosch C.E. Characterizating bladder and external urethral sphincter function using a model of cauda equine injury. Exp Neurol. Submitted and under review.

Abstracts

CE Hulsebosch, JP Yang, RJ Grill, SJ Davies, JE Daves, DJ Deyo, GC Unabia, Z Ye, **BA Rooney**, KM Johnson and GL Clifton. Sheep – A large mammalian model for translational research in central and peripheral nervous system injuries. Presented at the 33rd annual Society for Neuroscience meeting, New Orleans, LA. 2003.

BA Rooney, CE Hulsebosch and DJ McAdoo. Injury induced increases in extracellular excitatory amino acid concentrations in the rat spinal cord: A model of failed back surgery syndrome. Presented at the 34th annual Society for Neuroscience meeting, San Diego, CA. 2004.

BA Rooney, K Kintner and CE Hulsebosch. Model of cauda equine injury: effects on bladder detrusor and external urethral spincter coordination. Presented at the 35th annual SfN meeting, Washington DC. 2005.

BA Rooney, CE Hulsebosch and DJ McAdoo. Preemptive analgesia with lidocaine prevents failed back surgery syndrome. Presented at the 36th annual SfN meeting, Atlanta, GA. 2006.

BA Rooney, JE Davies and CE Hulsebosch. Cauda equine injury: effects on bladder functionand dorsal horn neurochemical cytoarchitecture. Presented at the 37th annual SfN meeting, San Diego, CA. 2007.

BA Rooney and CE Hulsebosch. The effects of cauda equine injury on lower urinary tract function and dorsal horn afferent innervations. Presented at Mission Connect Meeting, Houston, TX. 2007.

BA Rooney and CE Hulsebosch. Bladder-sphincteric functional deficits and permanent loss of dorsal horn afferentation after cauda equine injury. Presented at Neurotrauma 2008: First joint symposium of the International and National Neurotrauma Societies, Orlando, FL. 2008

BA Rooney and CE Hulsebosch. Artemin induced axonal regeneration across the DREZ promotes improvements in bladder function and delays the increased expression of phosphacan. Presented at the National Neurotrauma Symposium, Las Vegas NV, 2010.

INVITED SPEAKER:

Preemptive analgesia with lidocaine prevents Failed Back Surgery Syndrome. Anesthesia and Neuroscience Combined Conference (ANCC), University of Texas, Medical Branch, Galveston, TX. June 2007.

Preemptive analgesia with lidocaine prevents Failed Back Surgery Syndrome. American Spinal Injury Association (ASIA): "Treatment Strategies for Improved Recovery after Spinal Cord Injury" workshop. June 20th, 2008.

AWARDS:

Oslerian Essay Award for Translational Research, National Student Research Forum, Galveston, Texas, 2007.

Travel Grant Recipient: National Neurotrauma Society annual meeting, Kansas City, MI, 2007.

Top 16 Abstract Award: National Neurotrauma Society annual meeting, Kansas City, MI, 2007.

Mason Guest Memorial Award for the Best Poster Presentation in Physiology. National Student research forum, Galveston, TX, 2008.

Sigma Xi Award for a Poster Presentation. National Student research forum, Galveston, TX, 2008.

UTMB James E. Beall II Award for Best Neuroscience Poster Presentation. National Student research forum, Galveston, TX, 2008.

Joint recipient of Best Student Research Poster, Neuroscience and Cell Biology Department Annual Retreat, UTMB, Galveston, TX, July 2008.

Travel Grant recipient: Society for Neuroscience meeting, Washington DC, 2008.

Top 16 Abstract Award: National Neurotrauma Society annual meeting, Las Vegas, NV, 2010.

Permanent Address: 6 Abbeylands, Duleek, County Meath, Ireland.

This dissertation was typed in full by Brian Rooney.